

1229357
[0081544#]

RPP-RPT-56430, Rev. 0

Three-Dimensional Surface Geophysical Exploration of the U Tank Farm

Author Name: N. Crook, M. McNeill, G. Noonan, hydroGEOPHYSICS, Inc.
Columbia Energy and Environmental Services, Inc.
Washington River Protection Solutions, LLC
Richland, WA 99352
U.S. Department of Energy Contract DE-AC27-08RV14800

EDT/ECN: DRF

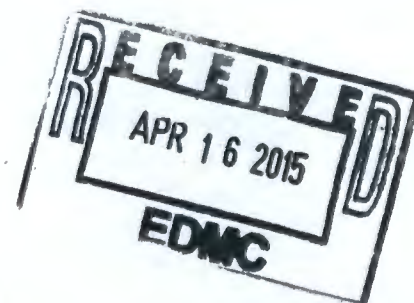
UC:

Cost Center:

Charge Code:

B&R Code:

Total Pages: 82 JDA 1/29/14



Key Words: Surface Geophysical Exploration, SGE, Survey Report, U Tank Farm

Abstract: A surface geophysical exploration (SGE) survey that included direct current electrical resistivity was conducted within the U Tank Farm on the Hanford Site near Richland, Washington. This survey was the first full tank farm surface geophysical exploration survey. The survey was accomplished with the Geotection™-180 Resistivity Monitoring System which facilitated a much larger survey size and faster data acquisition rate. The primary objective of the U Tank Farm SGE survey was to provide geophysical data and subsurface imaging results to support regulatory interim measures.

TRADEMARK DISCLAIMER. Reference herein to any specific commercial product, process, or service by trade name, trademark, manufacturer, or otherwise, does not necessarily constitute or imply its endorsement, recommendation, or favoring by the United States Government or any agency thereof or its contractors or subcontractors.

APPROVED

By Janis D. Aardal at 8:08 am, Jan 29, 2014

Release Approval

Date

DATE:
Jan 29, 2014

**HANFORD
RELEASE**

Release Stamp

Approved For Public Release

S-2-4

WMA-U

80

EXECUTIVE SUMMARY

A surface geophysical exploration survey using a direct current electrical resistivity method was conducted within the 241-U Tank Farm on the Department of Energy Hanford Site near Richland, Washington. This survey was the first full tank farm surface geophysical exploration survey. The survey was accomplished with the Geotecton™-180 Resistivity Monitoring System which facilitated a much larger survey size and faster data acquisition rate. The survey included electrical current transmission and voltage measurements on 490 surface electrodes, within an orthogonal grid, 10 depth electrodes, and 54 wells, acting as long electrodes. Data collection took place between May 16, 2013 and June 28, 2013.

The surface electrode and depth electrode data from the survey were combined to produce an inversion model for the U Tank Farm. The results indicate low resistivity targets between storage tanks U-104, U-105, U-107, and U-108 and between storage tanks U-110 and U-111, between elevations of approximately 637 and 616 feet (194 and 188 meters) above mean sea level, with a deeper large region of low resistivity within the footprint of storage tanks U-104 through U-109, between elevations of approximately 594 and 466 feet (181 and 142 meters) above mean sea level. Figure ES-1 displays two depth slices from the inversion modeling results at elevations just below the base of the tank level and within the conductive region at depth. Figure ES-2 displays a plan view of the distribution of low resistivity within the tank farm. Two contours of low resistivity values are highlighted:

- Opaque value (dark blue) representing 0.5 ohm-meter
- Transparent value (light blue) representing 1.0 ohm-meter.

Modeling of the well-to-well data for U Tank Farm showed three low resistivity targets; between storage tanks U-102 and U-103, to the west of storage tank U-104, and in the southern portion of the survey area to the west of storage tank U-110 (Figure ES-3). The footprint of these low resistivity targets generally coincide with expectations based on knowledge of past releases in the tank farm. Again, two contours of low resistivity values are highlighted:

- Opaque value (dark green) representing 12 ohm-meter
- Transparent value (light green) representing 15 ohm-meter.

Figure ES-1. Plan View Depth Slices of Calculated Resistivity for Filtered Surface to Surface Dataset.

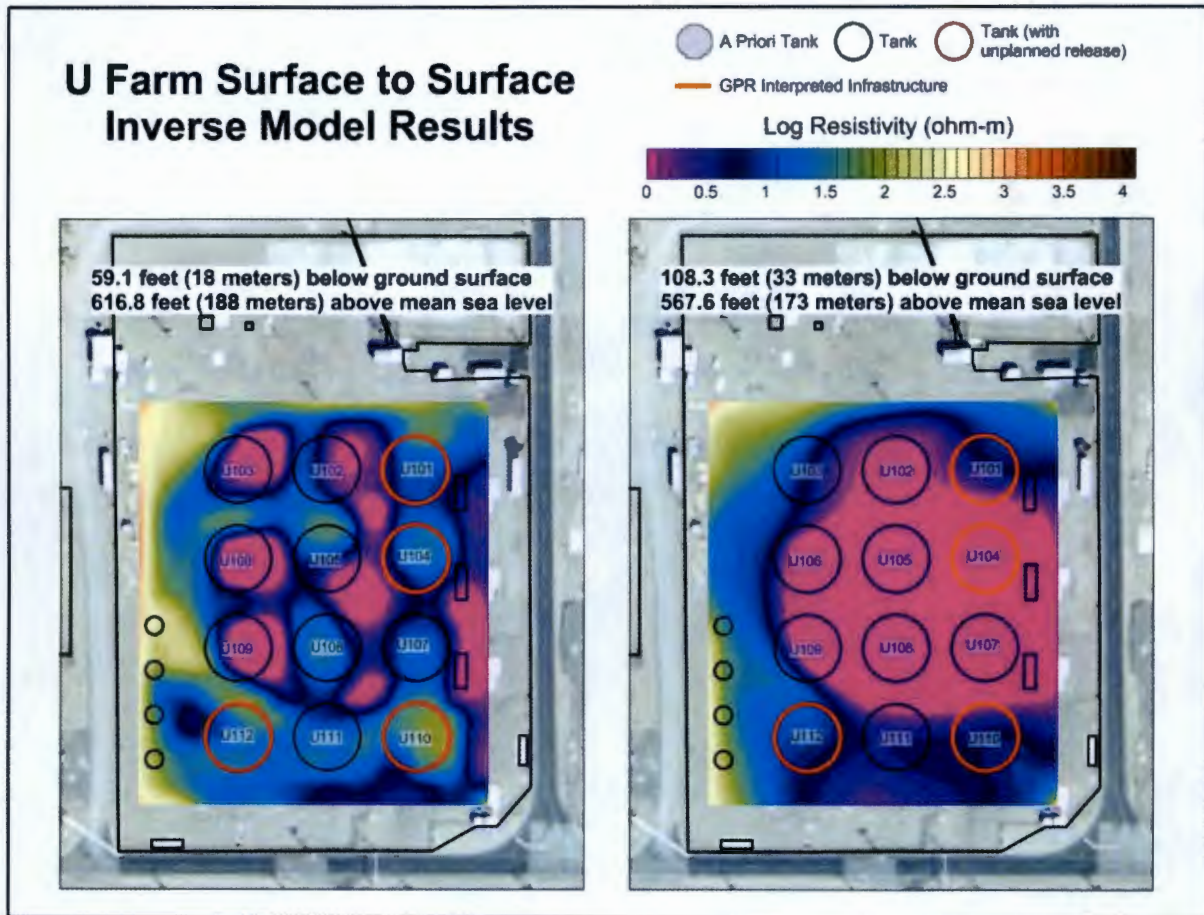


Figure ES-2. Three-Dimensional Rendered Bodies of the Low Resistivity Targets using Surface to Surface Dataset in the U Tank Farm, Plan View. (Plan View).

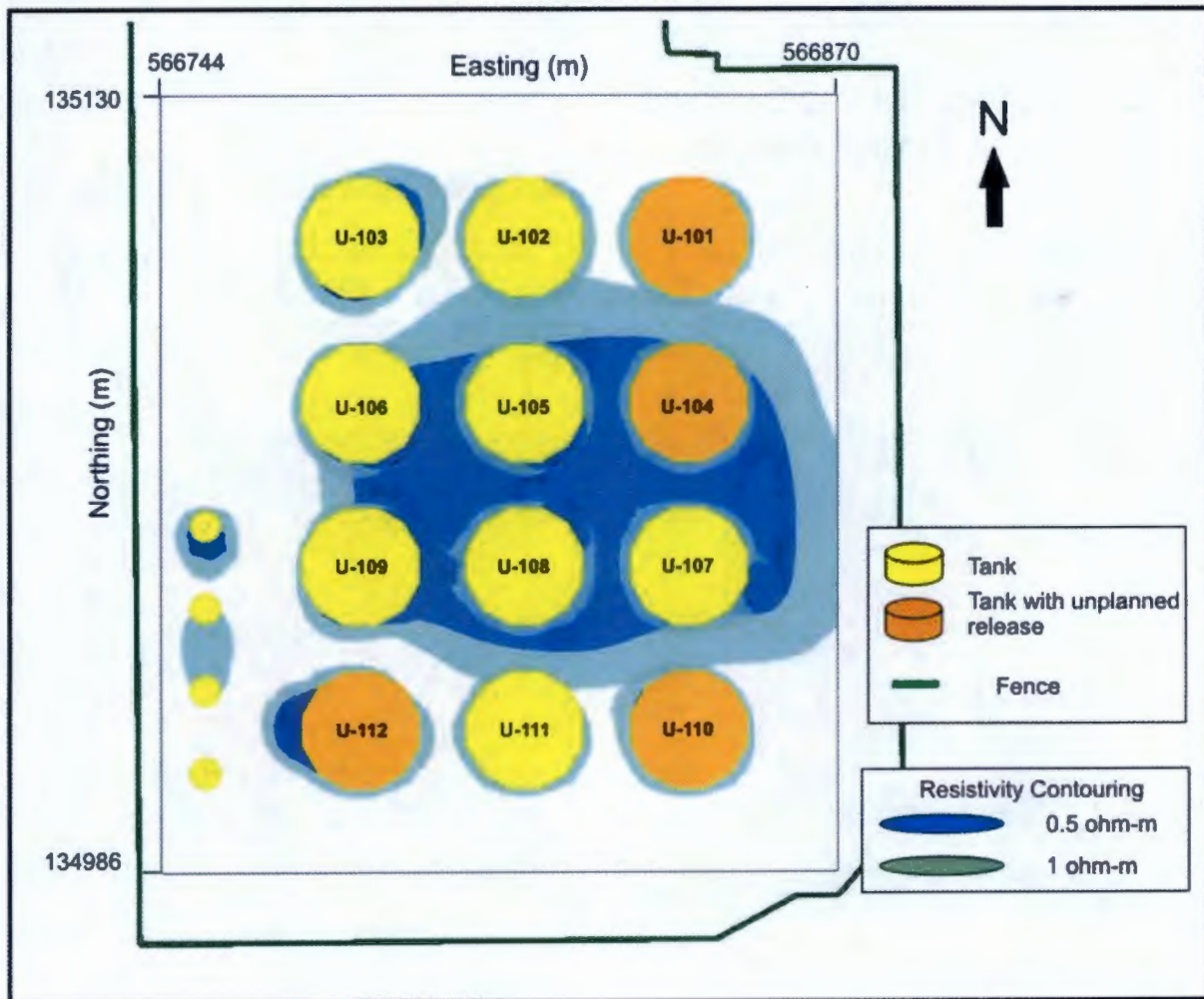


Figure ES-3. Well-to-Well Inversion Model Results for the U Tank Farm; from 2013.

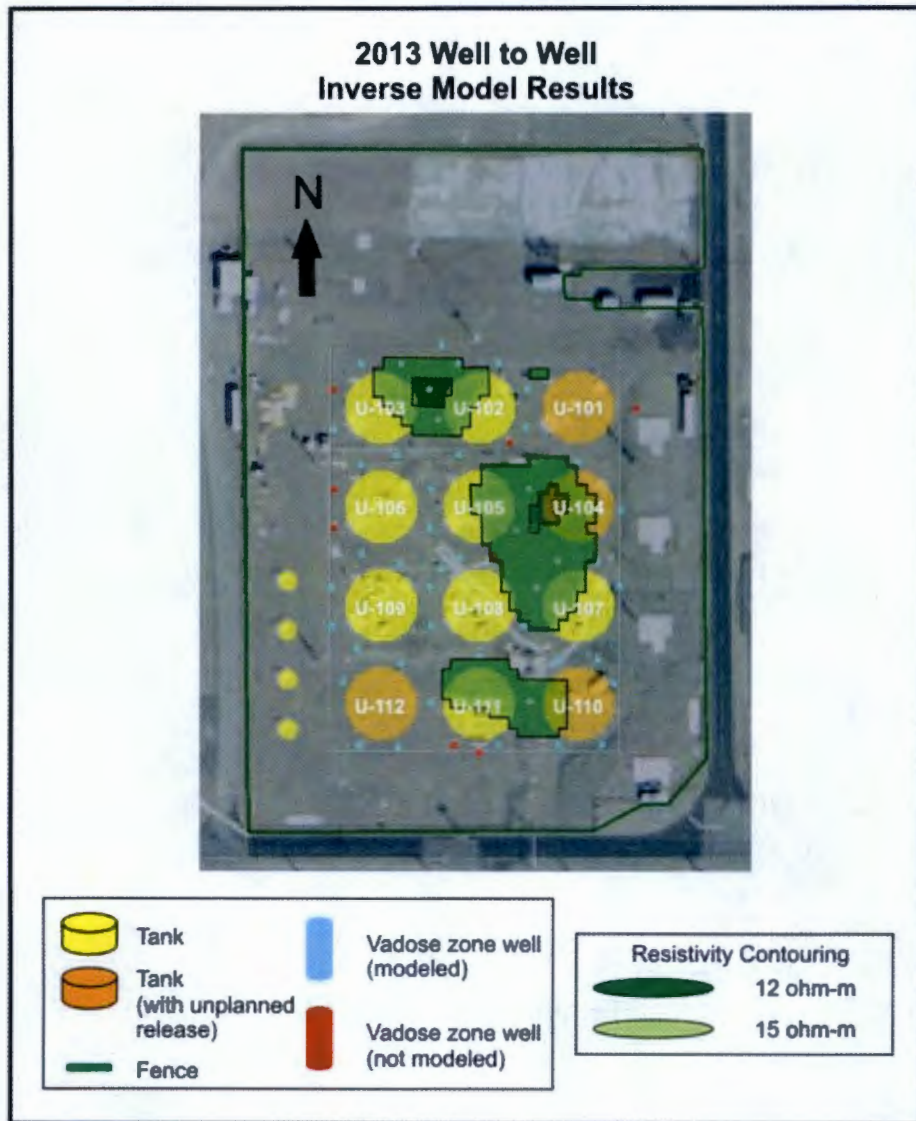


TABLE OF CONTENTS

| | | |
|-------|--|----|
| 1.0 | INTRODUCTION | 1 |
| 1.1 | SCOPE | 1 |
| 1.2 | OBJECTIVES | 1 |
| 1.3 | REPORT LAYOUT | 1 |
| 2.0 | BACKGROUND | 2 |
| 2.1 | SITE DESCRIPTION | 2 |
| 2.2 | OPERATIONAL HISTORY | 5 |
| 2.3 | PREVIOUS CHARACTERIZATION EFFORTS | 8 |
| 2.3.1 | Drywell Gamma Logging | 8 |
| 2.3.2 | Direct Push Sampling | 17 |
| 3.0 | DATA ACQUISITION AND PROCESSING METHODOLOGY | 18 |
| 3.1 | SURVEY DESIGN | 18 |
| 3.1.1 | 2D Survey | 19 |
| 3.1.2 | 3D Survey | 20 |
| 3.2 | EQUIPMENT | 26 |
| 3.2.1 | Electrode and Cable Layout | 26 |
| 3.2.2 | Geotection™ 180 Resistivity Monitoring System (3D Resistivity) | 26 |
| 3.2.3 | SuperSting Resistivity Meter (2D Resistivity) | 27 |
| 3.2.4 | Quality Assurance | 27 |
| 3.3 | ACQUISITION METHODOLOGY | 28 |
| 3.3.1 | 2D Acquisition | 28 |
| 3.3.2 | 3D Acquisition | 28 |
| 3.4 | DATA PROCESSING | 29 |
| 3.4.1 | Data Reduction | 29 |
| 3.4.2 | Depth Electrode Performance | 31 |
| 3.4.3 | Inverse Modeling | 32 |
| 4.0 | MODELING RESULTS | 33 |
| 4.1 | 2D ELECTRICAL RESISTIVITY SURVEY RESULTS | 33 |
| 4.1.1 | North Survey Lines | 34 |
| 4.1.2 | East Survey Lines | 36 |
| 4.1.3 | South Survey Lines | 38 |
| 4.1.4 | West Survey Lines | 38 |
| 4.2 | 3D POINT ELECTRODE MODELING | 40 |
| 4.3 | LONG ELECTRODE MODELING (WELL-TO-WELL INVERSION) | 52 |
| 4.4 | INTEGRATED 2D AND 3D SURVEY ANALYSIS | 54 |

| | | |
|-----|------------------|----|
| 5.0 | CONCLUSIONS..... | 56 |
| 6.0 | REFERENCES | 58 |

LIST OF APPENDICES

| | | |
|---|------------------------|-----|
| A | QUALITY ASSURANCE..... | A-i |
|---|------------------------|-----|

LIST OF FIGURES

| | | |
|------------|---|----|
| Figure 1. | Location of the U Tank Farm within the 200 West Area of the Hanford Site. | 3 |
| Figure 2. | General Configuration of Tank Construction in U Tank Farm..... | 4 |
| Figure 3. | Surficial Fluid Discharge Summary (Gallons) to U Tank Farm..... | 7 |
| Figure 4. | Visual Interpretation of Drywell Logging Activity at 4 ft (1.2 m) bgs (671.9 ft [204.8 m] amsl). | 9 |
| Figure 5. | Visual Interpretation of Drywell Logging Activity at 11 ft (3.4 m) bgs (664.9 ft [202.6 m] amsl). | 10 |
| Figure 6. | Visual Interpretation of Drywell Logging Activity at 23 ft (7m) bgs (652.9 ft [199 m] amsl). | 11 |
| Figure 7. | Visual Interpretation of Drywell Logging Activity at 36 ft (11 m) bgs (639.9 ft [195 m] amsl). | 12 |
| Figure 8. | Visual Interpretation of Drywell Logging Activity at 50 ft (15.2 m) bgs (625.9 ft [190.8 m] amsl). | 13 |
| Figure 9. | Visual Interpretation of Drywell Logging Activity at 56 ft (17.1 m) bgs (619.9 ft [188.9 m] amsl). | 14 |
| Figure 10. | Visual Interpretation of Drywell Logging Activity at 67 ft (20.4 m) bgs (608.9 ft [185.6 m] amsl). | 15 |
| Figure 11. | Visual Interpretation of Drywell Logging Activity at 88 ft (26.8 m) bgs (587.9 ft [179.2 m] amsl). | 16 |
| Figure 12. | Visual Interpretation of Drywell Logging Activity at 100 ft (30.5 m) bgs (575.9 ft [175.5 m] amsl). | 17 |
| Figure 13. | Map of 2D Resistivity Survey Coverage for FY2006 (Blue) and FY2013 (Green). | 19 |
| Figure 14. | Resistivity Cable and Surface Electrode Layout. | 21 |
| Figure 15. | 3D Survey Depth Electrode and Well Distribution. | 25 |
| Figure 16. | The SuperSting R8 resistivity meter (top) and Geotecton™ -180 Resistivity Monitoring System (bottom)..... | 27 |
| Figure 17. | Remote Locations Used for the Pole-Pole Array..... | 29 |
| Figure 18. | Data Distribution for Raw (Combined Reciprocal) and Reduced V/I Data for the 3D Survey (Surface and Depth Electrode Data). | 30 |
| Figure 19. | North Line 2D Model Surface Resistivity Results for the FY2013 (Top) and FY2006 (Bottom) Surveys..... | 35 |

| | | |
|------------|---|----|
| Figure 20. | East Line 2D Model Surface Resistivity Results for the FY2013 (Top) and FY2006 (Bottom) Surveys..... | 37 |
| Figure 21. | South Line 2D Model Surface Resistivity Results for the FY2013 Survey. | 38 |
| Figure 22. | West Line 2D Model Surface Resistivity Results for the FY2013 (Top) and FY2006 (Bottom) Surveys..... | 39 |
| Figure 23. | Size And Position of the Inverse Model Grid Used to Model the U Tank Farm Point Electrode Data. | 41 |
| Figure 24. | <i>A Priori</i> Model Blocks Added to the Inverse Modeling Domain..... | 42 |
| Figure 25. | Distribution of Modeled Resistivity Values for the U Tank Farm (Blue) and BY Tank Farm (Red) Inversion Results..... | 43 |
| Figure 26. | Expanded Plan View for the Depth Slice at 6.6 Ft of Calculated Resistivity for Filtered Surface to Surface, with Linear Interpretations from the FY2012 Ground Penetrating Radar Site Clearance Survey of U Tank Farm (left image). | 44 |
| Figure 27. | Plan View Depth Slices of Calculated Resistivity for Filtered Surface to Surface Dataset. | 45 |
| Figure 28. | Plan View Depth Slices of Calculated Resistivity for Filtered Dataset..... | 46 |
| Figure 29. | Three-Dimensional Rendered Bodies of the Low Resistivity Targets using Surface to Surface Dataset in the U Tank Farm, View From Southeast..... | 50 |
| Figure 30. | Three-Dimensional Rendered Bodies of the Low Resistivity Targets using Surface to Surface Dataset in the U Tank Farm, Plan View..... | 51 |
| Figure 31. | Three-Dimensional Rendered Bodies of the Low Resistivity Targets using Surface to Surface Dataset in the U Tank Farm, View From the South..... | 51 |
| Figure 32. | Well-to-Well Inversion Model Results for the U Tank Farm, 2006 (reprocessed) and 2013. | 53 |
| Figure 33. | Integrated 2D and 3D Survey Anomaly Map. | 55 |

LIST OF TABLES

| | | |
|----------|---|----|
| Table 1. | Locations for Depth Electrodes in 241-U Tank Farm (in Washington State Plane, m, NAD83)..... | 22 |
| Table 2. | Well Locations in 241-U Tank Farm (in Washington State Plane, m, NAD83). (3 sheets) | 22 |
| Table 3. | Number of Data Points Retained During Data Reduction Steps (Surface and Depth Electrode Data). | 31 |
| Table 4. | Number of Data Points Retained During Data Reduction Steps (Well-to-Well Data). | 31 |
| Table 5. | Depth Electrode Performance Measure for U Tank Farm. | 32 |
| Table 6. | Model Resistivity Values from the Inversion Output for the RES2DINV Code for the FY2006 and FY2013 Surveys. | 34 |
| Table 7. | Inverse Modeling Convergence and Error Statistics. | 40 |

LIST OF TERMS

Abbreviations and Acronyms

| | |
|-------|--|
| 2D | two-dimensional |
| 3D | three-dimensional |
| AC | alternating current |
| AGI | Advanced Geosciences, Inc. |
| amsl | above mean sea level |
| bgs | below ground surface |
| CAD | computer-aided design |
| DOE | U.S. Department of Energy |
| ft | feet |
| FY | fiscal year |
| GPR | ground penetrating radar |
| GPS | global positioning system |
| HGI | hydroGEOPHYSICS, Inc. |
| m | meter |
| NIST | National Institute of Standards and Technology |
| PUREX | plutonium-uranium extraction |
| REDOX | reduction oxidation |
| RMS | root-mean-square |
| SGE | surface geophysical exploration |
| SST | single-shell tank |
| UL | Underwriters Laboratories |
| WRPS | Washington River Protection Solutions, LLC |
| WTW | well-to-well |

LIST OF TRADEMARKS

AutoCAD is a registered trademark of AutoDesk, Inc.

Geotecton is a trademark of hydroGEOPHYSICS, Inc.

Leica is a registered trademark of Leica Technology.

Rock Works is a registered trademark of RockWare, Inc.

SuperSting R8 is a registered trademark of Advanced Geosciences, Inc.

Surfer is a registered trademark of RockWare, Inc.

1.0 INTRODUCTION

This report documents the results of the surface geophysical exploration (SGE) survey completed within the 241-U Tank Farm at the U.S. Department of Energy (DOE) Hanford Site in Washington State in fiscal year (FY) 2013. hydroGEOPHYSICS, Inc. (HGI) and Columbia Energy and Environmental Services, Inc., with support from technical staff of Washington River Protection Solutions, LLC (WRPS), conducted a three-dimensional (3D) survey of the subsurface using electrical resistivity. A limited scope geophysical survey of the U Tank Farm was previously completed in FY2006 and is documented in RPP-RPT-31557, *Surface Geophysical Exploration of U Farm at the Hanford Site*. The FY2013 3D results were compared to results obtained in FY2006 where applicable. In addition, two-dimensional (2D) electrical resistivity lines were surveyed outside of U Tank Farm for characterization purposes near historic trenches and for comparison to the 2006 survey. Data acquisition and analysis were performed in accordance with RPP-PLAN-54501, *Work Plan for 3D Electrical Resistivity Survey at the 241-U Tank Farm*. The 3D electrical resistivity data were acquired using 490 surface electrodes (located at the ground surface), 10 depth electrodes, and 54 wells completed within the U Tank Farm region. A reanalysis of the 2006 2D electrical resistivity profiles was conducted prior to modeling to provide an assessment of the changes, if any, in the analysis of the U Tank Farm resistivity anomalies using the latest generation of inverse modeling software. Further details on the reanalysis can be found in RPP-RPT-54500, *241-U Farm: Two-Dimensional Electrical Resistivity Reanalysis*.

1.1 SCOPE

The scope of this electrical resistivity characterization survey included:

- Data acquisition on surface electrodes, depth electrodes, and wells
- Statistical evaluation of depth electrodes to ensure quality in data acquisition
- Compilations of 3D electrical resistivity cross-sections of the U Tank Farm.

1.2 OBJECTIVES

The primary objective of the U Tank Farm SGE survey is to provide geophysical data and subsurface imaging results to support regulatory interim measures. Interim measures, like interim surface barriers, are initial actions intended to mitigate the impact of subsurface contaminants to the surrounding environment while more permanent measures are assessed.

1.3 REPORT LAYOUT

The overall scope and content of this report is divided into several main sections as follows:

- **Section 1.0, Introduction** – Describes the scope and objectives of the investigation.
- **Section 2.0, Background** – Describes the geologic and hydrologic setting and information regarding the disposal activities in and around U Tank Farm.
- **Section 3.0, Data Acquisition and Processing** – Presents general layout of the data acquisition and processing with methods and controls used to ensure the quality and control of data collection, reduction, and processing used in this study.

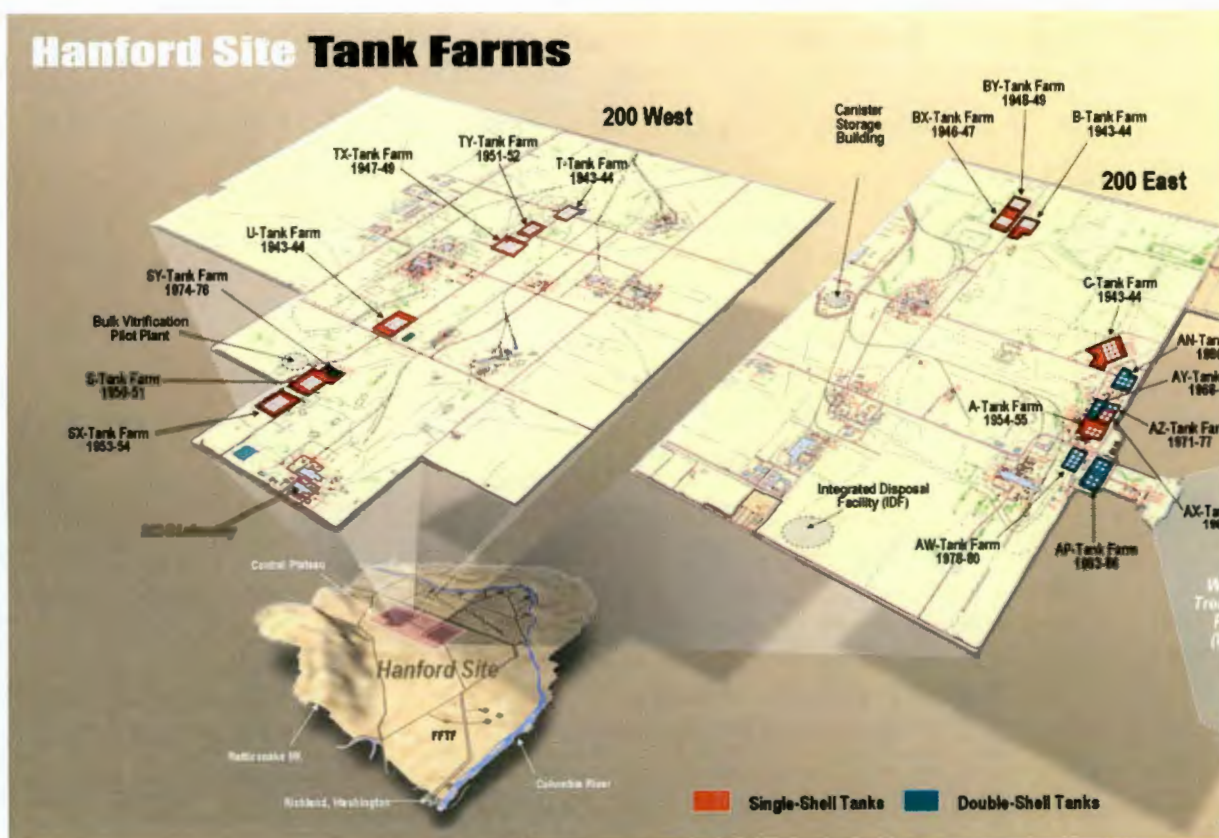
- **Section 4.0, Results and Interpretations** – Presents the preliminary modeling results from the electrical resistivity surveying effort.
- **Section 5.0, Conclusions** – Provides a summary and conclusions drawn from the results and interpretations.
- **Section 6.0, References** – Provides a listing of references cited in the report.
- **Appendix A, Quality Assurance** – Presents general methods and controls used to ensure the quality and control of data collection, reduction, and processing and configuration control of software and database changes used in this study.

2.0 BACKGROUND

2.1 SITE DESCRIPTION

U Tank Farm is one of 12 single-shell tank (SST) farms on the Hanford Site. U Tank Farm is located in the central portion of 200 West Area at the DOE Hanford Site (Figure 1). U Tank Farm contains twelve 100-Series SSTs and four 200-Series SSTs that were constructed between 1943 and 1944, put into service in 1946, and currently out of service pending final waste retrieval actions. Because of its long operational history, the U Tank Farm received waste generated by the majority of the major chemical processing operations at the Hanford Site. This included waste from the bismuth phosphate fuel processing, uranium recovery, plutonium-uranium extraction fuel processing, and fission product recovery (RPP-15808, *Subsurface Conditions Description of the U Waste Management Area*). Information on the geology and hydrology of the U Tank Farm area can be found in RPP-35485, *Field Investigation Report for Waste Management Area U*, and RPP-23748, *Geology, Hydrogeology, Geochemistry, and Mineralogy Data Package for the Single- Shell Tank Waste Management Areas at the Hanford Site*. Additional background information on the construction of U Tank Farm, remaining waste inventory, and subsurface conditions is available in RPP-PLAN-53808, *200 West Area Tank Farms Interim Measures Investigation Work Plan*. A brief description of site infrastructure and waste inventory as it pertains to the U Tank Farm investigation follows.

Figure 1. Location of the U Tank Farm within the 200 West Area of the Hanford Site.

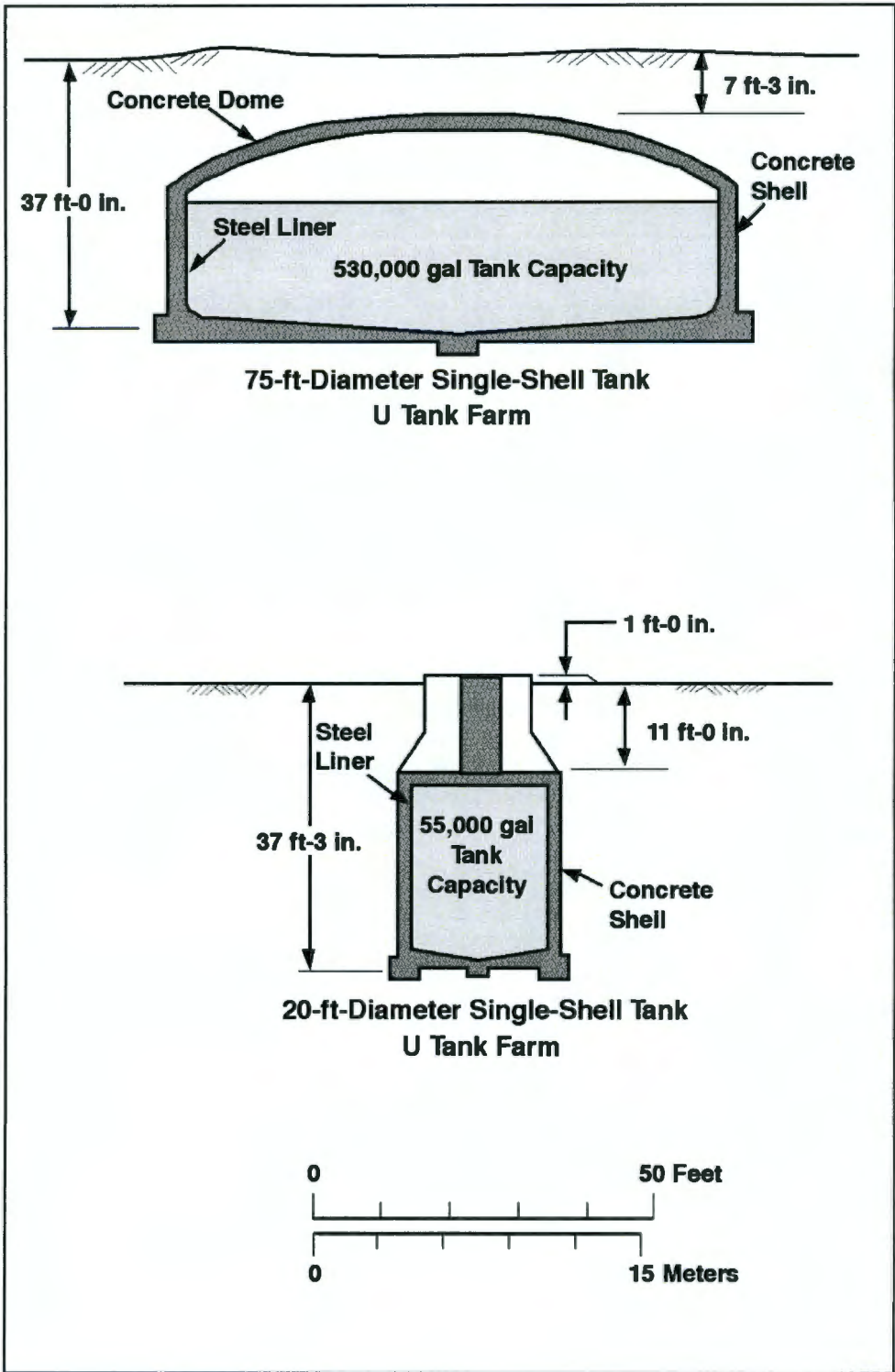


The U Tank Farm comprises the following:

- Twelve 100-Series SSTs with a 530,000-gallon (2.0×10^6 liter) capacity
- Four 200-Series SSTs with a 55,000-gallon (0.21×10^6 liter) capacity
- Waste transfer lines
- Leak detection systems
- Tank ancillary equipment.

The 100-Series tanks are 75 ft (22.9 m) in diameter and 30 ft (9.1 m) tall. The tanks have a 15-ft (4.6-m) operating depth, and an operating capacity of 530,000 gallons (2.0×10^6 liters) each. The 200-Series tanks are 20 ft (6.1 m) in diameter and 37 ft (11.3 m) tall from base to dome. The tanks have a 24-ft (7.3-m) operating depth and an operating capacity of 55,000 gallons (0.21×10^6 liters) each. Typical tank configuration and dimensions are shown in Figure 2.

Figure 2. General Configuration of Tank Construction in U Tank Farm.



The basic tank structure consists of a carbon steel liner covered with a reinforced concrete shell that completely encases the steel liner and extends continuously above the liner wall to form a dome cover over the tank. Between the steel liner and concrete shell is a 3/8 inch (0.95 centimeter) thick asphalt membrane that serves as a waterproofing layer. The 100-Series tanks and 200-Series tanks are situated entirely below ground surface (bgs), with approximately 7 and 11 ft (2.0 and 3.4 m) of backfill covering the concrete tank dome respectively.

Infrastructure within the tank farm consists of buried waste transfer lines, instrument and electrical lines, abandoned water lines, and concrete structures associated with valve pits and diversion boxes.

The backfill that covers the SSTs came from screened (i.e., large stones removed), excavated soil material. The heavy equipment that was used for excavation and for completing the tank construction is thought to have produced a compaction layer under and around each tank. The backfill between and over the tanks is relatively homogeneous compared with the undisturbed soil under the tanks.

The U Tank Farm 100-Series tanks were constructed in four cascades each consisting of a three-tank cascade series. Each successive tank in the cascade series is sited at a lower elevation that allowed gravity flow of liquid between tanks. Each tank is surrounded by several drywells in which radiometric instruments are used to detect changes in activity levels in the sediments surrounding the borehole (RPP-7580, *Historical Vadose Zone Contamination from U Tank Farm Operations*). U Tank Farm has 59 of these leak detection drywells, completed between 1944 and 1979, ranging in depth between 80 and 150 ft (24.0 and 45.7 m) bgs. These drywells served as both primary and secondary leak detection devices. In addition, a number of groundwater monitoring wells are located in the U Tank Farm area. The FY2006 geophysical survey completed measurements on drywells and groundwater wells within and surrounding the perimeter of U Tank Farm (RPP-RPT-31557). The current FY2013 geophysical survey used drywells (vadose zone wells) only.

2.2 OPERATIONAL HISTORY

Unintentional discharges in or near U Tank Farm and intentional discharges to ground near U Tank Farm have occurred through waste management operations (RPP-7580; RPP-15808). Unintentional discharges in or near the U Tank Farm include the following.

- In 1950, during construction at diversion boxes 241-U-151 and 241-U-152, a leak occurred whose source and volume were unspecified (UPR-200-W 6).
- In 1953, metal waste spray was ejected from a riser in the 244-UR vault created by a violent chemical reaction in the vault (UPR-200-W-24). The contamination spread to the southeast covering the eastern half of the tank farm.
- In 1956, two events occurred. Five hundred gallons (1,900 liters) of metal waste overflowed from the 241-UR-151 diversion box at the northeast corner of U Tank Farm (UPR-200-W-132), and tank U-104 leaked an estimated 55,000 gallons (208,000 liters) of metal waste (UPR-200-UW-155).
- Tank U-101 was reported to have leaked 30,000 gallons (114,000 liters) of reduction oxidation (REDOX) high-level waste in 1959 (UPR-200-W-154). Drywell monitoring data around tank U-101 do not support a tank leak of this volume.

- Tank U-110 was reported to have leaked 8,000 gallons (31,000 liters) of REDOX coating waste in 1969.
- Tank U-112 was reported to have leaked 10,000 gallons (38,000 liters) of REDOX high-level waste in 1975.
- In 1971, an inadvertent cut in an underground waste line near tank U-103 resulted in minor contamination (UPR-200-W-128).
- Tank U-104 was reported to have leaked 55,000 gallons (208,000 liters) of uranium-rich metal waste in the early 1950s. Subsequent drywell logging showed spectral gamma uranium activity that extended to the south and southwest of tank U-104. The uranium plume is between 52 ft (16 m) and 92 ft (28 m) bgs and extends in an oval shape oriented toward the south-southwest with a major axis of about 225 ft (69 m) and a minor axis of about 100 ft (30 m).

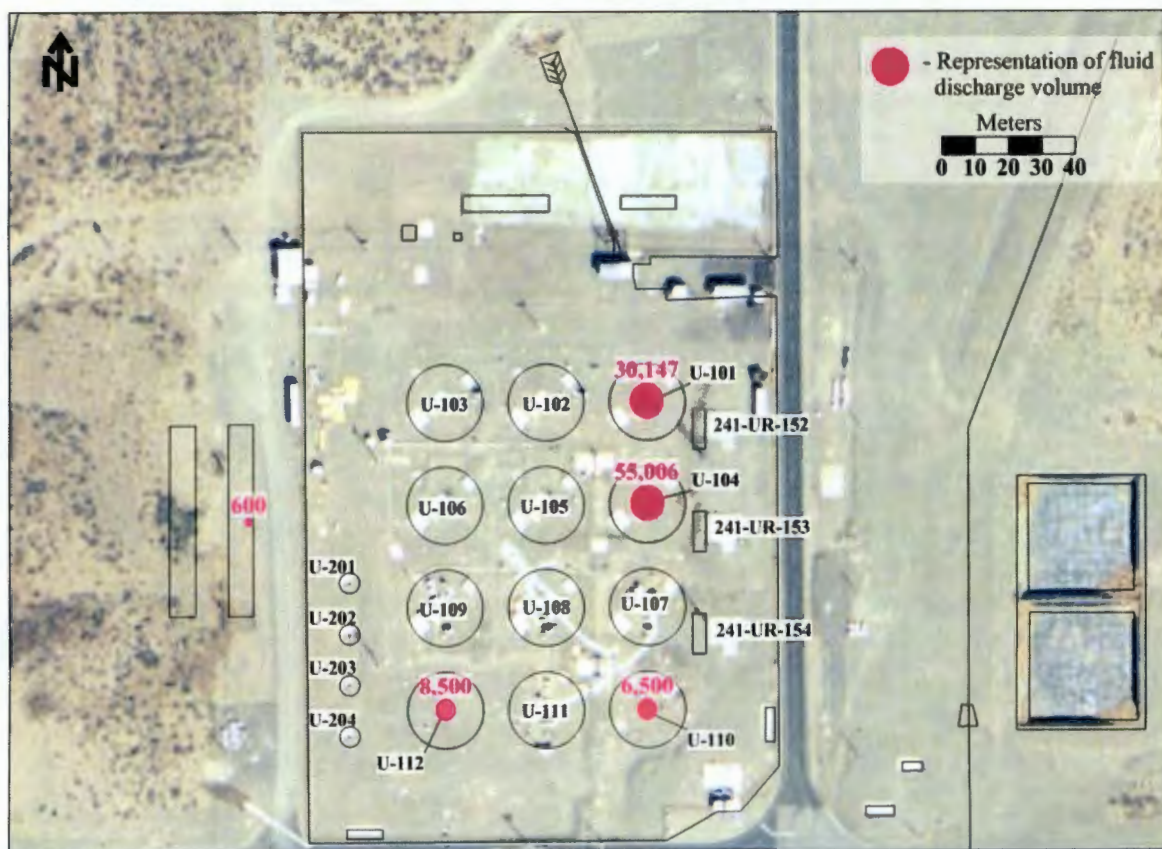
Intentional discharges to ground near U Tank Farm include the following (RPP-7580; RPP-15808).

- Wastewater from the 283-W water treatment plant, 284-W powerhouse, 2723-W mask cleaning station, and 2724-W laundry facility was discharged to the 216-U-14 ditch. Laundry discharges ended in 1981; discharges from the powerhouse ended in 1984.
- Cooling water, steam condensate, floor drainage from the 231-Z Plutonium Isolation Building, Plutonium Finishing Plant storm water runoff and chemical sewer waste were discharged to U Pond via the 216-Z-1D ditch. The volume of water discharged to the ditch was not recorded but is estimated at approximately 211 million gallons (800 million liters) per year.
- Cooling water and cell drainage from the tri-butyl phosphate, uranium trioxide (UO_3), and U Plants were discharged to the 216-U-14 ditch. This increased flow through the ditch from approximately 290 million gallons (1.1 billion liters) per year to over 2 billion gallons (8 billion liters) per year. After 1958, when U Plant was shut down, the UO_3 plant continued to process waste from the REDOX and Plutonium-Uranium Extraction (PUREX) Plants and discharge cooling water and chemical sewer waste to the 216-U-14 ditch, but the volume of discharge was reduced from over 2 billion gallons (8 billion liters) per year to approximately 530 million gallons (2 billion liters) per year.
- Beginning in 1956, increased plutonium production of the REDOX plant increased wastewater discharges to the 216-Z-1D ditch from 211 million gallons (800 million liters) per year to approximately 1 billion gallons (4 billion liters) per year.
- In 1954, the tank U-110/U-111/U-112 cascade was filled with combined REDOX high-level and coating waste. Because the waste was self-boiling a reflux condenser was added to tank U-110 and tank condensate was transferred to the 216-U-3 French drain (identified as the 216-U-3 crib) until the tanks stopped boiling. In 1954 and 1955, about 208,000 gallons (790,000 liters) were discharged to this facility.
- Wastewater discharges from the 231-Z building ended in 1957. In 1959, an unknown amount of plutonium and americium was inadvertently released from 231-Z in the 216-Z-1D ditch.

- During the 1960s, contaminated sludge from the bottom of the 207-U retention basin was scraped out and consolidated in two pits adjacent to the north and south walls of the basin (UPR-200-W-111 and UPR-200-W-112).
- The UO_3 Plant continued to discharge as much as 850 million liters per year of cooling water to the 216-U-14 ditch. To facilitate decommissioning part of the ditch, the 216-U-16 crib was built near U Plant in 1984 to receive UO_3 cooling water. Discharges to this crib flushed uranium out of the 216-U-1 and 216-U-2 cribs into the groundwater. Use of the 216-U-16 crib was discontinued and the UO_3 Plant cooling water was redirected back to the 216-U-14 ditch. Shutdown of the PUREX Plant in 1988 reduced the amount of UO_3 plant wastewater to the ditch to approximately 250 million liters per year. The UO_3 Plant was shut down in 1993.
- In 1986, approximately 625 gallons (2,400 liters) of recovered nitric acid, containing approximately 86 pounds of uranium, was accidentally released from the UO_3 Plant into the chemical sewer and the 207-U basin.

Figure 3, showing the major planned and unplanned releases of liquid waste to the soil, was generated from data presented in Section 2.2 and from RPP-26744, *Hanford Soil Inventory Model*. It is likely that since the releases, the resulting plumes have migrated away from the source due to a number of higher than normal precipitation periods and rapid snowmelt events. These recharge events would have an effect on the distribution of contaminants and moisture in the vadose zone.

Figure 3. Surficial Fluid Discharge Summary (Gallons) to U Tank Farm.



The tanks in the U Tank Farm currently contain an estimated total volume of 2,930,000 gallons (11.1×10^6 liters) of mixed wastes consisting of various bismuth phosphate, REDOX, and PUREX processing waste streams (HNF-EP-0182, *Waste Tank Summary Report for Month Ending July 31, 2013*). General tank content (i.e., liquid and solid volumes) data and some tank monitoring data are summarized monthly in waste tank summary reports (e.g., HNF-EP-0182). Tanks U-101, U-104, U-110, and U-112 are classified as assumed/confirmed leakers. These tanks are currently estimated to have leaked a total of 98,500 to 101,600 gallons (373,000 to 385,000 liters) of tank waste.

As a result of the discharges around U Tank Farm, some of the inorganic tank and crib constituents may have reached the groundwater. Current information on groundwater contamination is available in DOE/RL-2013-22, *Hanford Site Groundwater Monitoring Report for 2012*.

Results of a reassessment of estimated release volumes and associated inventory as provided in RPP-26744 and HNF-EP-0182 are presented in RPP-RPT-50097, *Hanford 241-U Farm Leak Inventory Assessment Report*. The reassessment provides an updated comparison to the tank loss estimates contained in HNF-EP-0182. The reassessment findings for this report state that no additional releases were indicated for tanks already classified as "sound" in 241-U Tank Farm. The revised loss estimate for tank U-104 showed the most significant increase, from 55,000 gallons to 109,000 gallons (208,000 to 413,000 liters). Tanks U-110 and U-112 show potential increases as well but the estimated increases are more uncertain and original estimates may indeed be correct. Tank U-101, listed as an assumed leaker in HNF-EP-0182 with a tank waste loss of 30,000 gallons (114,000 liters), is recommended for a revaluation of integrity with an updated tank waste loss of 0 to 30,000 gallons (0 to 114,000 liters). Based on a review of operational history, the assessment contains findings for potential new unplanned releases as a result of pipeline failures that were not previously documented in DOE/RL-88-30, *Hanford Site Waste Management Units Report*. The volume of this potentially discharged waste was unable to be determined due to insufficient information. RPP-23405, *Tank Farm Vadose Zone Contamination Volume Estimates*, also suggests modifications of official tank leak totals stating that some attributed leak events may actually have been from evaporation of waste, spare inlet overflows, line leaks or spills during process operations.

2.3 PREVIOUS CHARACTERIZATION EFFORTS

2.3.1 Drywell Gamma Logging

A series of cross-section visualizations based on spectral gamma drywell measurements are provided (Figures 4 through 12), taken directly from GJO-97-1-TARA, *Hanford Tank Farms Vadose Zone: Addendum to the U Tank Farm Report*. A review of these figures indicates relatively wide spread gamma contamination near the tank farm surface and three distinct contamination areas at 56 ft (17 m) bgs (619.9 ft [188.9 m] amsl) near the base of tanks U-104, U-110, and U-112. A uranium plume is indicated southwest of tank U-104, a cesium plume is indicated southwest of tank U-110 from one drywell (60-10-07), and a cesium plume is indicated northeast of tank U-112 from one drywell (60-12-01).

Figure 4. Visual Interpretation of Drywell Logging Activity at 4 ft (1.2 m) bgs (671.9 ft [204.8 m] amsl).

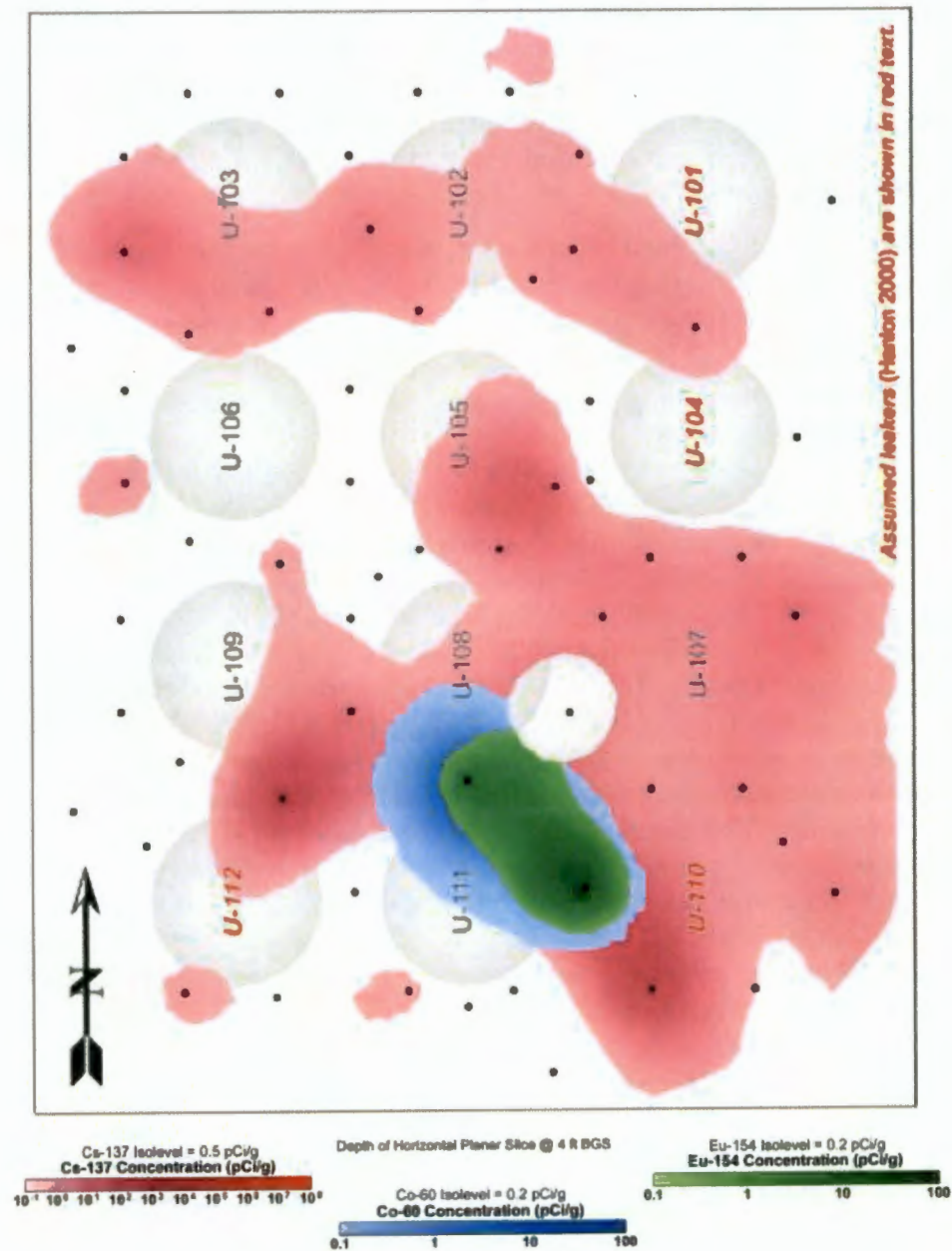


Figure 5. Visual Interpretation of Drywell Logging Activity at 11 ft (3.4 m) bgs (664.9 ft [202.6 m] amsl).

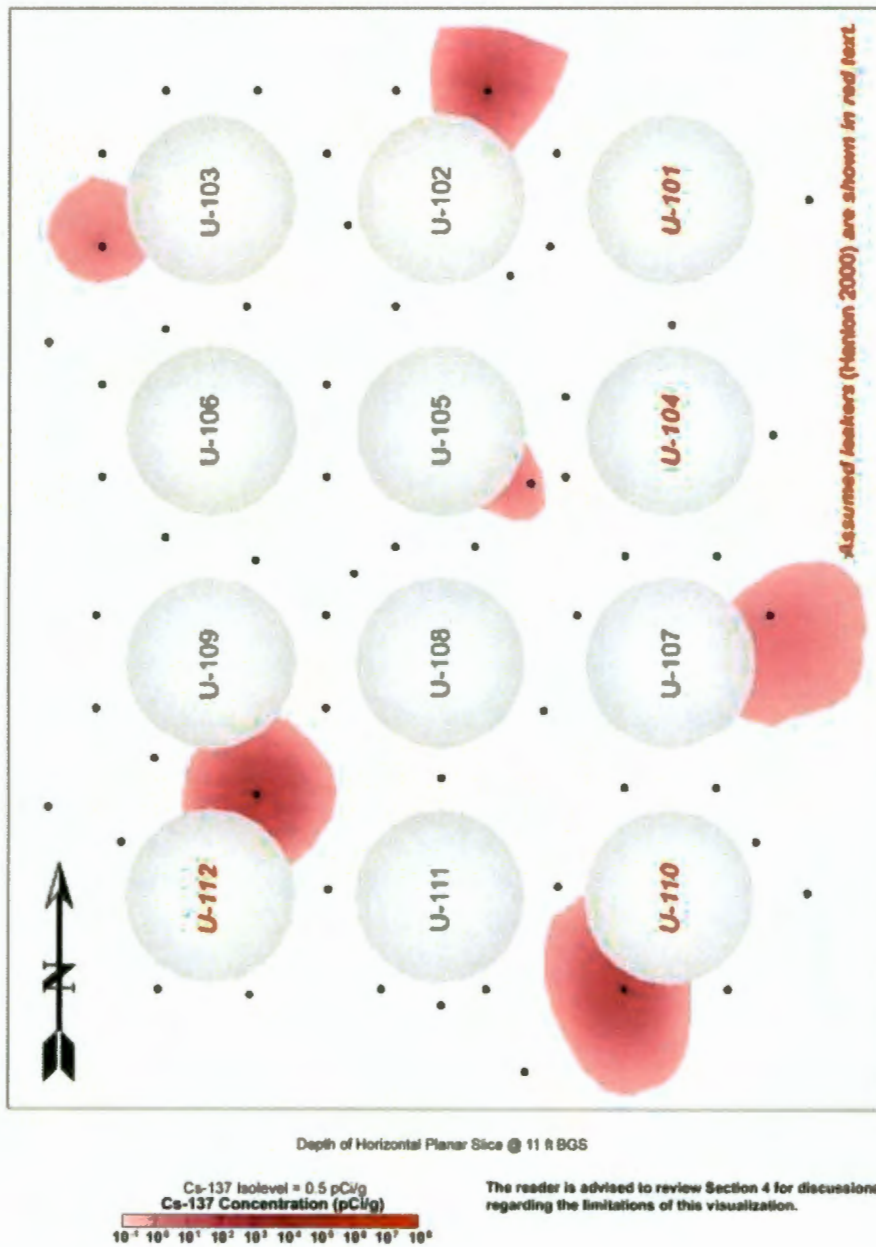


Figure 6. Visual Interpretation of Drywell Logging Activity at 23 ft (7m) bgs (652.9 ft [199 m] amsl).

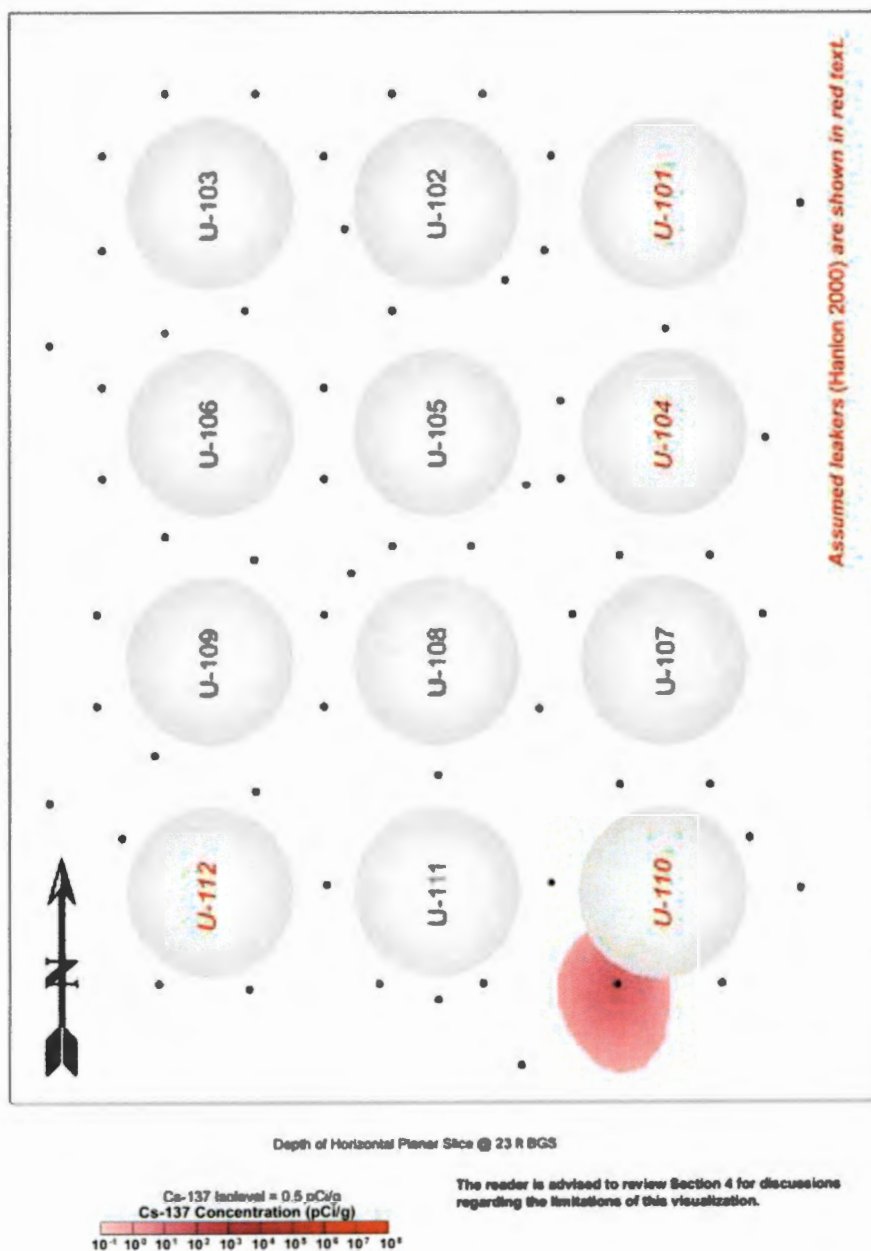


Figure 8. Visual Interpretation of Drywell Logging Activity at 50 ft (15.2 m) bgs (625.9 ft [190.8 m] amsl).

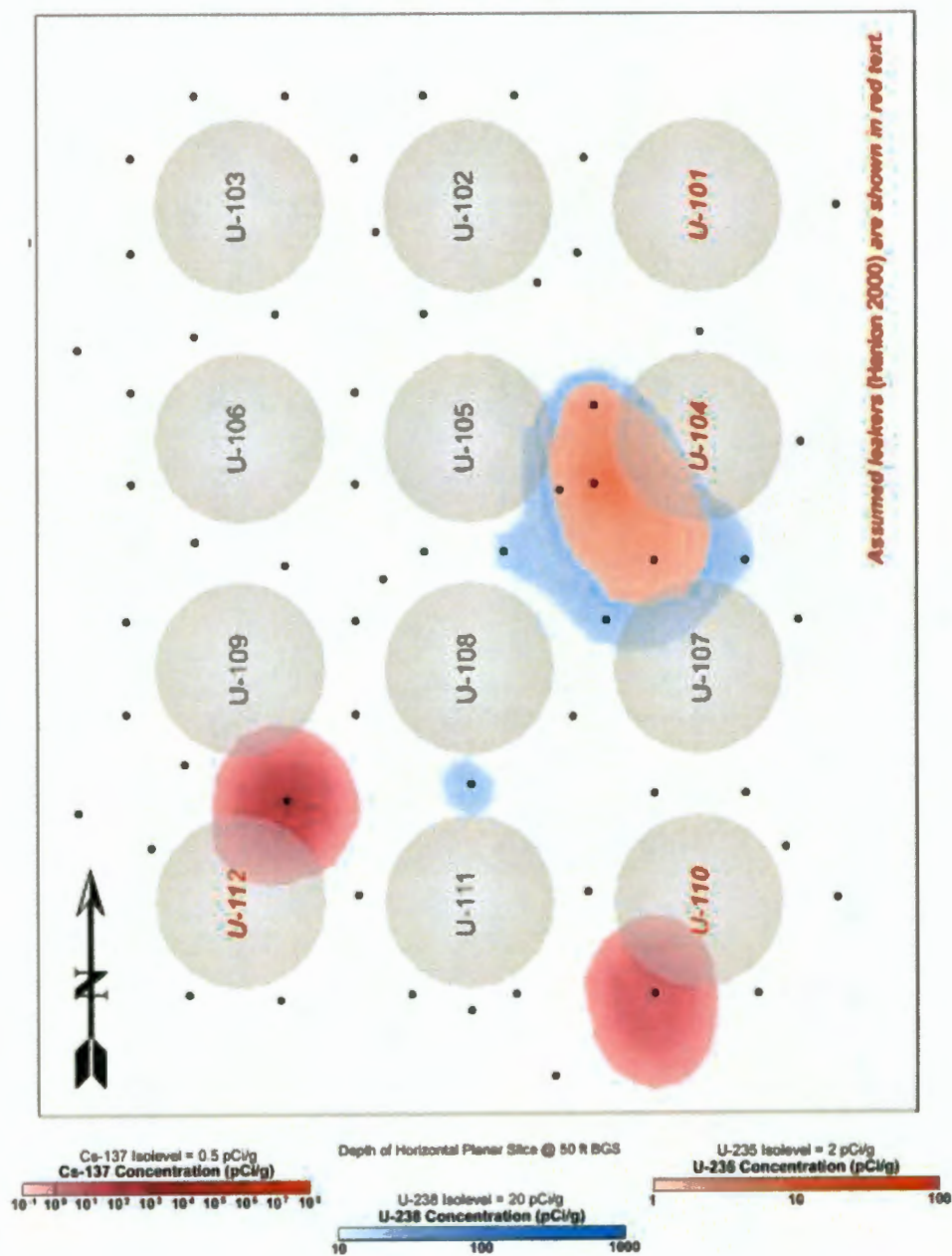


Figure 9. Visual Interpretation of Drywell Logging Activity at 56 ft (17.1 m) bgs (619.9 ft [188.9 m] amsl).

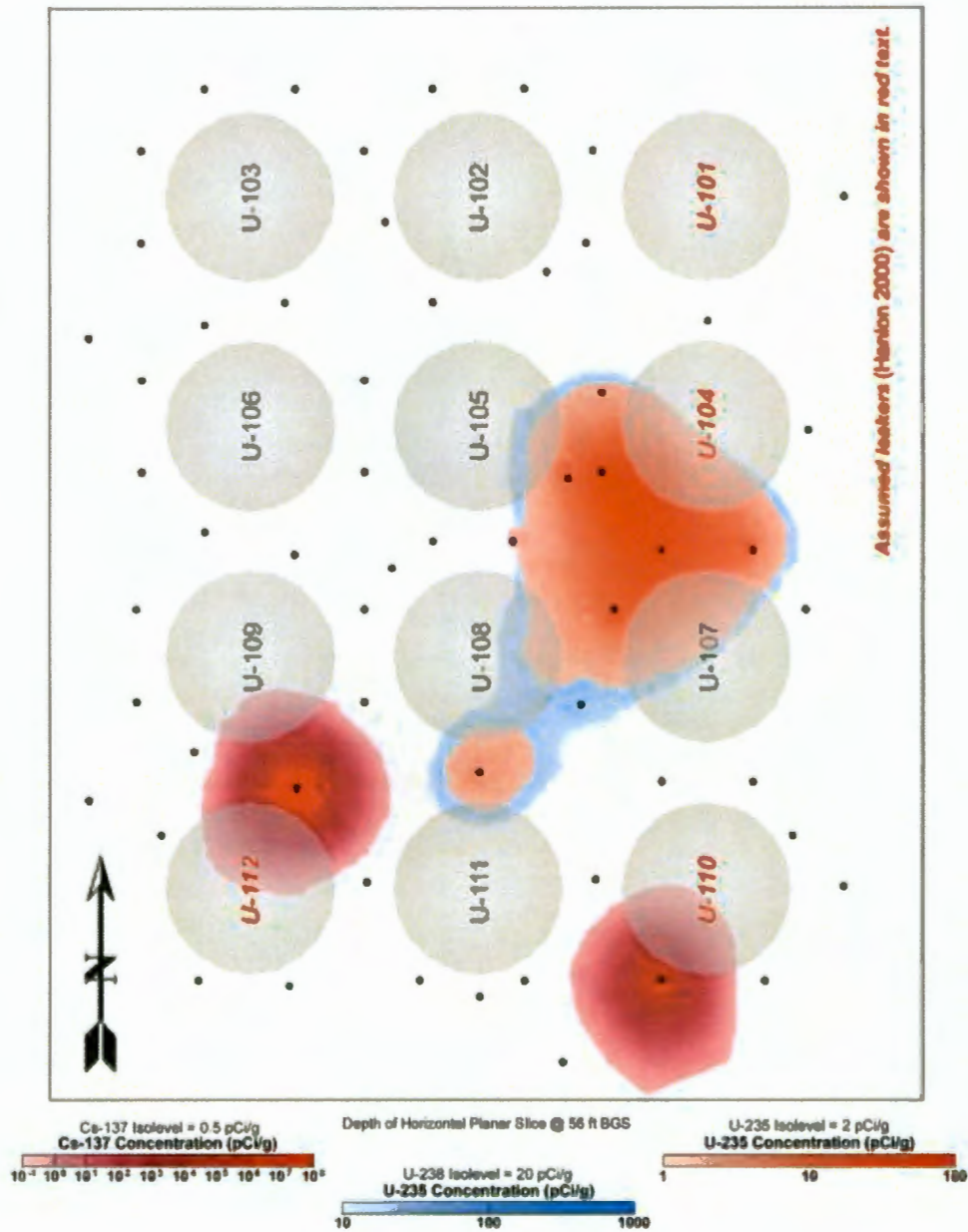


Figure 10. Visual Interpretation of Drywell Logging Activity at 67 ft (20.4 m) bgs (608.9 ft [185.6 m] amsl).

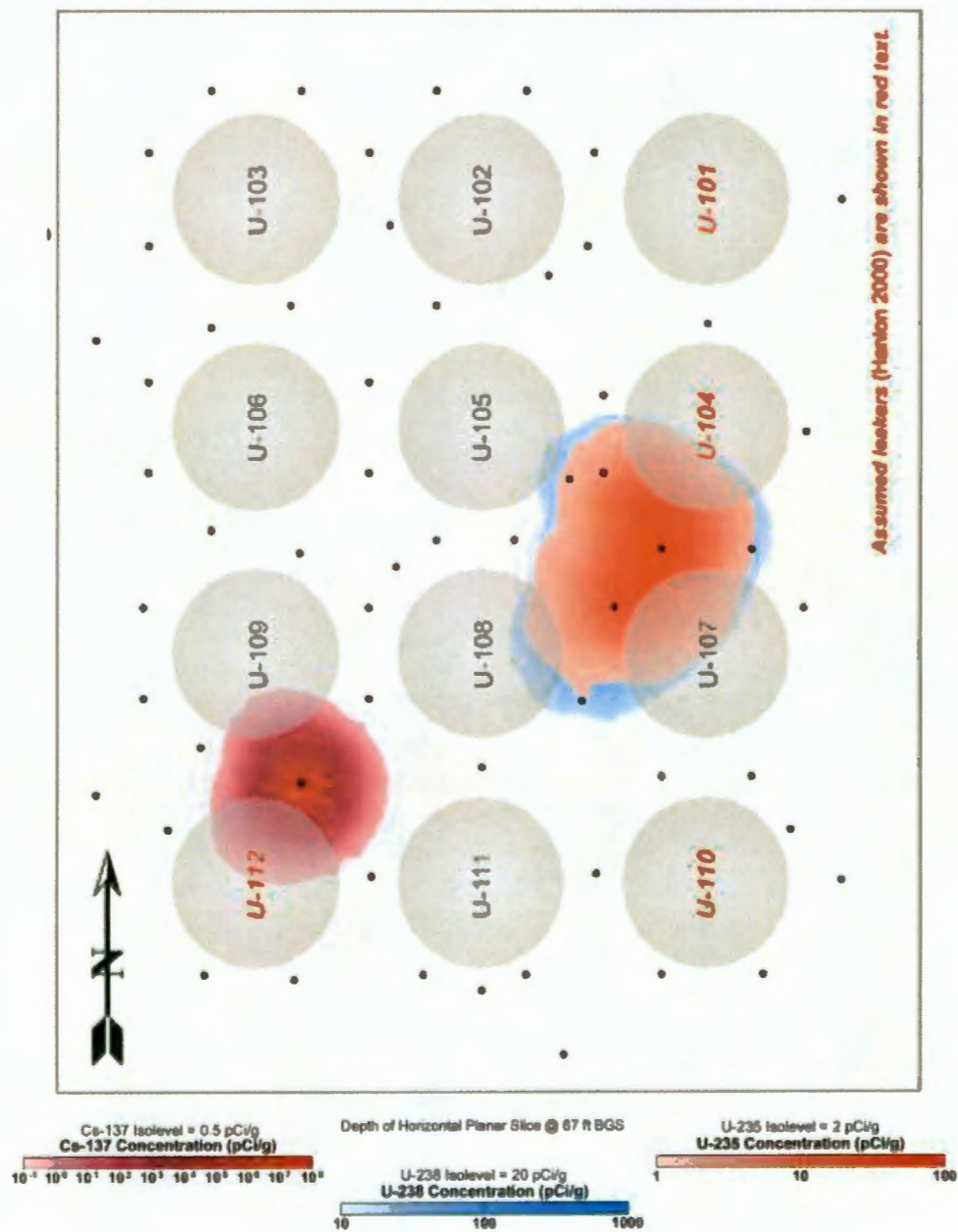


Figure 11. Visual Interpretation of Drywell Logging Activity at 88 ft (26.8 m) bgs (587.9 ft [179.2 m] amsl).

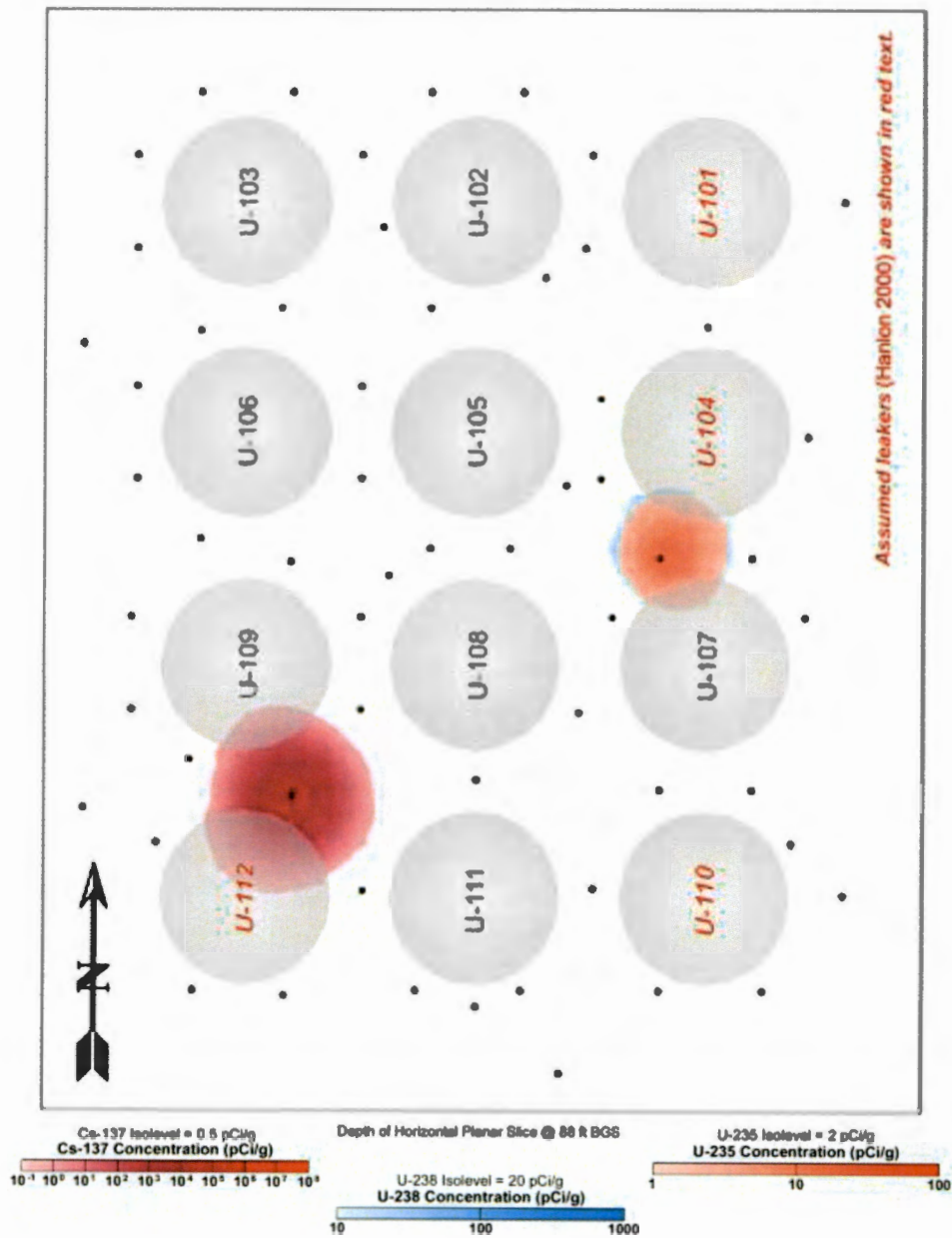
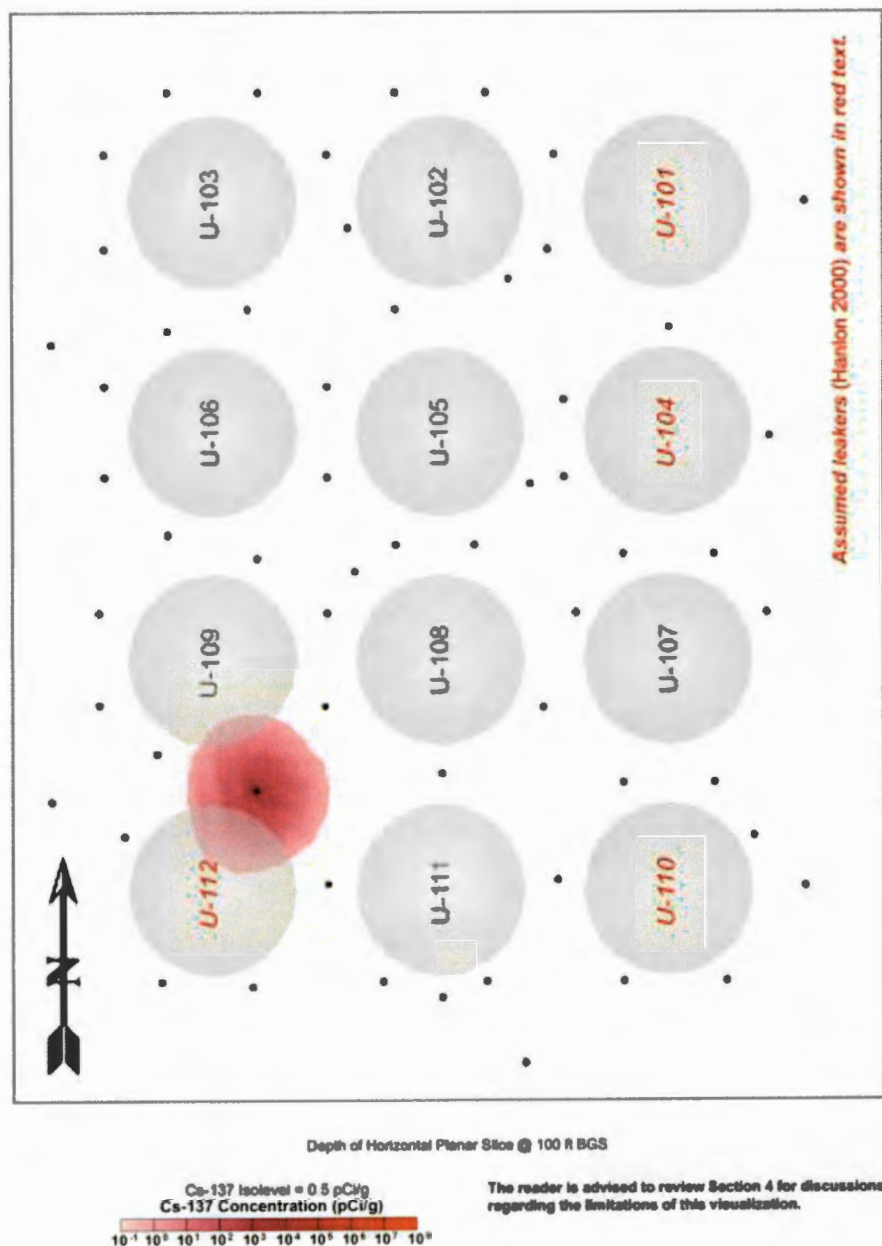


Figure 12. Visual Interpretation of Drywell Logging Activity at 100 ft (30.5 m) bgs (575.9 ft [175.5 m] amsl).



2.3.2 Direct Push Sampling

Direct push probe holes were completed at U Tank Farm in 2007 to install resistivity electrodes at depth and to obtain soil sediment samples for later geochemical analysis (RPP-35968). The results of these geochemical analyses are found in PNNL-17163, *Characterization of Direct Push Vadose Zone Sediments from the 241-U Single-Shell Tank Farm*.

A total of 20 direct pushes were driven at 10 locations within the U Tank Farm for moisture and gamma logging, and to retrieve samples for later testing. For comparison purposes, background samples from outside the tank farm were also taken for analysis. With respect to contamination due to tank-related waste, the most significant findings came from direct pushes in the vicinity of tanks U-104 and U-105. Lesser amounts of tank-related waste were detected near tanks U-110 and U-112.

Background samples were taken down to a depth of 144 ft (43.9 m) bgs (531.8 ft [162.1 m] amsl), penetrating the Hanford formation (units H1 and H2) and the upper sub-unit of the Cold Creek formation (CCU). Sampling results for moisture and gamma found the following:

- Average moisture contents ranging from around 4 wt% in the H1 and H2 units, and around 16 wt% in the Cold Creek formation
- No anthropogenic elements that produce gamma radioactivity.

Direct push samples were retrieved down to approximately 100 ft (30.5 m) bgs (575.8 ft [175.5 m] amsl). All samples contained moisture contents within the range of the background samples. The highest moisture contents measured from direct push samples was 19.8 wt%, whereas the highest background measurement was 18.3 wt%. In fact, the report concludes that “no correlation can be made between moisture content and the potential presences of tank waste in the sediment.” Push holes near tanks U-104 and U-105 detected trace activities of uranium, consistent with the drywell gamma logging results, and technetium-99 down to a depth of at least 92 ft (28.0 m) bgs (584 ft [178 m] amsl). Samples near tank U-110 showed indications of a high sodium-bearing waste stream, with elevated concentrations of technetium-99 and nitrates down to a depth of 98 ft (29.9 m) bgs (577.8 ft [176.1 m] amsl). Two samples from near tank U-112 contained trace amounts of uranium. Because contamination was detected in several of the deepest samples, the vertical extent of contamination cannot be derived from the direct push sampling results.

Further detail on the sampling results can be found in PNNL-17163.

3.0 DATA ACQUISITION AND PROCESSING METHODOLOGY

Data acquisition for a 3D and 2D electrical resistivity survey at the U Tank Farm began on May 16, 2013 and was completed on June 28, 2013. The geophysical survey was initiated to collect data on surface electrodes; electrodes buried beneath the surface (i.e., depth electrodes); and wells (i.e., long electrodes).

Data collection activities, equipment, and data processing are described in the following sections.

3.1 SURVEY DESIGN

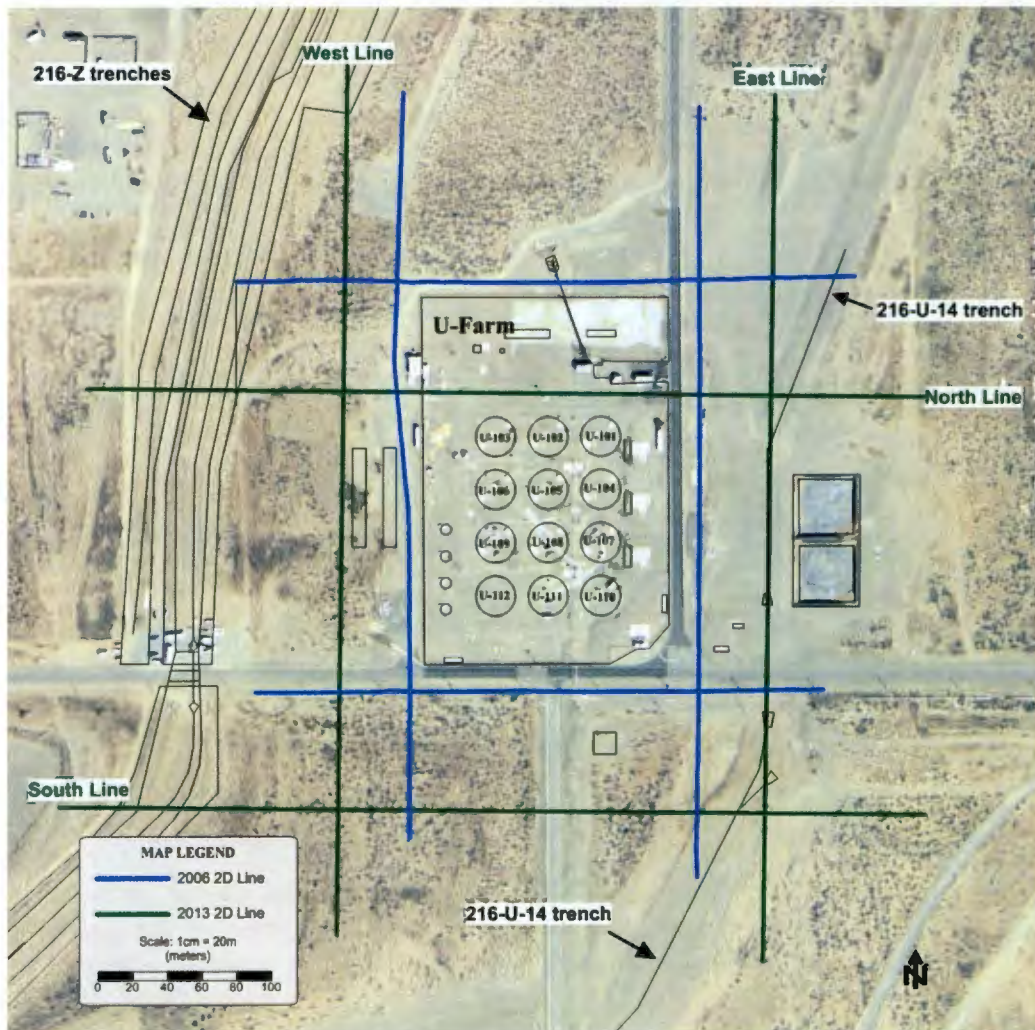
In FY2006 an SGE survey was completed in U Tank Farm, with both 2D and well-to-well (WTW) electrical resistivity surveys being completed. Prior to the FY2013 survey, an updated review of the 2D electrical resistivity data acquired in FY2006 was completed by reprocessing three of the four 2D survey lines, taking advantage of recent advances in inversion software. Results of this review and reprocessing were used to optimize the field efforts for the FY2013

2D survey. Details on the reanalysis can be found in RPP-RPT-54500. The FY2013 2D electrical resistivity survey complements the FY2006 2D results obtained, while the 3D electrical resistivity survey augments the FY2006 WTW survey.

3.1.1 2D Survey

A 2D electrical resistivity survey consisting of four survey lines was performed at U Tank Farm. Three of the survey lines (East, South, and West lines) were located entirely outside the perimeter fence of U Tank Farm, while the North line ran partially through the northern section of U Tank Farm (Figure 13). The four survey lines were approximately 1,640 ft (500 m) in length and were positioned to complement the four survey lines acquired in FY2006 (shown in blue, Figure 13) and support continued characterization of subsurface conditions outside the U Tank Farm perimeter fence. The body of this report focuses on the 3D electrical resistivity results; the 2D results are presented in Appendix A.

Figure 13. Map of 2D Resistivity Survey Coverage for FY2006 (Blue) and FY2013 (Green).



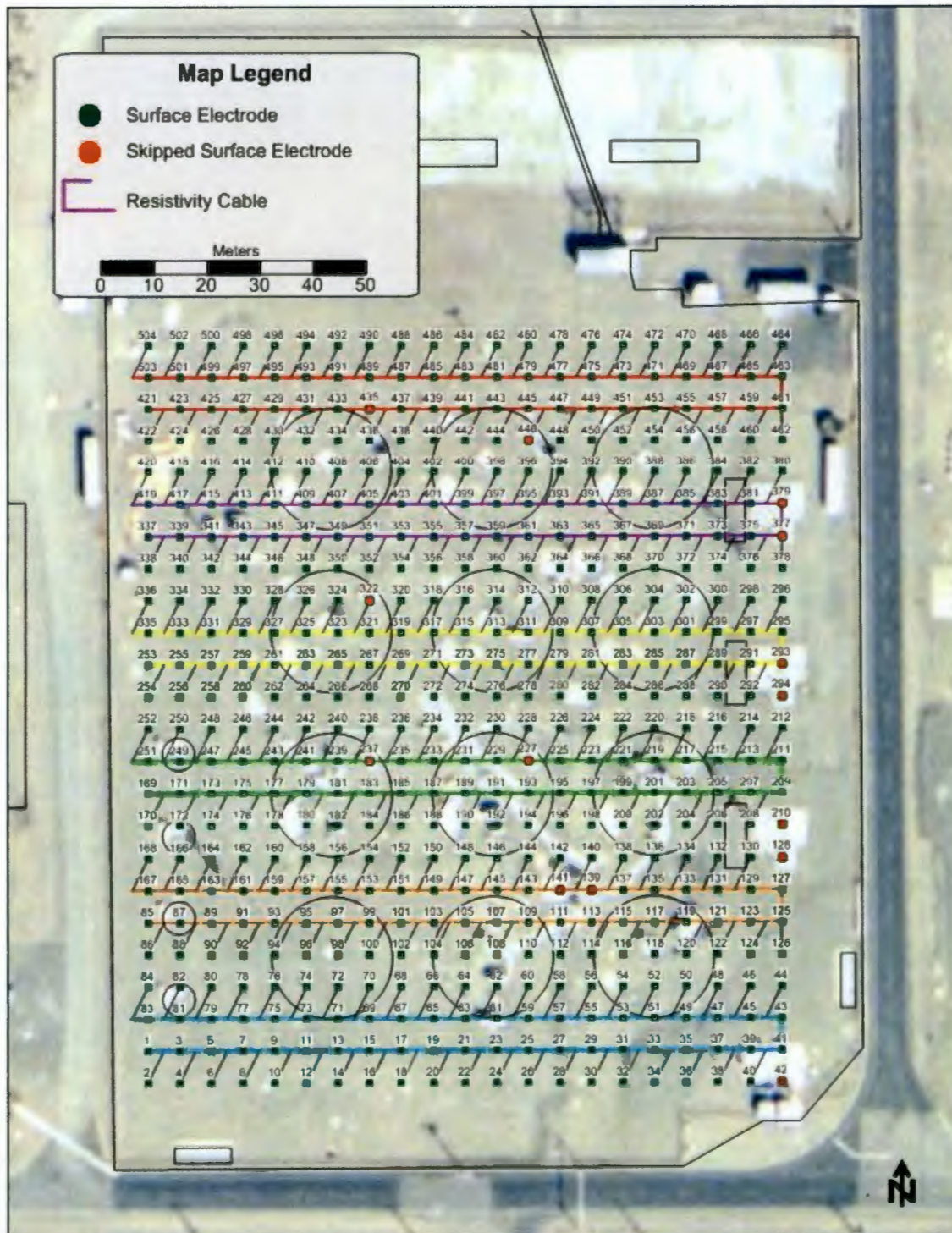
Electrode spacing along the survey lines was 9.8 ft (3 m). An optimized measurement set was used where the 9.8 ft (3 m) electrode spacing was collected for near-surface measurements and a coarser 19.7 ft (6 meter) spacing was used for deeper measurements. The finer electrode spacing increased the subsurface resolution and data density in the near-surface compared to the original FY2006 2D electrical resistivity survey.

3.1.2 3D Survey

The 3D electrical resistivity data were collected on surface electrodes, depth electrodes, and wells within the U Tank Farm perimeter fence. Data were collected based on a 3D data acquisition method that utilized numerous different electrode arrangements. The surface electrodes were distributed across a uniform grid to optimize the numerical inversion models used in the data analysis and interpretation. The significantly larger amounts of data associated with a 3D survey, relative to a 2D survey, makes an optimized geometry crucial to reduce modeling run times and analysis. For the 3D U Tank Farm survey, 490 surface electrodes were distributed across a grid, with dimensions 452.8 ft by 393.7 ft (138 m by 120 m) and electrodes spaced nominally every 19.7 ft (6 m) in the east-west and north-south directions. Some positions within this grid were skipped based on proximity to buried near-surface infrastructure or surface obstructions. Figure 14 shows the layout of the surface electrodes with associated resistivity and jumper cables.

To minimize interference, the 3D grid of surface electrodes was positioned to avoid dense clusters of above ground and near-surface infrastructure based on the results from field observations and the FY2013 ground penetrating radar (GPR) survey. The GPR survey was designed specifically to map the subsurface infrastructure in support of this resistivity survey (RPT-2013-004, *Summary of U-farm Site Clearance Survey*).

Figure 14. Resistivity Cable and Surface Electrode Layout.



Further resolution improvements are possible by adding depth electrodes to a surface electrode geometry, whereby electrical current and voltage measurements can be made near or within a target in the subsurface. Depth electrodes have the added benefit of being further from near-surface infrastructure and associated electrical interference and noise. For the U Tank Farm 3D electrical resistivity survey, 10 boreholes with single depth electrodes were incorporated into the survey. The location of the depth electrode did not necessarily align to the surface electrode grid. Table 1 displays the locations and depths associated with each depth electrode for the current survey per RPP-35968, *Completion Report for U Tank Farm Hydraulic Rotary Hammer Direct Push Drilling, Probe Installation and Sampling*.

**Table 1. Locations for Depth Electrodes in 241-U Tank Farm
(in Washington State Plane, m, NAD83).**

| Borehole ID | Easting | Northing | Depth (m) | Elevation (m) | Depth (ft) | Elevation (ft) |
|-------------|---------|----------|-----------|---------------|------------|----------------|
| C5589 | 566839 | 135121 | 29 | 177 | 95 | 580.8 |
| C5591 | 566858 | 135113 | 29 | 177 | 95 | 580.8 |
| C5593 | 566864 | 135080 | 29 | 177 | 95 | 580.8 |
| C5595 | 566816 | 135091 | 29 | 177 | 95 | 580.8 |
| C5597 | 566799 | 135081 | 29 | 177 | 95 | 580.8 |
| C5599 | 566799 | 135061 | 29 | 177 | 95 | 580.8 |
| C5601 | 566822 | 135065 | 29 | 177 | 95 | 580.8 |
| C5603 | 566753 | 135062 | 29 | 177 | 95 | 580.8 |
| C5605 | 566794 | 135020 | 29 | 177 | 95 | 580.8 |
| C5607 | 566840 | 134998 | 29 | 177 | 95 | 580.8 |

Fifty four vadose zone dry wells within the U Tank Farm perimeter fence were used as 'long electrodes' in the 3D data acquisition; this method has been used in past survey designs to improve data quality in areas of increased buried infrastructure. Recent advances in inversion software allow for the simultaneous processing of point source electrodes (surface and depth electrodes) and linear electrodes (wells). Table 2 lists the dry wells used in the survey design.

**Table 2. Well Locations in 241-U Tank Farm (in Washington State
Plane, m, NAD83). (3 sheets)**

| Well Name | Tank Farm | Easting (m) | Northing (m) | Elevation (m) | Casing Length (ft) |
|-----------|-----------|-------------|--------------|---------------|--------------------|
| 60-00-02 | U | 566860 | 135104 | 206.271 | 154 |
| 60-00-11 | U | 566800 | 135123 | 203.846 | 131 |
| 60-01-08 | U | 566826 | 135098 | 204.218 | 125 |
| 60-01-10 | U | 566826 | 135109 | 204.07 | 102 |
| 60-02-01 | U | 566817 | 135118 | 203.968 | 102 |
| 60-02-05 | U | 566821 | 135093 | 204.095 | 102 |
| 60-02-07 | U | 566805 | 135089 | 204.082 | 125 |
| 60-02-08 | U | 566799 | 135100 | 203.863 | 98 |
| 60-02-10 | U | 566796 | 135109 | 203.77 | 125 |

Table 2. Well Locations in 241-U Tank Farm (in Washington State Plane, m, NAD83). (3 sheets)

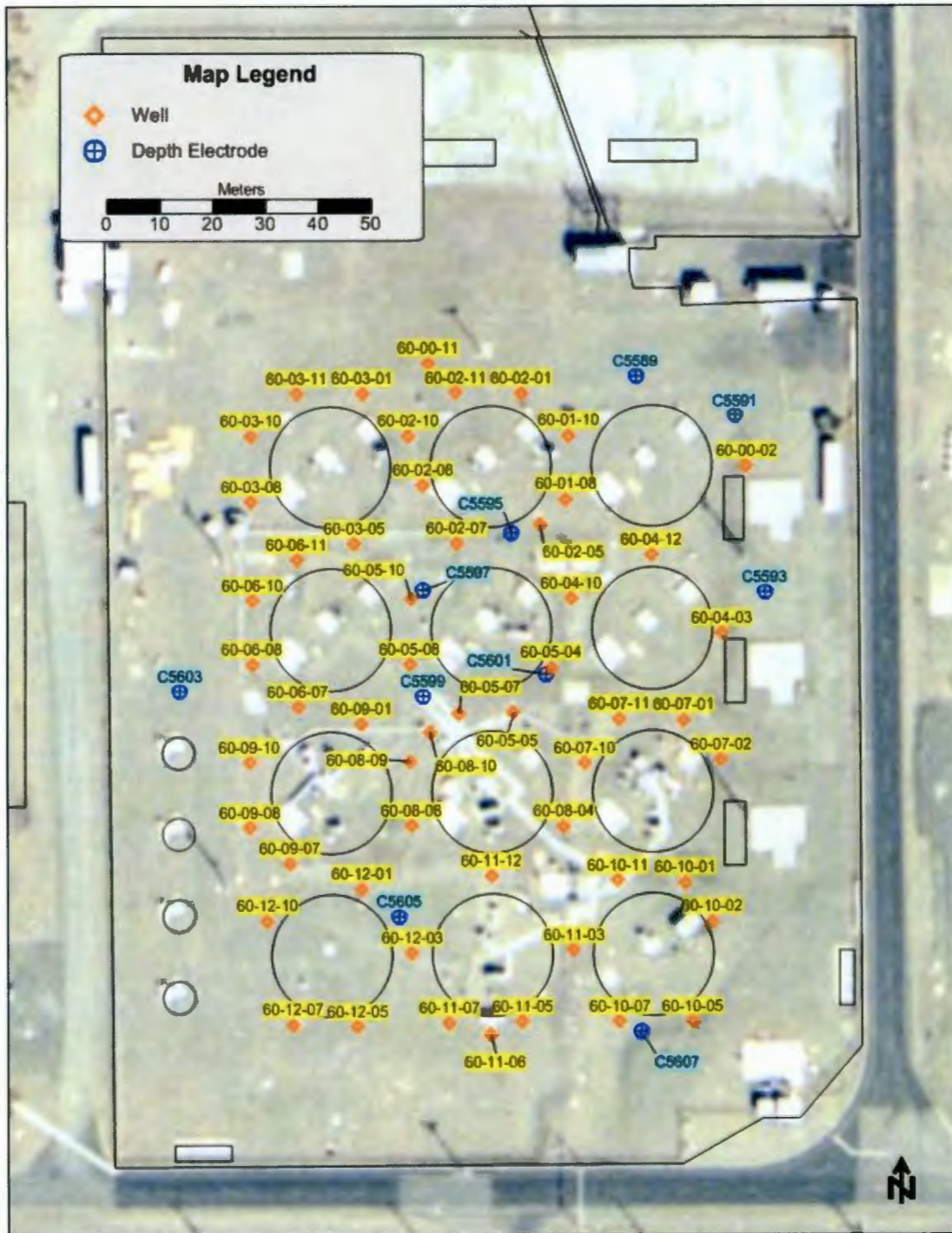
| Well Name | Tank Farm | Easting (m) | Northing (m) | Elevation (m) | Casing Length (ft) |
|------------------|------------------|--------------------|---------------------|----------------------|---------------------------|
| 60-02-11 | U | 566805 | 135118 | 203.84 | 131 |
| 60-03-01 | U | 566787 | 135118 | 203.676 | 98 |
| 60-03-05 | U | 566786 | 135089 | 203.83 | 125 |
| 60-03-08 | U | 566766 | 135097 | 203.601 | 128 |
| 60-03-10 | U | 566766 | 135109 | 203.489 | 102 |
| 60-03-11 | U | 566775 | 135117 | 203.525 | 125 |
| 60-04-03 | U | 566855 | 135072 | 204.967 | 125 |
| 60-04-10 | U | 566827 | 135079 | 204.822 | 118 |
| 60-04-12 | U | 566842 | 135087 | 204.376 | 125 |
| 60-05-04 | U | 566823 | 135066 | 204.015 | 72 |
| 60-05-05 | U | 566816 | 135058 | 204.14 | 125 |
| 60-05-07 | U | 566806 | 135058 | 203.788 | 125 |
| 60-05-08 | U | 566796 | 135067 | 203.707 | 125 |
| 60-05-10 | U | 566797 | 135079 | 203.696 | 102 |
| 60-06-07 | U | 566775 | 135059 | 203.531 | 125 |
| 60-06-08 | U | 566766 | 135067 | 203.628 | 125 |
| 60-06-10 | U | 566766 | 135079 | 203.602 | 125 |
| 60-06-11 | U | 566775 | 135086 | 203.703 | 98 |
| 60-07-01 | U | 566848 | 135056 | 204.32 | 98 |
| 60-07-02 | U | 566855 | 135049 | 204.836 | 128 |
| 60-07-10 | U | 566829 | 135048 | 204.365 | 98 |
| 60-07-11 | U | 566836 | 135056 | 204.454 | 125 |
| 60-08-04 | U | 566825 | 135036 | 204.776 | 128 |
| 60-08-08 | U | 566797 | 135037 | 203.855 | 98 |
| 60-08-09 | U | 566796 | 135049 | 203.682 | 125 |
| 60-08-10 | U | 566800 | 135054 | 203.753 | 144 |
| 60-09-01 | U | 566787 | 135056 | 203.621 | 98 |
| 60-09-07 | U | 566773 | 135030 | 203.584 | 98 |
| 60-09-08 | U | 566766 | 135036 | 203.555 | 118 |
| 60-09-10 | U | 566766 | 135048 | 203.433 | 125 |
| 60-10-01 | U | 566848 | 135026 | 205.024 | 125 |
| 60-10-02 | U | 566853 | 135018 | 205.018 | 98 |
| 60-10-05 | U | 566850 | 135000 | 204.523 | 125 |
| 60-10-07 | U | 566836 | 135000 | 204.348 | 121 |
| 60-10-11 | U | 566836 | 135026 | 204.848 | 98 |
| 60-11-03 | U | 566827 | 135013 | 204.95 | 125 |
| 60-11-05 | U | 566818 | 135000 | 204.106 | 125 |

Table 2. Well Locations in 241-U Tank Farm (in Washington State Plane, m, NAD83). (3 sheets)

| Well Name | Tank Farm | Easting (m) | Northing (m) | Elevation (m) | Casing Length (ft) |
|------------------|------------------|--------------------|---------------------|----------------------|---------------------------|
| 60-11-06 | U | 566812 | 134998 | 204.082 | 125 |
| 60-11-07 | U | 566804 | 135000 | 203.984 | 125 |
| 60-11-12 | U | 566812 | 135027 | 204.406 | 125 |
| 60-12-01 | U | 566787 | 135025 | 203.675 | 125 |
| 60-12-03 | U | 566797 | 135013 | 203.769 | 125 |
| 60-12-05 | U | 566786 | 134999 | 203.794 | 98 |
| 60-12-07 | U | 566774 | 134999 | 203.59 | 102 |
| 60-12-10 | U | 566769 | 135019 | 203.511 | 98 |

Figure 15 shows the distribution of wells and depth electrodes within the 3D survey area.

Figure 15. 3D Survey Depth Electrode and Well Distribution.



3.2 EQUIPMENT

3.2.1 Electrode and Cable Layout

The first stage of the project was to assemble all available infrastructure maps for the U Tank Farm area. The resulting maps were combined into an AutoCAD® drawing and subsequently used to define the coordinates for electrode placement. The maps containing infrastructure locations, including subsurface pipes/structures and surface structures, were digitized and combined with the electrode locations. These maps were supplemented with infrastructure interpretation results obtained from the FY2013 GPR survey. Electrode locations were then modified to avoid being directly over infrastructure where possible. Electrode placement was limited by maintaining a uniform 6-meter grid layout to support data processing procedures. The final electrode layout was then uploaded into a Leica® 1200 global positioning system (GPS) that was used to mark electrode locations on the ground surface. The Leica system has sub-centimeter accuracy, ensuring the survey geometry is retained.

The electrodes are connected to the resistivity acquisition systems by way of multi-cored cables. For the U Tank Farm 3D survey, a total of six cables were deployed; each cable allowing up to 84 electrodes to be connected. The cables were placed in a serpentine pattern, with jumpers connecting the stainless steel probe to the electrode cable. In some areas, the specific location of the cable was modified to accommodate the storage tanks. Extension cables were deployed from the survey area to the Geotecton™-180 data acquisition trailer, located as close to the cable layout as possible while being outside the tank farm perimeter fence. For the 2D survey, switch boxes (multiplexers), manufactured by Advanced Geosciences, Inc. (AGI), acted as junction boxes to connect the SuperSting R8 resistivity meter to the various electrode cables.

3.2.2 Geotecton™ 180 Resistivity Monitoring System (3D Resistivity)

For 3D resistivity data acquisition, the Geotecton-180 Resistivity Monitoring System, designed and fabricated by HGI, was used (Figure 17). The Geotecton system is Underwriter's Laboratories (UL)-compliant and is contained in a mobile trailer and powered by a 220 volt AC source (for this survey a portable generator was used as a power source).

The Geotecton-180 Resistivity Monitoring System has 180 channels, in comparison to the 8 channels available on the SuperSting R8 system, manufactured by AGI. This equates to a data collection rate that is 15 to 20 times faster than previous SGE projects using the SuperSting R8 system. In addition, because the Geotecton-180 Resistivity Monitoring System has a greater number of channels, the number of times the depth electrodes are transmitted on decreases significantly. On previous surveys it was possible to overuse the depth electrodes through continuous current transmission, which increased the contact resistance of the electrode by reducing the available moisture. The improved dynamic range allows the output electrical power to be reduced while still producing a usable signal, improving the lifespan of the historically poor performing depth electrodes.

3.2.3 SuperSting Resistivity Meter (2D Resistivity)

A SuperSting R8 resistivity meter, manufactured by AGI, was used for the 2D electrical resistivity data acquisition (Figure 16). The meter is capable of full eight-channel acquisition, whereby eight simultaneous measurements of voltage can be made during electrical current transmission. The SuperSting R8 resistivity meter has been used for many SGE projects and has proven to be reliable for short or long-term, continuous acquisition campaigns.

Figure 16. The SuperSting R8 resistivity meter (top) and Geotection™ -180 Resistivity Monitoring System (bottom).



3.2.4 Quality Assurance

Intensive quality assurance was completed before and after the survey to ensure the equipment was functioning appropriately and the quality of data was acceptable. Calibration requirements are described for hardware used to collect geophysical data in CEES-0360, *Surface Geophysical Exploration System Design Description*. As an example, the manufacturer (AGI) of the SuperSting R8 resistivity meter recommends a yearly calibration of internal calibration resistors. The calibration is performed at the manufacturer's facility and a certificate of calibration is provided. A copy of the calibration documentation, serial numbers, and expiration dates are maintained in project files.

Daily inspection of the receiver calibration was also performed onsite using the manufacturer-supplied calibration resistor test box. The supplied test box is connected to the Geotection-180 Resistivity Monitoring System or SuperSting R8 resistivity meter before commencing the daily

survey. A specific calibration test firmware is provided within the SuperSting R8 resistivity meter and provides the operator with a pass/fail indication for each of the eight receiver channels. For the Geotection-180 Resistivity Monitoring System, a specific calibration test sequence file is used to test all possible measurement combinations. The resulting data file is copied into a controlled spreadsheet that contains the known National Institute of Standards and Technology (NIST) resistance values. The sheet identifies if any of the channels fail, and if so, a recalibration or repair is required.

3.3 ACQUISITION METHODOLOGY

For the 2D electrical resistivity survey, data collection was initialized on May 16, 2013 and completed on May 23, 2013. The 3D electrical resistivity survey data collection occurred between June 10, 2013 and June 28, 2013. Data were collected approximately 8 hours a day. Personnel were maintained onsite at all times during acquisition to monitor data collection and to keep the cable area clear of vehicles and equipment that could damage cables and impact data quality.

Both forward and reverse data sets were collected during data acquisition in order to increase the resolution of the resistivity survey and evaluate data quality. Forward and reverse measurements are acquired by switching the transmitting and receiving electrodes to produce a reciprocal dataset. The two sets of data ensured that each electrode acted as both transmitter and receiver; both are needed for quality control. The theory of reciprocity implies that a homogeneous earth should allow for consistent measurements in both forward and reverse measurement conditions. Thus, by varying selected reciprocal percent difference thresholds, the ratio between data quality and quantity can be assessed. For this survey effort, data measurements with a relative percent difference greater than 3 percent (well-to-well combinations) or 5 percent (surface and depth electrode combinations) were considered unacceptable and removed from the dataset before numerical inverse modeling.

3.3.1 2D Acquisition

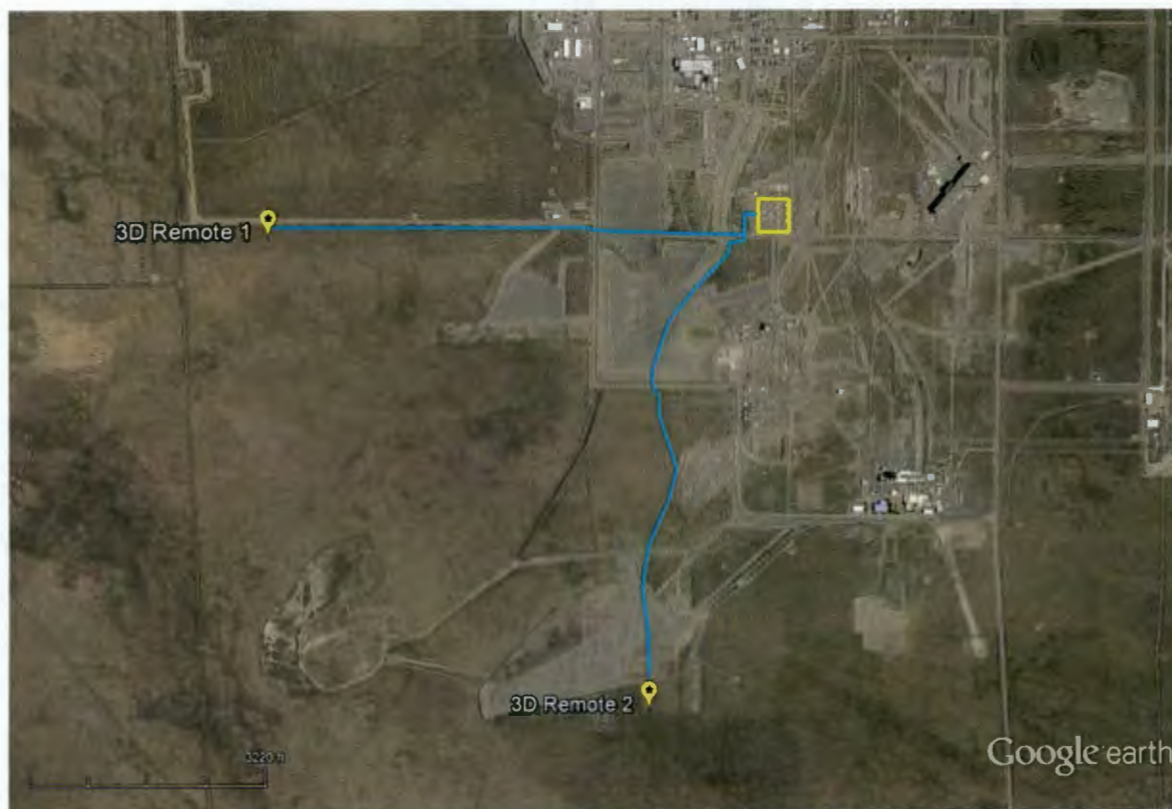
For the 2D electrical resistivity survey the Schlumberger array was selected, due to logistical considerations. The term “array” refers to a particular arrangement of four electrodes that are used to transmit current and receive the potential voltages. An electric field is established by applying electrical power (I) between two electrodes (transmitting pair or Tx). Electric potential (V) is measured by sampling received voltages using a data acquisition card connected to two additional electrodes (receiving pair or Rx). In the Schlumberger array the Tx dipole is located at a fixed location along the line while the Rx dipole expands outward, with increased dipole spacing, through a series of different pairs. For each pair a “transfer resistance” value (V/I) is obtained by dividing the electrical potential (V) by the applied electrical current (I). This process happens sequentially until all feasible locations along the line have been occupied by the Tx pair.

3.3.2 3D Acquisition

For the 3D electrical resistivity survey a pole-pole array was selected; where one electrode from each of the transmitting and receiving electrode pairs were placed effectively at infinity. Practically, these poles are placed remotely, anywhere from two to five times the maximum in

farm electrode distance away from the survey area in opposite directions. Figure 17 shows the locations of the remotes used in the FY2013 3D SGE project at U Tank Farm.

Figure 17. Remote Locations Used for the Pole-Pole Array.



Source: © 2013 Google.

3.4 DATA PROCESSING

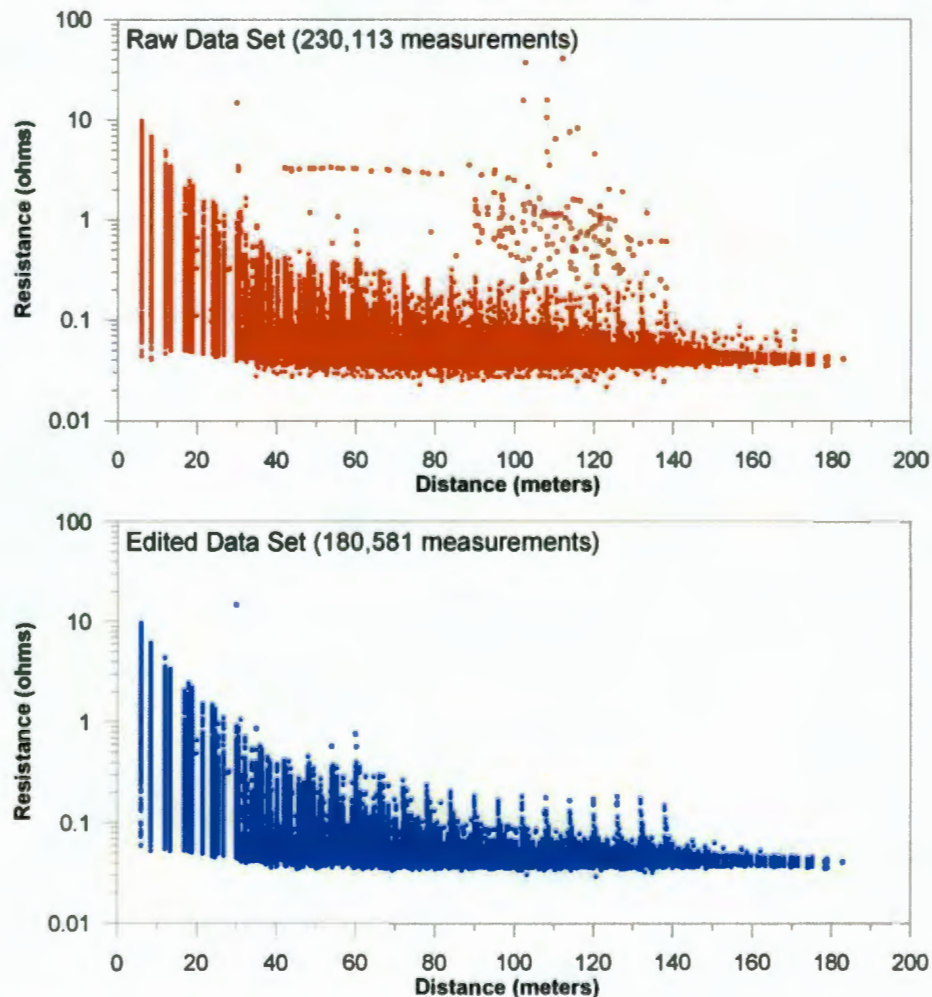
3.4.1 Data Reduction

All raw data collected at the site were compiled into a relational database. Raw data included both electrical resistivity data and GPS positional data to geo-reference the resistivity data. A set of queries was designed to segregate reciprocal pair data points. This information included electrode type (surface, depth, well) and a sequential electrode number (as designated in the survey design). Additional data fields were added for the calculated distance between electrodes and percent error between reciprocal data. The data were then exported from the database for graphical filtering and plotting in a spreadsheet.

Four important diagnostic data parameters from the raw data include voltage/current (V/I ; resistance), point (repeat) error, reciprocal error, and electrical current output. The point error is a calculated percent error between cycled/repeated measurements. A plot of these data can provide information with regards to the statistical variation of the data population.

The process of data reduction identifies and eliminates data points, but no data modification (rounding, averaging, smoothing, or splining) is permitted. The rationale is to seek out and remove spurious points that do not conform to the data population or points that violate potential theory. The first step in this reduction process was to remove data outside of the statistical population; negative V/I values, high repeat or point errors, low output current values, low measured voltage, and high contact resistance. The next step in data reduction was to apply a data quality filter based on reciprocity. Reciprocal measurements were used to assess the quality of the results. Secondary reciprocal measurements were generated for each initial data point by switching the transmitting and receiving electrodes. Electrical theory suggests that the measurements should be exactly the same. All data with a reciprocal percent difference greater than 3 percent was removed from the well-to-well dataset, and greater than 5 percent was removed for all other models. Figure 18 displays the 3D data distribution before and after filtering. The process used to filter the raw data is further described in CEES-0360.

Figure 18. Data Distribution for Raw (Combined Reciprocal) and Reduced V/I Data for the 3D Survey (Surface and Depth Electrode Data).



Data distribution for Raw (top) and Reduced (bottom) V/I data.
All are plotted against the distance between transmitting/receiving electrode pairs.

Table 3 and Table 4 display the percentages of data retained during steps of the reduction process.

Table 3. Number of Data Points Retained During Data Reduction Steps (Surface and Depth Electrode Data).

| | Forward | Reverse | Sum | Percent of Total |
|--|---------|---------|---------|------------------|
| Total Raw | 237,508 | 236,826 | 474,334 | 100 |
| Total Combined Reciprocal | 230,113 | 230,113 | 460,226 | 97.0 |
| Total Remaining (<5% Reciprocal Error) | 180,581 | 180,581 | 361,162 | 76.1 |

Table 4. Number of Data Points Retained During Data Reduction Steps (Well-to-Well Data).

| | Forward | Reverse | Sum | Percent of Total |
|--|---------|---------|-------|------------------|
| Total Raw | 2,862 | 2,862 | 5,724 | 100 |
| Total Combined Reciprocal | 2,862 | 2,862 | 5,724 | 100 |
| Total Remaining (<3% Reciprocal Error) | 2,746 | 2,746 | 5,492 | 95.9 |

3.4.2 Depth Electrode Performance

The U Tank Farm depth electrodes were installed in August 2007 and were part of the first generation of single depth electrodes to be installed within the tank farms. All of the boreholes were constructed in the same manner, with resistivity probes placed at a depth of 97 ft (29.6 m). The construction details are provided below (RPP-35968):

- Once logging was completed in a borehole, the drive tip was knocked out of the bottom of the tubing, and the tubing back pulled approximately 5 ft (1.52 m). The probe hole was filled with silica sand from bottom to the depth at which the resistivity probe was to be placed. The resistivity probe was placed and additional silica sand (approximately 5 ft [1.52 m]) was then added to the hole, encasing the probe in sand. Fifteen to 19 liters (4 to 5 gallons) of saline water were then added. Bentonite crumbles were then placed from the top of the silica sand to surface while pulling back the tubing. This was done with the remainder of the borehole to surface. A protective steel casing was cemented in place approximately 12 inches (30.48 centimeters) deep to protect the protruding probe wiring.

A statistical performance analysis is performed on all depth electrode data to ensure only high quality data are included in the numerical inversion modeling. A benefit in using the HGI designed Geotection-180 Resistivity Monitoring System is that it provides unique recorded survey performance parameters that can be directly used in the analysis. The performance from

the different types of electrodes was explored through output current, point error, reciprocal error, and contact resistance. Table 5 lists the summary statistics from each of the electrodes. Four of the ten depth electrodes were deemed unacceptable for inclusion in the 3D inversion models based on the performance parameters in Table 5, these electrodes are highlighted in red. Each of these underperforming depth electrodes displayed low current output, accompanied with high contact resistance, resulting in high point (repeat) error. While the remaining six depth electrodes performed well based on this performance analysis, they were omitted from the inversion model as they fell outside the acceptable ranged during the data reduction phase (based on V/I versus distance statistical population).

Table 5. Depth Electrode Performance Measure for U Tank Farm.

| Electrode Name | Median Transmitting Current (mA) | Median Point Error (%) | Median Reciprocal Error (% difference) | Median Contact Resistance | Percentage of Data Below 5% Error Cutoff |
|----------------|----------------------------------|------------------------|--|---------------------------|--|
| C5589 | 39 | 1915.25 | 23.63 | 5896 | 32 |
| C5591 | 66 | 242.63 | 3.10 | 3519 | 65 |
| C5593 | 229 | 16.97 | 1.14 | 1000 | 87 |
| C5595 | 304 | 8.54 | 0.98 | 753 | 87 |
| C5597 | 91 | 131.76 | 3.12 | 2554 | 57 |
| C5599 | 651 | 3.77 | 0.88 | 352 | 88 |
| C5601 | 460 | 3.31 | 1.16 | 497 | 82 |
| C5603 | 74 | 168.23 | 2.57 | 3090 | 81 |
| C5605 | 908 | 1.21 | 1.01 | 250 | 81 |
| C5607 | 283 | 8.92 | 0.69 | 795 | 88 |

Note: Poorly performing depth electrodes are highlighted in red.

3.4.3 Inverse Modeling

Popular use of the RES3DINV and RES2DINV series (Geotomo Software, Malaysia) of resistivity inversion codes has led both professional and academic users to regard these codes as industry standard software. The software has been used in peer reviewed papers and extensively validated by HGI. The U Tank Farm modeling effort used RES2DINV for the 2D resistivity lines and RES3DINVx64, a 64-bit multi-threaded version developed specifically for a large number of electrodes, for the full tank farm resistivity survey.

In general, inverse modeling can be summarized in the following five steps.

1. The study site's voltage data has been measured and is discretized into grid nodes using a finite difference or finite element mesh. The meshing parameters used in either case, to design the computational grids, are dependent on electrode spacing used in site-specific data acquisition.
2. The inversion will set out to estimate the true resistivity at every grid node. An initial estimate of the subsurface properties is made based on the literal translation of the pseudo-section to a true resistivity, a constant value, or some other distribution from *a priori* information. A forward model run with these initial estimates is made to obtain

the distribution of voltages in the subsurface. The root-mean-square (RMS) error is calculated between the measured voltage and the calculated voltage resulting from the forward run.

3. Based on the degree of model fit to field measurements, the initial estimate of resistivity is changed to improve the overall model fit and the forward model with the updated estimates is rerun. The iterative method linearizes a highly nonlinear problem using Newton's method. Using this method, the inverse modeling code essentially solves the linearized problem to obtain the change in modeled resistivity (Δm) for the next iteration.
4. The resistivity model is updated using the general formula $m_{i+1} = m_i + \Delta m$, where m_{i+1} is the resistivity in a model cell at the next iteration, and m_i is the current value.
5. Steps 3 and 4 are repeated until the RMS error change between successive iterations reaches an acceptable level.

A-priori modeling of the major infrastructure reduces the effect of infrastructure, resulting in sufficient data quantity for inverse modeling of subsurface soil resistivity changes.

4.0 MODELING RESULTS

Upon completion of data filtering, measured apparent resistivity data from the U Tank Farm site were inverse modeled using the RES2DINV and RES3DINVx64 software packages (Geotomo Software, Malaysia). For specific details of the SGE electrical resistivity method and theoretical basis applied to inverse modeling, the reader is referred to discussions provided in RPP-34690, *Surface Geophysical Exploration of the B, BX, and BY Tank Farms at the Hanford Site*.

To accomplish the 2D and 3D inversion, every surface, depth, and long electrode was geo-referenced (using the Washington State Plane – Meters coordinate system) to allow absolute placement of an electrode within the inversion algorithm. The model was then run with a set of input parameters that have been demonstrated to work well in tank farm environments. After inversion, the final inversion results were interpolated to a regular grid and visualized using the Rock Works™ visualization software package (3D) and Surfer® surface contouring package (2D and 3D). The visualization allows discrimination of low resistivity targets that could be associated with increased moisture, increased ionic strength of the pore water, infrastructure, or a combination of these items. It is anticipated that mineralogy and porosity would have minimal effects on the resistivity outcome.

Two sets of 3D model results are presented below that include (1) using point electrodes on the surface and depth electrodes within boreholes, and (2) long electrodes in a WTW inversion.

4.1 2D ELECTRICAL RESISTIVITY SURVEY RESULTS

This section presents the inversion model results for the eight 2D electrical resistivity lines collected during the FY2006 and FY2013 SGE surveys (Figure 13). Four orthogonal lines were collected for each survey year; with the exception of the North line, the FY2013 lines were located a greater distance from U Tank Farm. In contrast, the FY2013 North line was located to the south of the equivalent FY2006 line, with a section running through U Tank Farm. The four

FY2013 survey lines were acquired to support continued characterization of subsurface conditions outside the U Tank Farm perimeter fence.

Data acquisition and inversion modeling details are previously described in Section 3.0; a summary of the inversion modeling results are provided in Table 6. A constant color scale is presented, and uses warmer hues to represent more resistive regions and cooler hues to represent less resistive regions. The color scale range was chosen to be similar to that used for previous SGE projects from differing areas at the Hanford Site.

Table 6. Model Resistivity Values from the Inversion Output for the RES2DINV Code for the FY2006 and FY2013 Surveys.

| Line | Survey Year | Inversion Model Resistivity (Ωm) | | |
|-------|-------------|--|---------|---------|
| | | Minimum | Maximum | Average |
| North | 2006 | 6.65 | 5,665 | 163.61 |
| North | 2013 | 1.30 | 6,779 | 442.38 |
| East | 2006 | 2.17 | 1,496 | 67.83 |
| East | 2013 | 0.15 | 9,681 | 733.60 |
| South | 2013 | 5.04 | 8,228 | 701.04 |
| West | 2006 | 3.36 | 2,796 | 143.52 |
| West | 2013 | 4.1 | 3,867 | 578.89 |

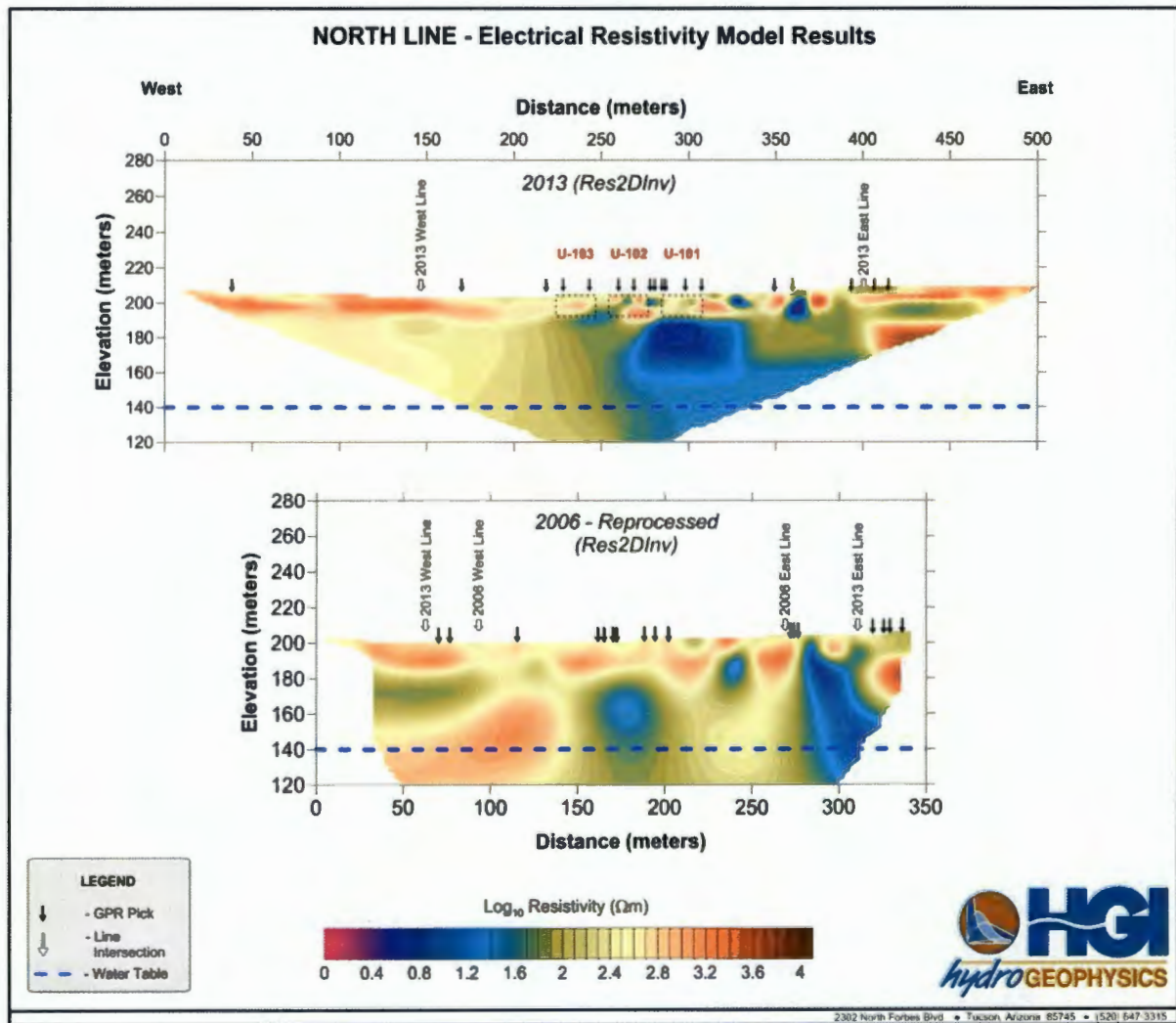
The inverse model results are shown in Figure 25 (North Line), Figure 26 (East Line), Figure 27 (South Line), and Figure 28 (West Line) in the following sections.

4.1.1 North Survey Lines

The inversion model results for the North line surveys are shown in Figure 19, the FY2006 survey line is offset to align with the FY2013 survey line. Picks from the GPR site clearance survey are included for both lines.

The model results for the North line generally displays a resistive near-surface layer, ranging between 33 and 66 ft (10 and 20 m) in thickness. A number of conductive targets are present in this near-surface layer, some of which can potentially be traced across the two survey lines. The conductive targets which potential span both lines are located at; 787 and 1076 ft (240 and 328 m) along the line for the FY2006 and FY2013 surveys respectively, 935 and 1194 ft (285 and 364 m) along the line for the FY2006 and FY2013 surveys respectively, and 1020 and 1266 ft (311 and 386 m) along the line for the FY2006 and FY2013 surveys respectively.

Figure 19. North Line 2D Model Surface Resistivity Results for the FY2013 (Top) and FY2006 (Bottom) Surveys.



The latter two targets, located to the east of the tank farm perimeter fence, are associated with GPR picks and could represent near-surface infrastructure running approximately perpendicular to the lines. The conductive target at 935 ft (285 m) along the FY2006 survey line appears to extend to the base of the model. The potential equivalent FY2013 target appears as an isolated bull's-eye response, possibly resulting from the different array type and electrode spacing improving the resolution in the near-surface. In addition, the near-surface infrastructure might be denser or more interconnected in the FY2006 survey line location leading to significantly larger responses in the resistivity. The conductive target located at 1076 ft (328 m) along the FY2013 survey line is located inside the tank farm, just to the north of where GPR surveying was performed, and so could potentially still represent near-surface infrastructure. The same is true for the conductive target at 787 ft (240 m) along the FY2006 survey line, where again no GPR collection was possible. There are a number of similar additional conductive targets present in

the FY2013 survey line between 820 and 984 ft (250 and 300 m) along the line that potentially represent near-surface infrastructure within the tank farm. These targets do not present conductive responses in similar locations on the FY2006 survey line.

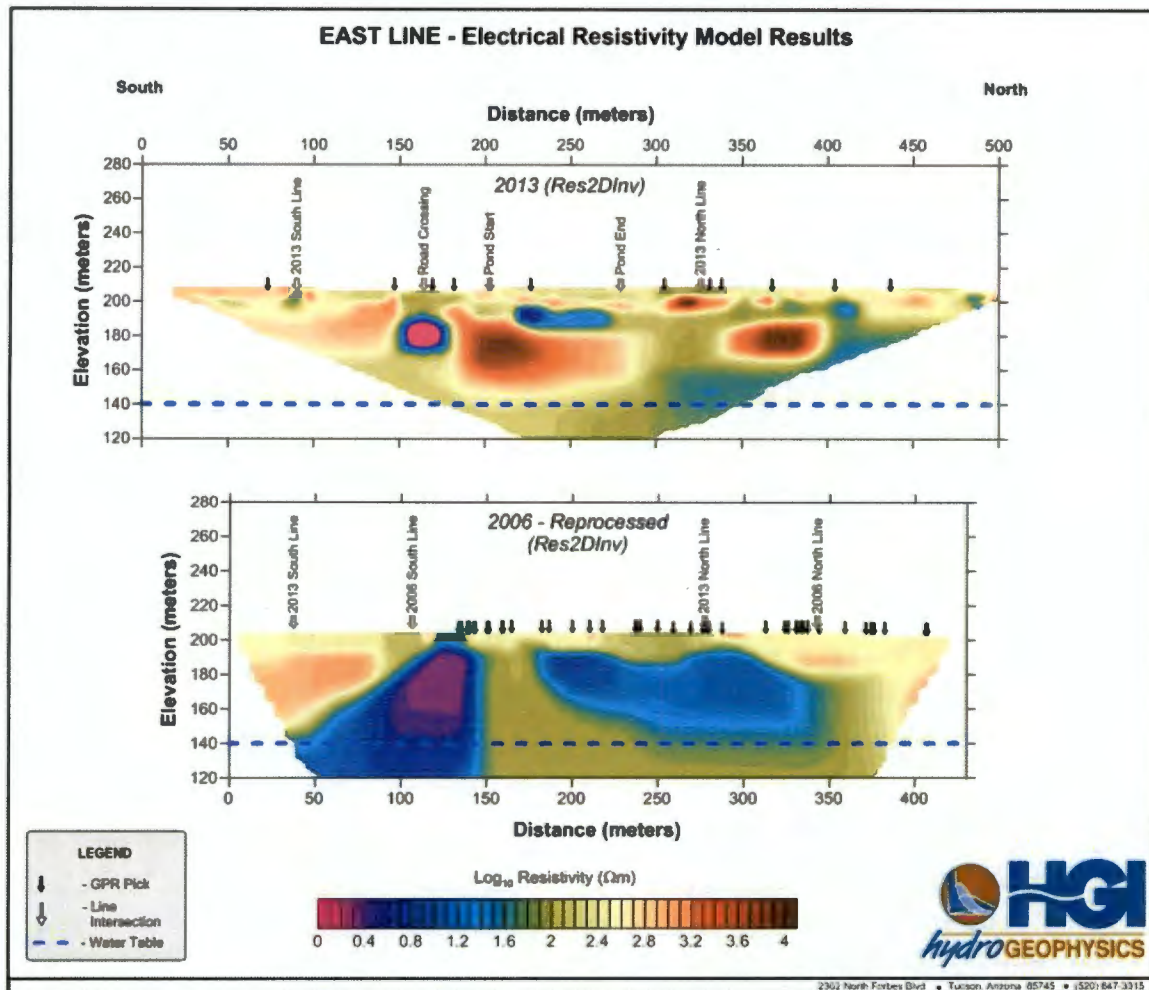
A large conductive target at depth is present in each of the survey lines, located at approximately 591 and 968 ft (180 and 295 m) along the line for the FY2006 and FY2013 surveys respectively. The FY2006 survey line target is located at a depth of approximately 98 ft (30 m) bgs (577.4 ft [176 m] amsl), and appears to extend down to the groundwater table. The location along the line for this target correlates well to the position of the French drain on the as built computer-aided design (CAD) drawings for U Tank Farm. Potentially, this target could reflect the increased soil moisture and ionic concentrations resulting from releases to this drain from the associated building septic system. The FY2013 survey line target appears more conductive, is located between a depth of approximately 59 and 131 ft (18 and 40 m) bgs (between 616.8 and 544.6 ft [188 and 166 m] amsl). This target again appears to extend to the groundwater table, although the conductivity decreases and the target appears more diffuse (most likely a result of the decreasing resolution with depth). The location along the line for this target correlates well to the building associated with the septic system from the previous conductive target in the FY2006 survey line. However, it is more likely, based on the line location on the northern edge of the 3D survey inversion model domain, to be a response to the conductive region below the storage tank level observed in the 3D modeling results. The depths of the target in the 2D line corresponds well to those observed in the 3D survey, namely between approximately 82 and 138 ft (25 and 42 m) bgs (between 593.8 and 538.1 ft [181 and 164 m] amsl).

4.1.2 East Survey Lines

The inversion model results for the East line surveys are shown in Figure 26, the FY2006 survey line is offset to align with the FY2013 survey line. Picks from the GPR site clearance survey are included for both lines.

The FY2013 model results display two obvious conductive targets, centered on 541 ft (165 m) and located between 722 and 902 ft (220 and 275 m) along the survey line respectively. These two targets aligned well with the location along the line and depth below surface of two conductive targets in the FY2006 survey line. The FY2006 targets are centered on 410 ft (125 m) and located between 591 and 738 ft (180 and 225 m) along the survey line. Both of these targets are associated with locations of significant amounts of infrastructure on the as-built CAD drawings, with the GPR picks confirming the presence of near-surface infrastructure. The depths of these targets, ranging between 23 and 49 ft (7 and 15 m) bgs (between 652.9 and 626.6 ft [199 and 191 m] amsl), appear deep for the majority of typical infrastructure. However, significant amounts of metallic infrastructure can interfere with electrical resistivity measurements, for example the pole-pole array results for the FY2006 survey display a broad target centered on 410 ft (125 m) along the survey line which extends to the depth limit of the model.

Figure 20. East Line 2D Model Surface Resistivity Results for the FY2013 (Top) and FY2006 (Bottom) Surveys.



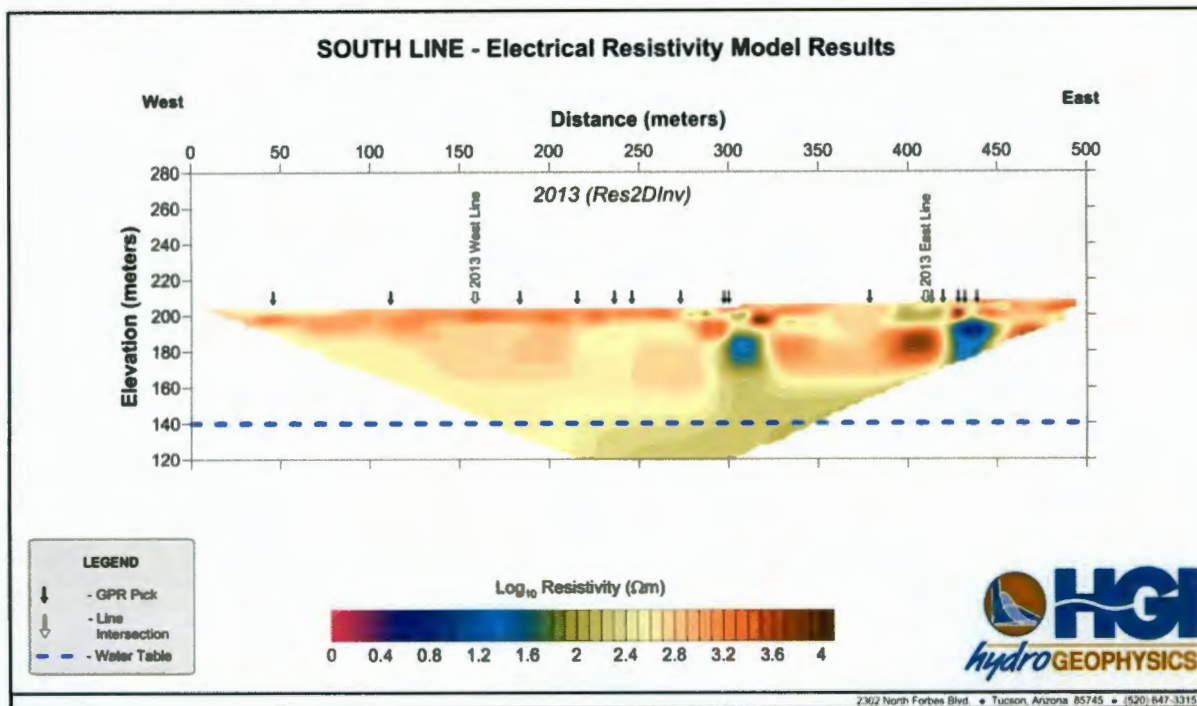
An additional conductive target is observed in the FY2006 survey line, located between 886 and 1066 ft (270 and 325 m) along the survey line at a depth similar to the target to the south. This target appears more diffuse than the previous two on this line, with lower conductivity values. The GPR results indicate a number of picks above this target, which could suggest a near-surface infrastructure response.

A number of smaller near-surface conductive targets are observed in the FY2013 survey line, located at approximately 295, 1247, 1345, and 1591 ft (90, 380, 410, and 485 m) along the line. These tend to be associated with GPR picks or locations on the as-built CAD corresponding to near-surface infrastructure.

4.1.3 South Survey Lines

The inversion model results for the South line survey are shown in Figure 21; only the FY2013 survey line is shown due to poor data quality in the FY2006 survey line. Picks from the GPR site clearance survey are included for the line.

Figure 21. South Line 2D Model Surface Resistivity Results for the FY2013 Survey.



The majority of the FY2013 survey line displays a fairly consistent structure, with a near-surface resistive layer, overlying a more homogenous layer which appears to become more conductive at depths coinciding with the groundwater table. A number of conductive targets are present, some are very near-surface, located at approximately 938, 1001, 1312, 1362, and 1427 ft (286, 305, 400, 415, and 435 m) along the survey line. These tend to be associated with GPR picks or features in the as-built CAD drawings indicating they are responses to near-surface infrastructure.

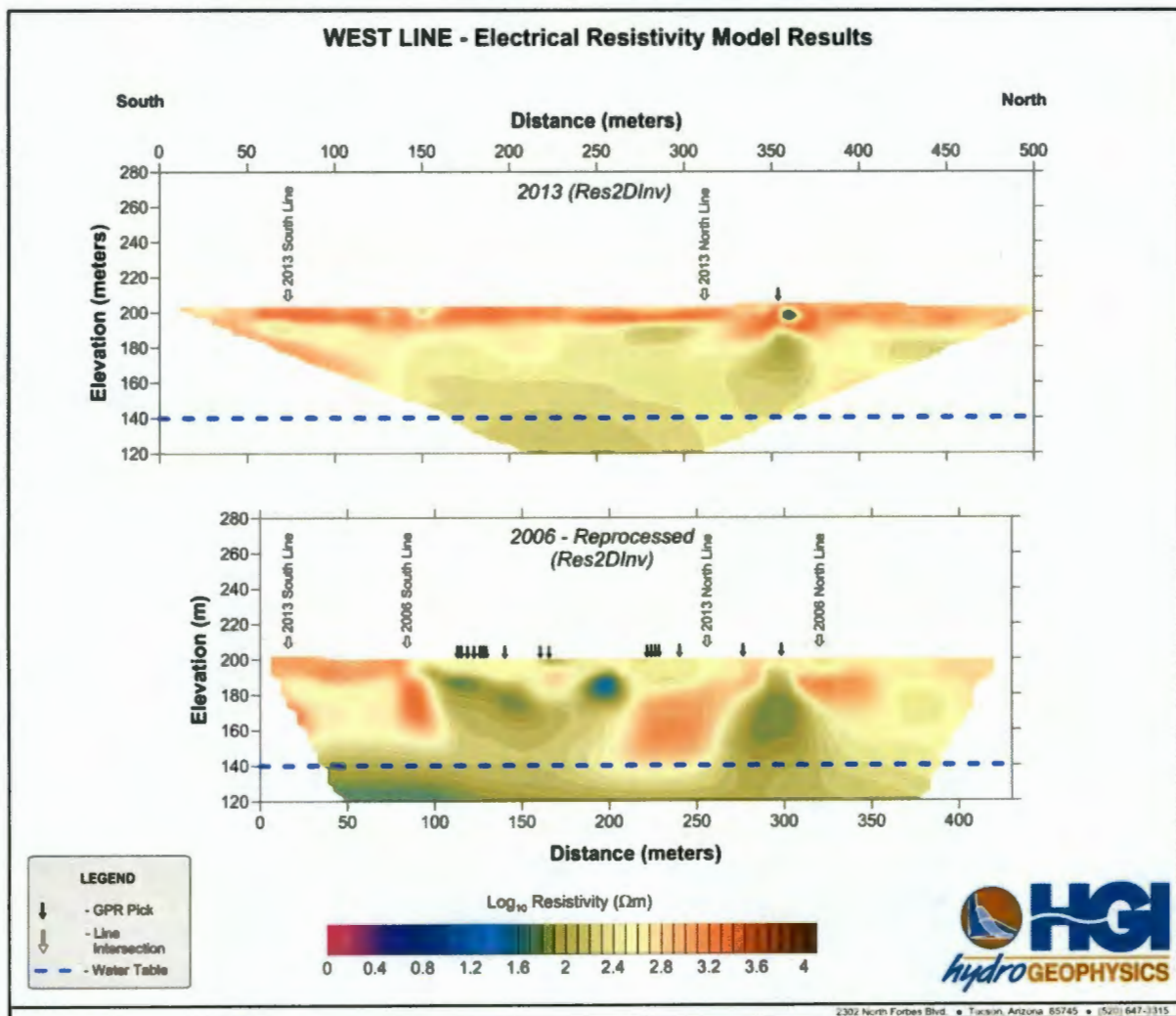
In addition, there are two obvious deeper conductive targets, with significantly lower resistivity values and larger dimensions than the previously described targets. Once again, both of these targets are associated with locations of significant amounts of infrastructure on the as-built CAD drawings, with the GPR picks confirming the presence of near-surface infrastructure.

4.1.4 West Survey Lines

The inversion model results for the West line surveys are shown in Figure 28, the FY2006 survey line is offset to align with the FY2013 survey line. Picks from the GPR clearance survey are included for both lines.

The FY2013 survey line displays a generally consistent resistive near-surface layer, approximately 33 ft (10 m) in thickness, overlying a more conductive layer. The lower layer appears to become increasingly more conductive at depths coinciding with the groundwater table. There appears to be only one near-surface conductive target of interest in this line, located at approximately 1181 ft (360 m) along the survey line. The target is bull's-eye in shape and is closely associated with the only GPR pick along this survey line, potentially indicating this is an infrastructure response. The inversion model beneath this feature, at a depth of approximately 59 ft (18 m) bgs (616.8 ft [188 m] amsl), appears more conductive than the surrounding regions. Whether this is an inversion modeling artifact produced by the very conductive target above or is indicative of another conductive feature is difficult to ascertain.

Figure 22. West Line 2D Model Surface Resistivity Results for the FY2013 (Top) and FY2006 (Bottom) Surveys.



The FY2006 survey line displays a conductive target at approximately 968 ft (295 m) along the survey line, which potentially aligns with the FY2013 conductive target. The FY2006 conductive target is also associated with a GPR pick, potentially indicating this is an infrastructure response. Additional conductive targets are located at 377 and 476 ft (115 and 145 m) along the survey line, these targets are associated with multiple GPR picks in this region, potentially indicating these are infrastructure responses. A very conductive target is located at 640 ft (195 m) along the survey line, although this is not associated with a GPR pick its shape and depth would tend to indicate an infrastructure response. The lower region of the model appears to become more conductive at depths coinciding with the groundwater table.

4.2 3D POINT ELECTRODE MODELING

Point electrode data from the U Tank Farm survey efforts were compiled for the current numerical inverse modeling. The initial starting points for the modeling included measurements on 490 surface electrodes and 10 depth electrodes. However, not all of these data were of acceptable quality and those data, including in some cases entire electrodes, were dropped from the model dataset. This included the depth electrode dataset, which did not meet data quality standards and was entirely removed prior to modeling as stated above. To create the final dataset for inversion, two types of data reduction occurred between the data acquisition and final inversion phases. First, data quality was inspected to eliminate unacceptable data that may have resulted from instrumentation error, electrical interference, or high data misfit with respect to neighboring points. The process of removing spurious data points is referred to as reducing and is performed prior to the first inversion run. Second, data were filtered after each inverse model was completed to remove data points that contributed to a high model RMS error. This process is referred to as a filter run, and the objective of a filter run was to reduce the final RMS to an acceptable level, usually below 10 percent. Each trial model run was assigned a model number which designated a specific data set or set of modeling parameters and each filter run was assigned a number. An example label for a model with a filter run is "Model_001i."

The initial model for point electrode data focused on the 3D data set using only the highest quality measured point electrode resistivity data, with no long electrodes. The high quality dataset for inversion was obtained by removing those data with reciprocal errors greater than 5 percent and anomalously low current and resistance (V/I) values. After data reduction, 174,597 measurements remained for inclusion in the initial inverse model. After completing a filter run to remove additional spurious data, 173,021 measurements remained. Table 7 lists the statistics for the modeling.

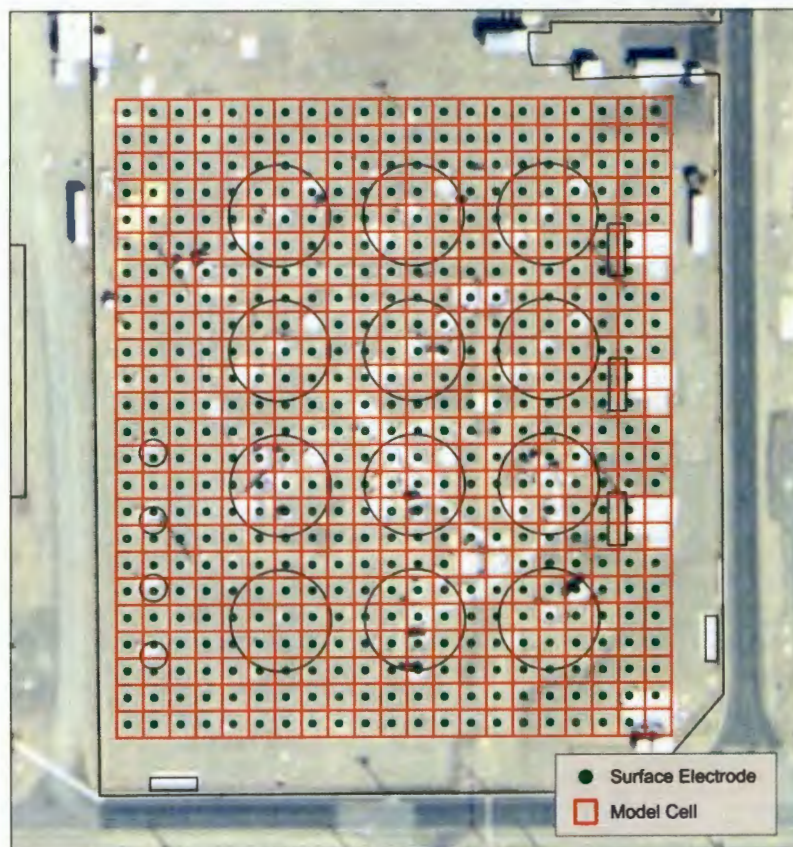
Table 7. Inverse Modeling Convergence and Error Statistics.

| Model | Surface to Surface | Model RMS Error (%) |
|---|--------------------|---------------------|
| Initial inversion input data file (U_Farm_StS_115) | 174,597 | 7.57 |
| Filtered inversion input data file (U_Farm_StS_115i) | 173,021 | 6.90 |
| Percent Data Remaining after filter run | 99.1% | |

A model mesh was created, as with any numerical modeling, whereby the subsurface was discretized into cells and nodes. The equations that describe the potential field during electrical current transmission are then solved at every node, with the appropriate boundary conditions. The RES3DINVx64 software automatically generates the model mesh for this forward model calculation by placing grid lines at the intersection of electrodes. Additional requirements of the numerical model include explicitly assigning every block an initial resistivity value and every node a current source (if any).

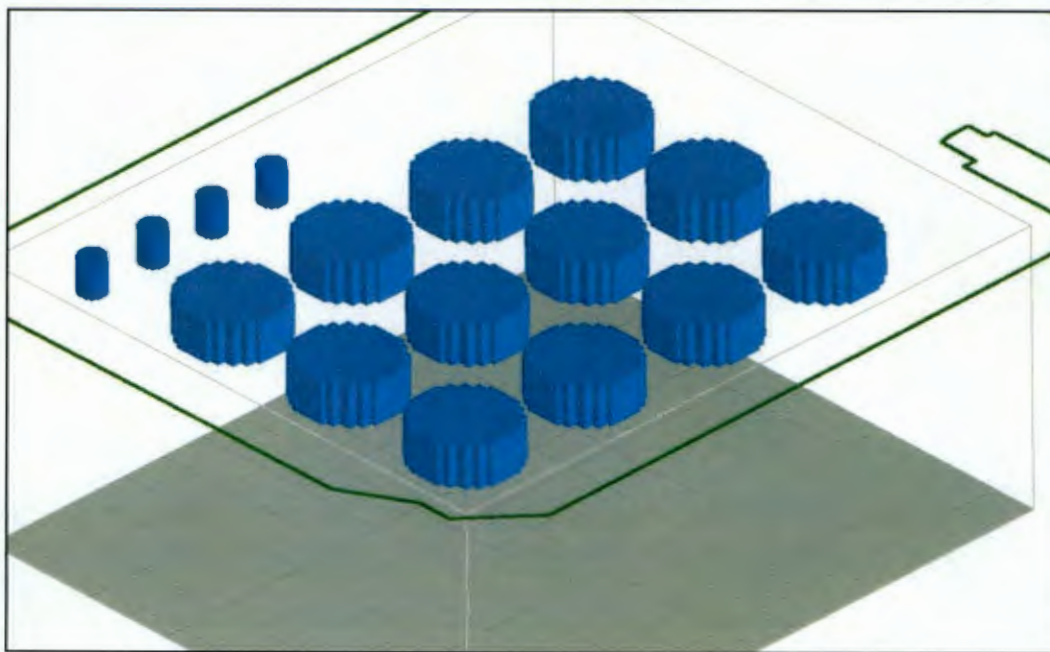
For the inverse model calculations, where the resistivity values are changed in the model domain until the measured and modeled voltages are nearly equal, a separate model mesh was created that did not align with the forward model mesh. The arbitrary gridding for the inverse model mesh prevented the creation of very small cells due to the depth electrode locations not being aligned to the surface electrode grid. We selected a 19.7 by 19.7 ft (6 by 6 meter) grid cell for the inverse model based on initial testing of a number of starting grid dimensions (Figure 29), which created 21 cells in the x-direction and 24 cells in the y-direction. There are a few cells which contain no electrodes within the model grid, usually due to infrastructure affecting surface electrode placement. In the z-direction, 14 layers were used. Although the model mesh extends to a depth of 515.1 ft (157 m) bgs (160.8 ft [49 m] amsl), the model sensitivity decreases significantly below 210 ft (64 m) bgs (465.9 ft [142 m] amsl) so these layers are not presented.

Figure 23. Size And Position of the Inverse Model Grid Used to Model the U Tank Farm Point Electrode Data.



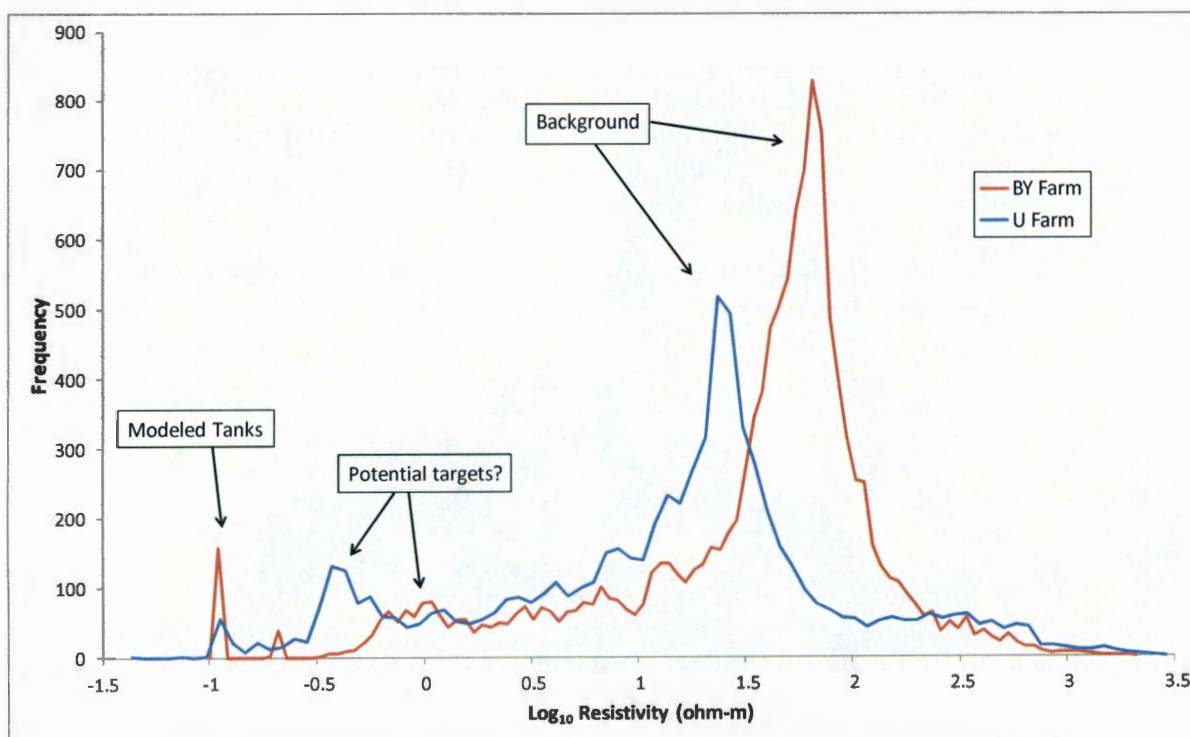
The locations of the storage tanks within the U Tank Farm were incorporated into the inverse model input file as *a priori* information, due to their known conductive effects. In past modeling efforts the storage tanks have been approximated using a simple rectilinear block representation. For the current U Tank Farm modeling, a series of models were run to determine whether an *a priori* shape resembling the actual circular tank would improve the resulting model. Previous modeling used a single rectangular block to approximate the tank. The circular storage tanks were more closely approximated during this modeling effort by using a series of overlapping blocks, extending between a depth of 7.2 and 37 ft (2.2 and 11.3 m) bgs (between 668.6 and 638.8 ft [203.8 and 194.7 m] amsl) for the 100-Series tanks and between a depth of 11.2 and 37.4 ft (3.4 and 11.4 m) bgs (between 664.7 and 638.5 ft [202.6 and 194.6 m] amsl) for the 200-Series tanks. Each block was assigned a resistivity value of 0.1 ohm-m by the modeler. Based on this testing, it was determined that the tank shape did not significantly affect the inverse model outcome. Upon entering *a priori* information in the RES3DINVx64 software, the user is given the option for stating the confidence of the chosen resistivity value given to these model blocks to account for the presence of the storage tanks (a confidence level ranging between 1 and 10). A low value is indicative of low confidence, and allows the model to change *a priori* information to improve the fit with the measured data. A high confidence would not allow the model to change the *a priori* information. For the final model we provided a confidence value of 2, thereby providing the model some flexibility to change the exact resistivity values of the tanks. Figure 30 displays the *a priori* blocks added to the model.

Figure 24. *A Priori* Model Blocks Added to the Inverse Modeling Domain.



In general, the average measured and modeled resistivity values within the U Tank Farm are considerably lower in comparison to values from other areas surveyed at the Hanford Site. To provide a point of reference, a distribution of resistivity values from U Tank Farm (FY2013 survey) and BY tank farm (FY2010 and 2011 surveys) is shown in Figure 25. The distributions share three similar features: (1) A localized peak at a \log_{10} resistivity value of -1 (0.1 ohm-m) representing the values of modeled metallic features (such as tanks and infrastructure), (2) a second localized peak possibly representing low resistivity targets, and (3) a third peak that may represent the higher background resistivity of the backfill and natural material. The bulk of the data from U Tank Farm is considerably lower in resistivity than the data from BY tank farm, with the background value peaks at \log_{10} resistivity values of 1.37 (23 ohm-m) and 1.81 (65 ohm-m), respectively.

Figure 25. Distribution of Modeled Resistivity Values for the U Tank Farm (Blue) and BY Tank Farm (Red) Inversion Results.



The results of the inverse modeling are displayed in Figure 20, Figure 21, and Figure 28. The figures were constructed from the output file for the second iteration of the filtered model run (with a final RMS error of 6.90 percent) and display slices at select depths within the model domain. The depths bgs are indicated in each subplot within the mosaic of different slices. Those layers with *a priori* tank information include a grayed out area indicating the modeled position of the tanks, with the intention being that blocking the highly conductive modeled tank will allow the viewer to observe the areas immediately surrounding the tank without being distracted by the modeled tanks themselves. Furthermore, the true outlines of the tanks are traced in black and red – the latter to denote tanks that are classified as historically leaking tanks to show their effects on the final resistivity distribution.

Figure 26. Expanded Plan View for the Depth Slice at 6.6 Ft of Calculated Resistivity for Filtered Surface to Surface, with Linear Interpretations from the FY2012 Ground Penetrating Radar Site Clearance Survey of U Tank Farm (left image).

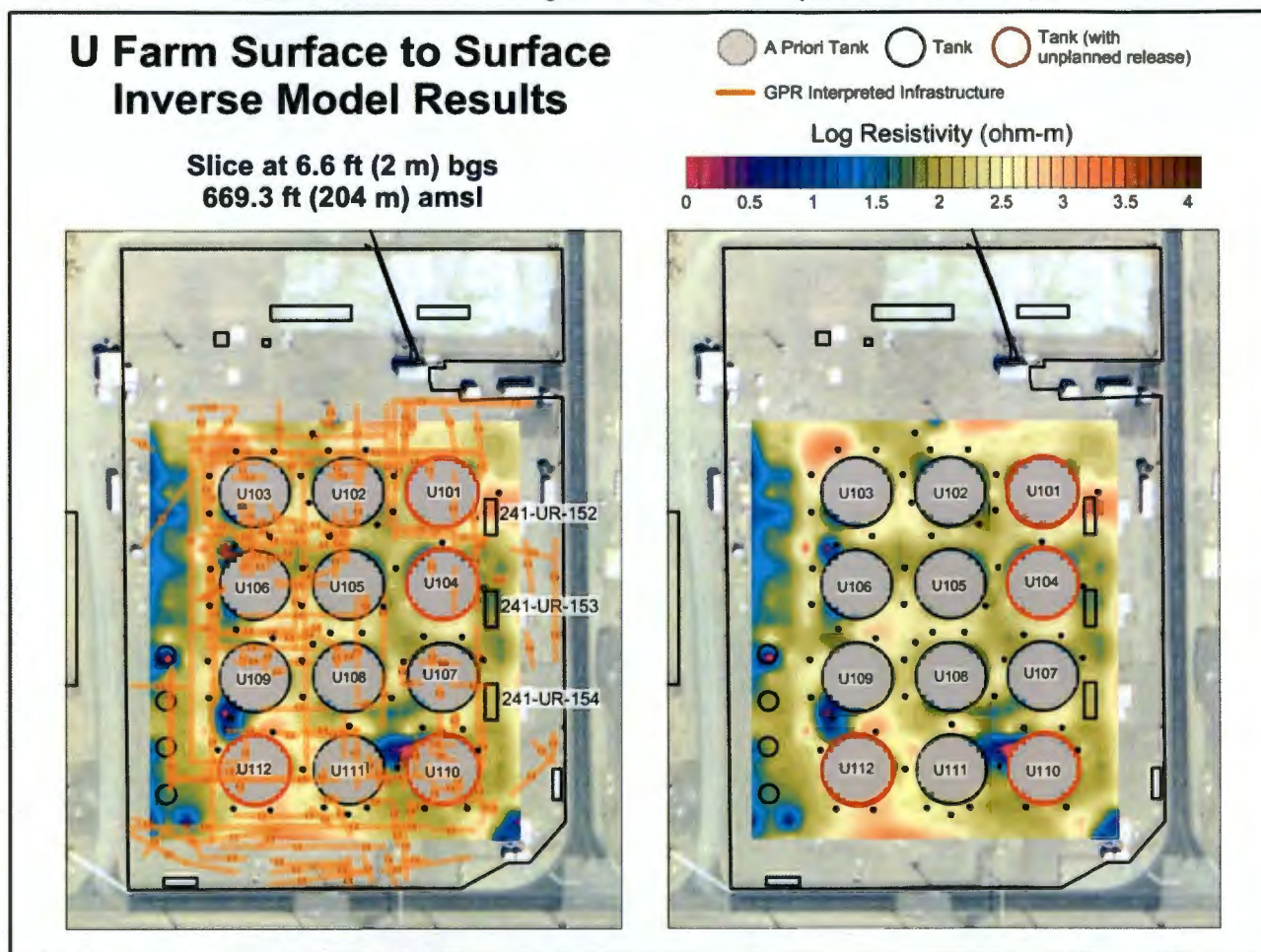


Figure 27. Plan View Depth Slices of Calculated Resistivity for Filtered Surface to Surface Dataset.

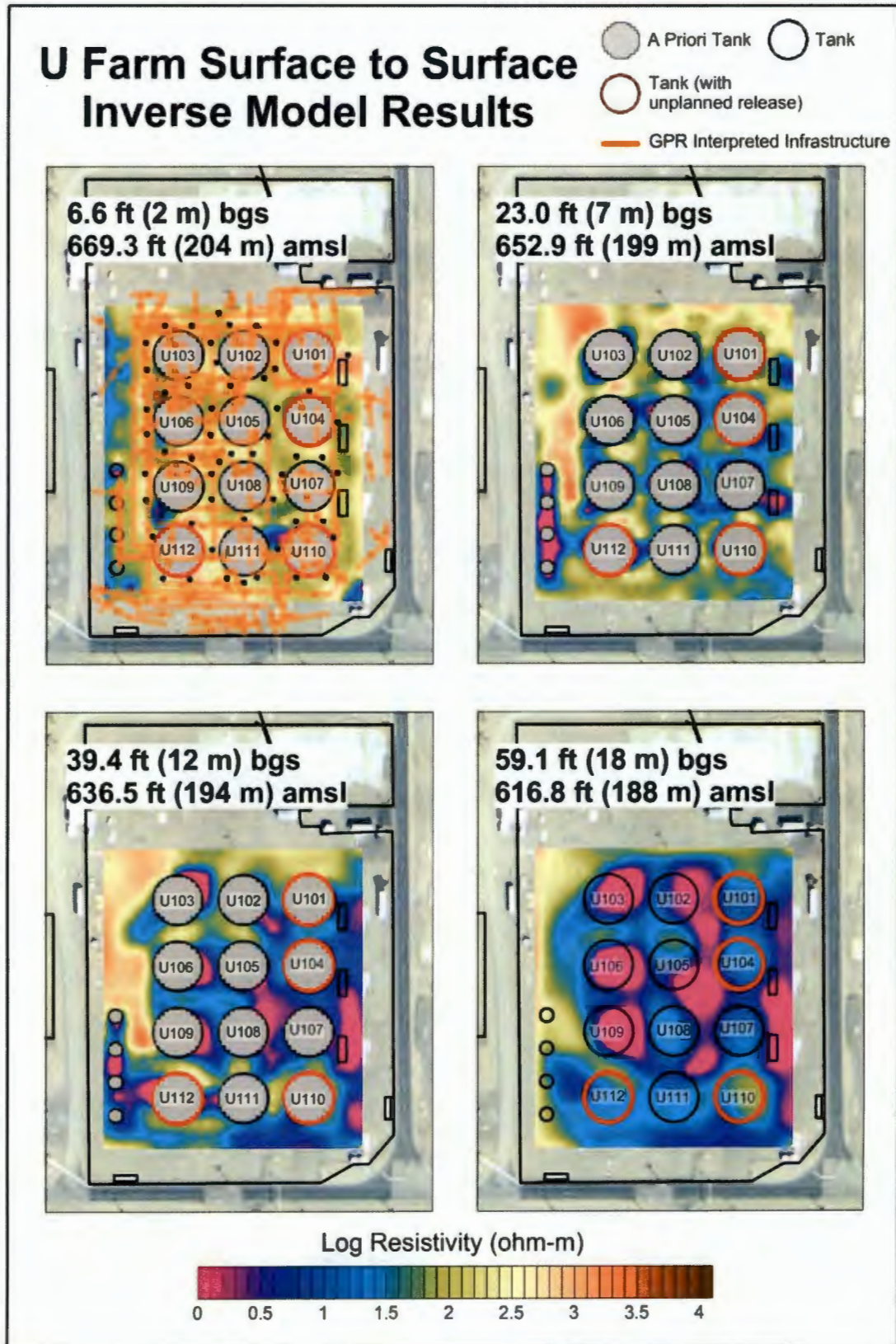
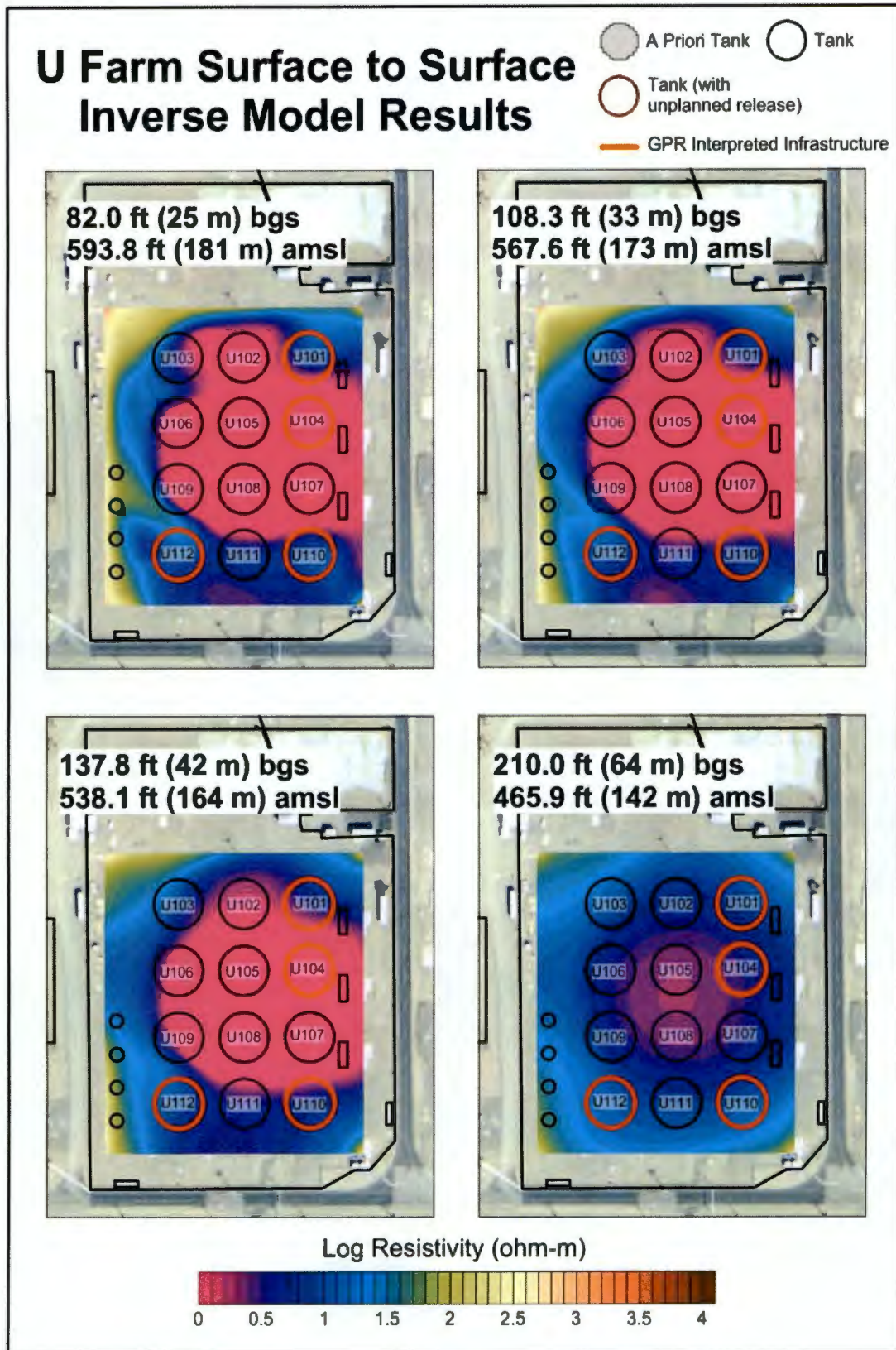


Figure 28. Plan View Depth Slices of Calculated Resistivity for Filtered Dataset.



The color scale uses warmer hues to represent more resistive regions and cooler hues to represent less resistive regions. The color scale range was chosen to be similar to that used for previous SGE projects from differing areas at the Hanford site. As highlighted in Figure 25, since the U Tank Farm modeled resistivity values are generally less resistive some of the warmer colors (reds and browns), representing resistive values, are not utilized in the slices.

The slice at 6.6 ft (2 m) bgs (669.3 ft [204 m] amsl) in Figure 25 and Figure 25, slightly above the top of the storage tanks (at approximately 7.2 ft [2.2 m] bgs [668.6 ft 203.8 m] amsl), displays relatively resistive values across the tank farm, taken to be representative of the farm background (backfill in this case). A number of conductive targets are observed; notably along the west edge of the inversion model and in proximity to the 200-Series tanks; extending between tanks U-109 and U-112, and U-110 and U-111; and extending to the north-west from tank U-106. A number of these targets approximate to linear in shape with resistivity values <3 ohm-m (\log_{10} resistivity values <0.5) and potentially represent subsurface infrastructure (pipelines for example) above or at the tank level. In addition, many of these targets are located in areas with a high density of linear interpretations identified in the FY2012 ground penetrating radar site clearance survey (Figure 27), for example around storage tank U-106 and in the vicinity of the 200-Series storage tanks. Geophysical logging data from dry wells around tank U-110 display an elevated gamma signature around this depth (3.9 ft [1.2 m] bgs [671.9 ft [204.8 m] amsl]). In particular, dry wells 60-11-03 and 60-11-12 display the only in-farm cobalt-60 and europium-154 signatures at this depth. Although not directly related to the resistivity data, the gamma logging can qualitatively indicate regions of past releases for ionic constituents.

The conductive target between tanks U-110 and U-111 correlates well to the elevated gamma signatures in this area and potentially represents a merged response from subsurface infrastructure and increased ionic concentrations related to a release. In addition, this target agrees well with a similarly located conductive target observed in the well-to-well inversion model. The slice at 23 ft (7 m) bgs (652.9 ft [199 m] amsl) in Figure 27, is about midway between the top and base of the 100-Series tanks, and approximately 11.5 ft (3.5 m) below the top of the 200-Series tanks. Numerous conductive targets can be observed in this depth slice, many of these anomalies approximate to linear in shape with resistivity values <3 ohm-m (\log_{10} resistivity values <0.5) and potentially represent subsurface infrastructure. The majority of the targets in this slice are observed extending between storage tanks, notably the targets between the 200-Series tanks, or are associated with the locations of the diversion boxes adjacent to tanks U-101, U-104, and U-107. There are regions to the south of tank U-110 and between tanks U-101, U-102, U-104, and U-105 where these targets appear less conductive and potentially are not associated with metallic infrastructure. Geophysical logging indicates an elevated gamma signature in a dry well to the south of tank U-110, between depths of approximately 11.5 and 55.8 ft (3.5 and 17 m) bgs (between 664.4 and 620.1 ft [202.5 and 189 m] amsl). These regions of lower conductivity anomalies could be indicative of a response to increased ionic concentrations related to a release or a more diffuse response from infrastructure.

Potential infrastructure responses continue to dominate the slice at 39.4 ft (12 m) bgs (636.5 ft [194 m] amsl) in Figure 27. At this depth, which is just slightly below the base of the modeled tanks, conductive targets are again observed between the 200-Series tanks, below the locations associated with the diversion boxes, and extending between a number of the 100-Series tanks. The majority of these targets are located in the same regions as the previous slice, but they appear more blurred potentially a result of the decreasing resolution with depth resulting in a

smearing of these features. The conductive target observed in the region to the south of tank U-110 is still present in this slice; it presents more like one cohesive anomaly now and is more conductive. Another conductive target of interest is the region between tanks U-104, U-105, U-107, and U-108. There is most likely a component of infrastructure response associated with this anomaly, but we observe a significant increase in conductivity of this region in areas where no infrastructure response was indicated in previous slices. This is notable around tank U-104 especially.

The slice at 59 ft (18 m) bgs (616.8 ft [188 m] amsl), in Figure 28, is completely below the base of the tanks, though it can be seen that in some areas the *a priori* modeled tanks are still having an influence at this level. This is primarily observed under tanks U-102, U-103, U-106, and U-109, where highly conductive regions still remain within the footprint of the tank. In addition, we observed highly conductive values for the regions beneath the diversion boxes on the eastern edge of the inversion model. The linear conductive targets discussed above, potential infrastructure responses, are predominantly absent in this slice, with the region around the 200-Series tanks returning to more resistive values indicative of the background for the tank farm. The conductive targets described in the previous slice above, to the south of tank U-110 and in the region between tanks U-104, U-105, U-107, and U-108 remain evident.

Known waste releases have occurred in U Tank Farm, the most significant of which is associated with tank U-104. Approximately 50,000 to 100,000 gallons (190,000 to 380,000 liters) of liquid waste was potentially leaked from tank U-104 into the surrounding area. Other smaller leaks may have occurred, associated with tanks U-101, U-110, and U-112. Gamma logging data, and in particular the U-235 and U-238 logging, from dry wells around tank U-104 display elevated signatures between 49.2 and 85.3 ft (15 and 26 m) bgs (between 626.6 and 590.6 ft [191 and 180 m] amsl). In addition, elevated signatures in the cesium-137 logging is observed near tanks U-110 and U-112 between depths of 49.2 and 55.8 ft (15 and 17 m) (between 626.6 and 620.1 ft [191 and 189 m] amsl), and 49.2 and 98.4 ft (15 and 30 m) bgs (between 626.6 and 577.4 ft [191 and 176 m] amsl), respectively.

The PNNL-17163 report indicates that the probe hole C5608, located directly south of tank U-110, displayed elevated (compared to the background samples collected) pore water conductivity values in samples collected between approximately 85 and 100 ft (26 and 30 m) bgs (between 590.1 and 577.4 ft [180 and 176 m] amsl). In addition, collected samples displayed elevated concentrations of water extractable anions, cations, and the mobile metals technetium-99 and chromium in the same depth range. It was concluded that a sodium-rich waste stream had migrated to at least 96 ft (29 m) bgs (580.7 ft [177 m] amsl) adjacent to tank U-110. The same report indicates that probe hole C5602, located directly southeast of tank U-105, displayed elevated concentrations of uranium-238 between depths of approximately 50 and 85 ft (15 and 26 m) bgs (between 626.6 and 590.6 ft [191 and 180 m] amsl), an obvious sign of tank-related fluid release.

The inversion model begins to change character in the slices below 82 ft (25 m) bgs (593.8 ft [181 m] amsl) in Figure 28, as the higher conductive responses coalesce into a larger mass below the tanks. A large low resistivity (high conductivity) region is seen encompassing the area below the northernmost nine tanks (U-101 through U-109), with the center of mass appearing closer to the central six tanks (U-104 through U-109). This response is relatively consistent in the slices at 82, 108.3, and 137.8 ft (25, 33, and 42 m) bgs (593.8, 567.6, and 538.1 ft [181, 173, and 164

m] amsl). The slice at 210 ft (64 m) bgs (465.9 ft [142 m] amsl), on Figure 28, then shows this highly conductive region beginning to dissipate, as the values become more resistive.

Electrical resistivity measurements are not sensitive to contaminants such as cesium and uranium; however it has been shown that conductive salts and nitrates present in the liquid waste releases can be associated with radioactive contaminants of concern. Increased levels of salts/nitrates in the ground will result in high conductivity (low resistivity) anomalies. The results of the U Tank Farm resistivity modeling clearly show a very conductive target residing below the tanks. This target could result from an increase in soil moisture at depth, although the low resistivity values, between 1 and 3 ohm-m, would tend to indicate a high percentage of ionic constituents present. There is little corroborating information in the gamma logging to support a release at these depths, although it is possible that the more mobile ionic constituents could potentially have migrated deeper than the less mobile radioactive isotopes. There is little indication of residual tank waste in the sediments analyzed to a maximum depth of approximately 100 ft (30 m) bgs (577.4 ft [176 m] amsl), and sufficient recharge was likely to have occurred to drive the bulk of the contamination deeper into the vadose zone (PNNL-17163). Possible influence of the *a priori* storage tank infrastructure was ruled out through testing the initial starting parameters assigned to the tanks in the inverse model. The conductive target appeared insensitive to changes in the starting resistivity of the *a priori* storage tanks.

Figure 29, Figure 30, and Figure 31 display three-dimensional renderings of the low resistivity features around the tanks in U Tank Farm. Figure 29 shows the isometric view of the tank farm, as viewed from the southeast (looking towards the northwest). Two levels of resistivity magnitude are presented, with the small opaque resistivity body in dark blue (resistivity value of 0.5 ohm-m) and the larger transparent resistivity body in light blue (resistivity value of 1 ohm-m). The main region of interest in the figure is the low resistivity feature beneath storage tanks U-104, U-105, U-106, U-107, U-108, and U-109. This feature represents a significant low resistivity anomaly within the U Tank Farm. However, these features, as modeled by RES3DINVx64, are likely represented larger than actual extent due to the smoothing process smearing information from the *a priori* tanks with any waste plume feature. Figure 31 shows a vertical profile view, from the south, with a dotted line representing the boundary of the Cold Creek geologic unit. This boundary is relatively close to the lower boundary of the conductive anomaly, and could be a potential controlling factor on the movement of constituents that are contributing to the anomaly.

Figure 29. Three-Dimensional Rendered Bodies of the Low Resistivity Targets using Surface to Surface Dataset in the U Tank Farm, View From Southeast.

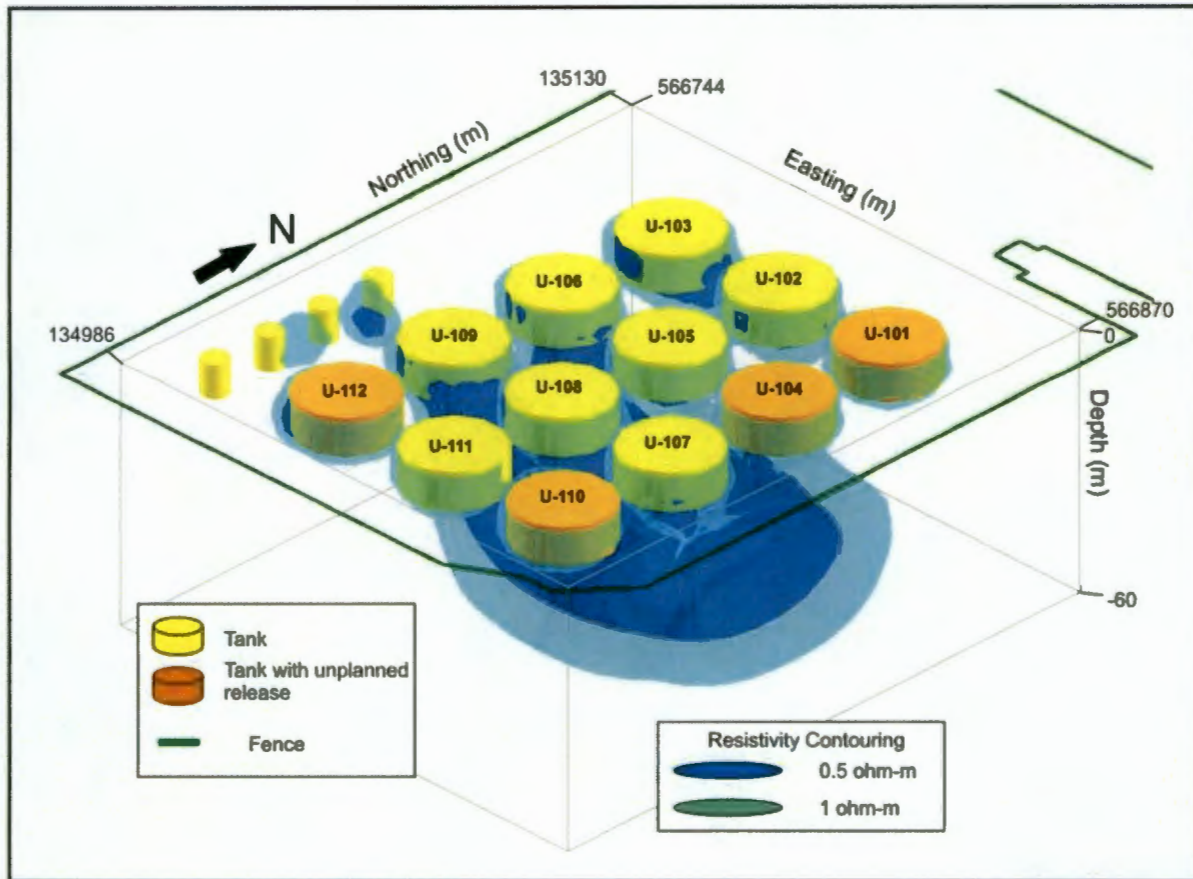


Figure 30. Three-Dimensional Rendered Bodies of the Low Resistivity Targets using Surface to Surface Dataset in the U Tank Farm, Plan View.

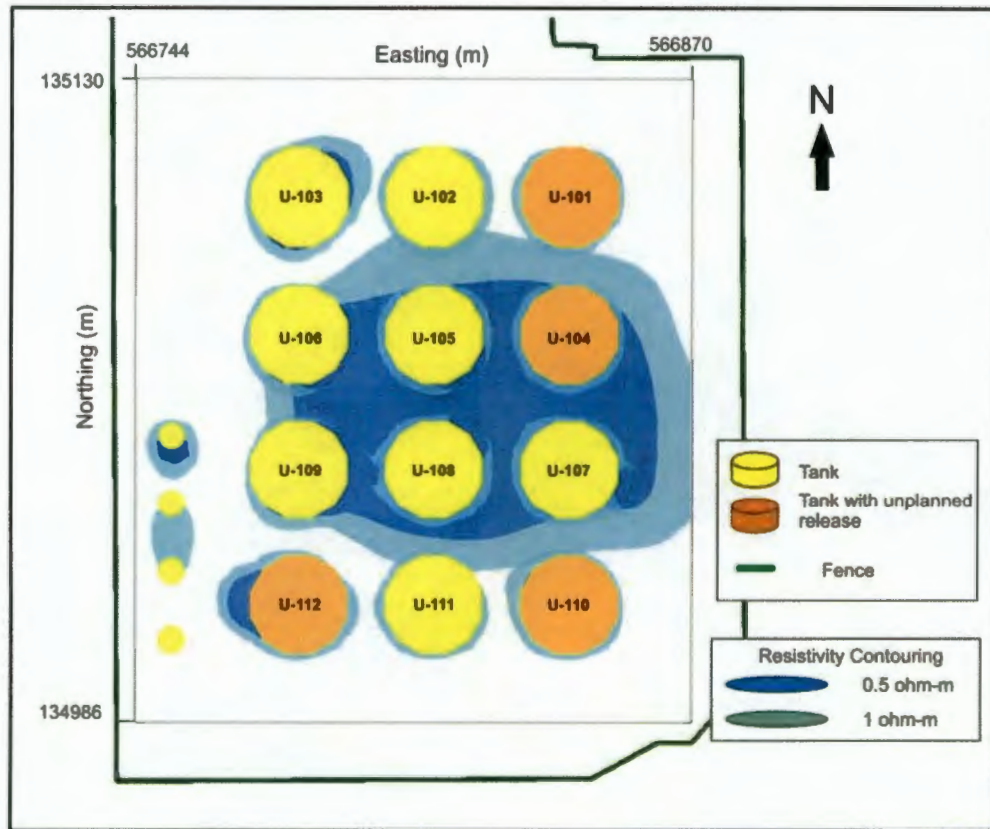
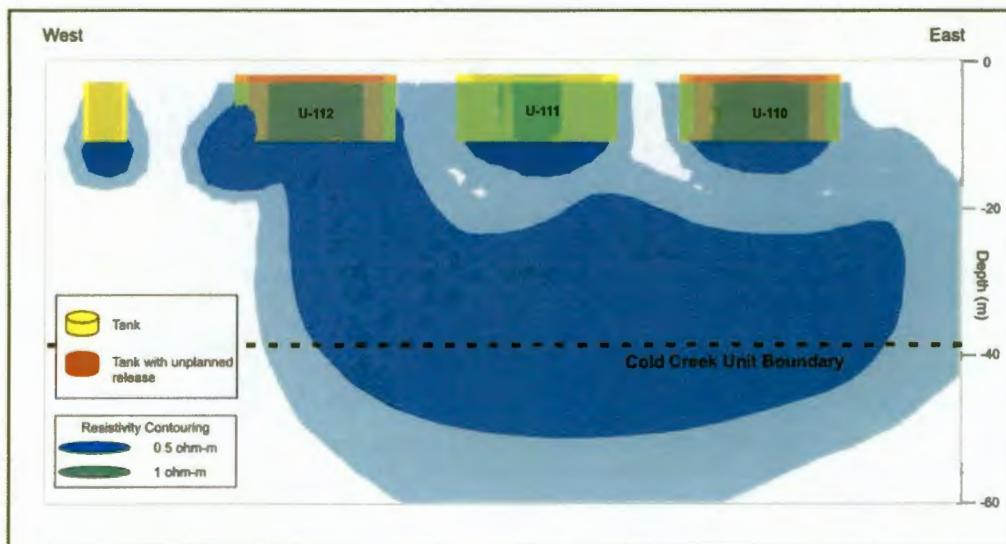


Figure 31. Three-Dimensional Rendered Bodies of the Low Resistivity Targets using Surface to Surface Dataset in the U Tank Farm, View From the South.



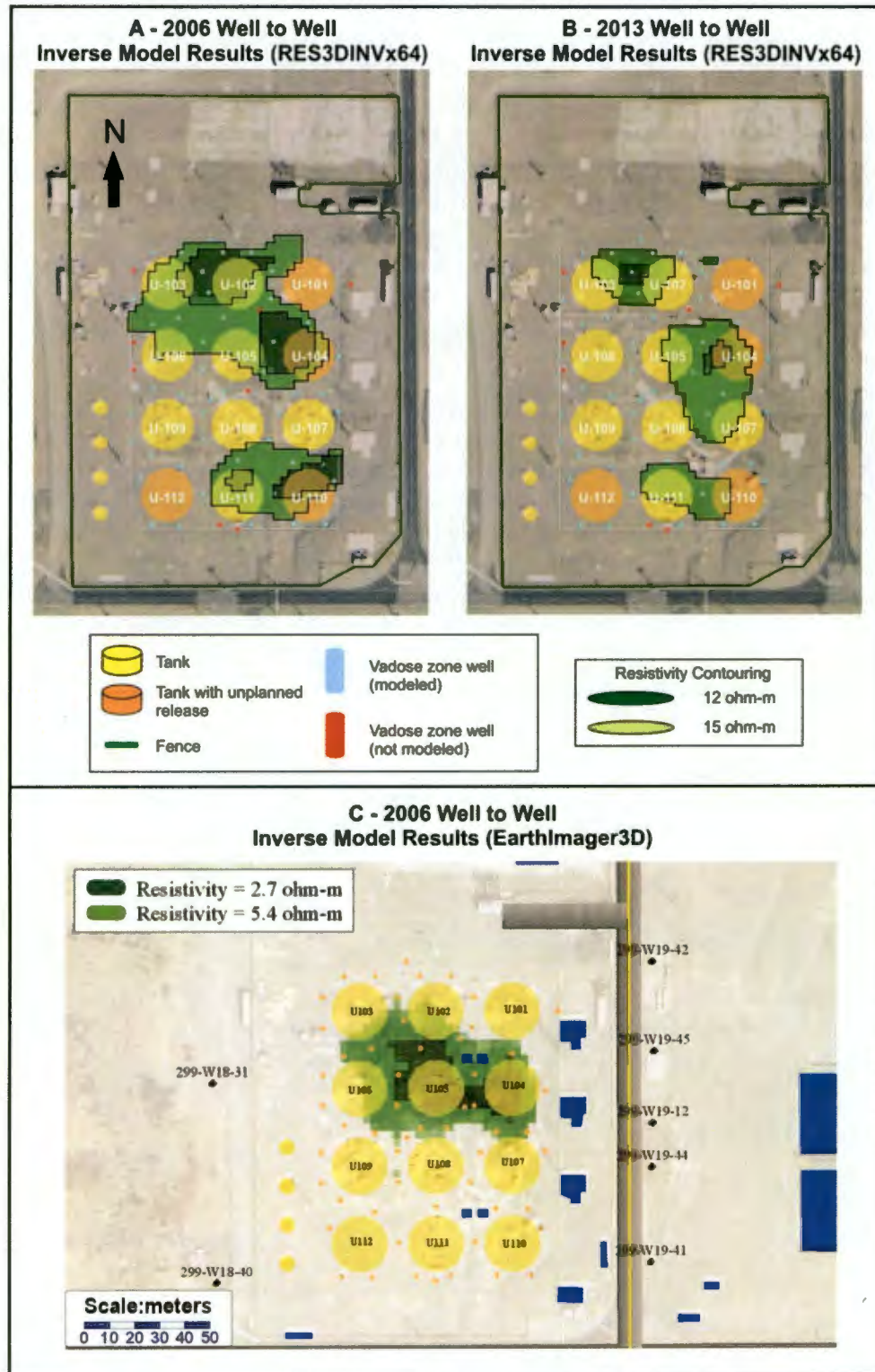
4.3 LONG ELECTRODE MODELING (WELL-TO-WELL INVERSION)

WTW data from the FY2013 efforts for the U Tank Farm survey were compiled for numerical inverse modeling. A total of 54 dry wells were used as long electrodes; 46 of which were retained for use in the final inversion model after eight were removed during the data reduction and filtering steps. The results from the previous FY2006 survey are also presented for comparison; further details can be found in RPP-RPT-31557. The two data sets were modeled independently instead of using a time-lapse modeling effort due to differences in survey logistics and locations of remote electrode arrays. Normally, data collected on the same set of electrodes at multiple time intervals could be used to assess temporal changes using a time-lapse modeling strategy, where the results from the first snapshot would be used as an initial condition of the following snapshots to help further constrain the temporal changes between models. In this case, comparison of independently modeled results can still provide a valid assessment of resistivity changes in a qualitative sense.

Figure 32 displays the results of the WTW inversion modeling for the FY2006 and FY2013 data. Two levels of resistivity values are presented in the plot, with the small opaque resistivity body in dark green representing a resistivity value of 12 ohm-m, and the larger transparent resistivity body in light green representing a resistivity value of 15 ohm-m. The FY2006 data were reprocessed and modeled in RES3DINVx64 to provide a direct comparison to the FY2013 data, using the same combination of dry well measurements. The bottom segment of Figure 32 shows the inverse model results of the FY2006 data as originally presented; at that time the data were modeled using the EarthImager3D (Advanced Geosciences) inversion software. The results for FY2013 and FY2006 display a good agreement between the locations of the center of mass for the three main conductive targets; namely between tanks U-102 and U-103, around tank U-104, and between tanks U-110 and U-111.

Based on the contour levels chosen, the exact shape of these conductive targets varies between survey years and is most likely a combination of the difference in remote electrode location between survey years and refinements in the inverse model grid between the two surveys (10 meter grid in FY2006 versus 3 meter grid in FY2013), based on optimization due to differing survey geometries and spatial area. Remembering that geophysical tools are most reliable as target recognition tools, the two inverse model results agree quite well. They also appear to agree well with the conductive target locations identified in the point electrode model, namely around tank U-110 and between tanks U-101, U-102, U-104, and U-105. The point electrode model also display a conductive target to the northeast of tank U-103, but it is uncertain if this is a response to the dense infrastructure in this region or an indication of increased ionic concentrations relating to a tank release.

Figure 32. Well-to-Well Inversion Model Results for the U Tank Farm, 2006 (reprocessed) and 2013.



There are a number of discrepancies between the FY2006 results that were reprocessed and modeled in RES3DINVx64 and the original EarthImager3D modeling. While the center of mass of the conductive target around tank U-104 is present in both models, the center of mass of the conductive target between tanks U-102 and U-103 in the reprocessed model seems to be shifted to the southeast in the original EarthImager3D model. In addition, the conductive target between tanks U-110 and U-111 is completely absent in the original EarthImager3D model. Upon further examination, this anomaly aligns well spatially with the spare inlet ports and the gamma logging information that detected near surface traces of cesium, cobalt, and europium. A major difference between the two inversions is the advancement in the way the long electrodes are incorporated into the model domain in the RES3DINVx64 inversion software. In addition, limitations with the EarthImager3D inversion software and hardware meant a much coarser inversion mesh was required. Advancements with the RES3DINVx64 inversion and in-house hardware allow for a much finer inversion mesh, leading to improvements in resolution.

4.4 INTEGRATED 2D AND 3D SURVEY ANALYSIS

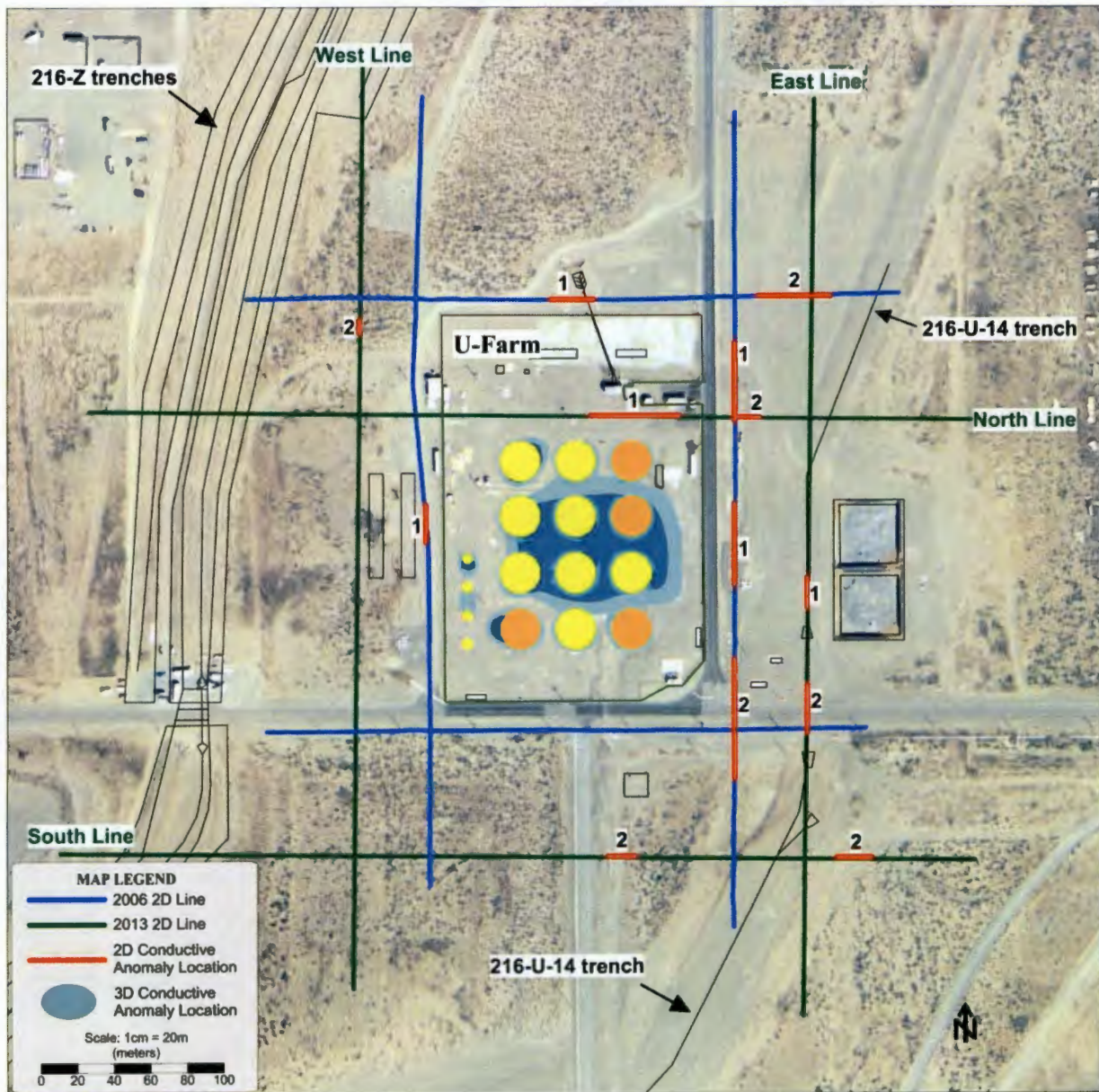
We have included a first attempt at integrating the 2D surveys from FY2006 and FY2013 with the FY2013 3D survey (Figure 33). The FY 2013 3D survey results (taken from Figure 30) include two levels of resistivity magnitude, with the small opaque resistivity body in dark blue (resistivity value of 0.5 ohm-m) and the larger transparent resistivity body in light blue (resistivity value of 1 ohm-m). The 2D lines were analyzed and sections of the line where conductive targets, in this case where the resistivity value was significantly lower than the average background reading, were located was noted. These sections were marked as red segments along the corresponding lines in Figure 33.

Many of the conductive targets in the 2D lines have a high probability of being responses to subsurface infrastructure and have been identified as such in previous sections; these are labeled with the number 2 in Figure 33. The conductive target associated with the FY2006 North 2D line (labeled with the number 1), corresponds well with the location of the French drain on the as-built drawings. In contrast, the conductive target in the FY2013 North 2D line potentially matches well to a conductive region in the 3D survey results that extends to the northern edge of the inversion model in the location of tanks U-101 and U-102. This region starts to become conductive at a depth of 59.1 ft (18 m) bgs (616.8 ft [188 m] amsl) which corresponds well to the depth of the top of the conductive target in the 2D North line.

The conductive target to the east of tanks U-104 and U-107 on the FY2006 East 2D line could potentially represent an extension to the conductive region observed on the eastern edge of the 3D survey inversion model in this location. The location and extent of the FY2006 East 2D line target aligns particularly well with the 3D results presented, however the 2D line target appears to be relatively shallow, with a maximum depth of approximately 49 ft (15 m) bgs (626.6 ft [191 m] amsl), compared to the depth of the 3D survey target. The conductive target associated with the FY2013 2D line could potentially be a response to the settling ponds to the east of the line based on the location and extent of this conductive target.

The conductive target on the FY2006 West 2D line does not appear to correlate with the 3D survey results and could potentially be related to releases in trenches to the west of this line or an infrastructure response.

Figure 33. Integrated 2D and 3D Survey Anomaly Map.



5.0 CONCLUSIONS

An SGE survey was conducted within the U Tank Farm on the Hanford Site. The survey consisted of four 2D electrical resistivity lines oriented around the perimeter of U Tank Farm, and a 3D electrical resistivity survey that encompassed the entire tank farm. The 3D survey included measurements on 490 surface electrodes placed within a grid, 10 depth electrodes, and 54 vadose zone dry wells acting as long electrodes. Data collection for the two surveys was completed between May 16, 2013 and June 28, 2013. Two inverse models were presented for the 3D electrical resistivity survey that included (1) point electrodes on the surface and (2) long electrodes (i.e., dry wells).

The combined point electrode inverse model had approximately 174,500 voltage measurements for the initial model run and 173,000 voltage measurements for the filter model run. The filter model run was conducted by removing those data that produced the highest error between modeled and measured voltage after the completion of the initial run. The filtered model run completed after five iterations with a root mean square error of 6.90 percent. The results of the model showed a continuous distribution of resistivity data within the U Tank Farm, with modeled resistivity spanning from 0.04 to 3321.4 ohm-m, or approximately 4.5 orders of magnitude difference between the lowest and highest resistivities. The low resistivity (high conductivity) targets, not associated with the underground storage tanks or interpreted infrastructure responses, were observed in the region between storage tanks U-104, U-105, U-107, and U-108, and to the south and west of tank U-110. The low resistivity targets can be verified by comparison to the WTW inversion modeling results. The validity of these targets was qualitatively verified by gamma logging data from the appropriate depths, obtained from the dry wells placed within the tank farm.

The dry wells located in the region between tanks U-104, U-105, U-107, and U-108 were the only ones in U Tank Farm to display elevated concentrations of U-235 and U-238, with elevated signatures occurring between approximately 49.2 and 85.3 ft (15 and 26 m) bgs (between 626.6 and 590.6 ft [191 and 180 m] amsl). The dry wells surrounding tank U-110 display elevated gamma signatures in the top 6.6 ft (2 m) of the subsurface; in particular dry wells 60-11-03 and 60-11-12 display the only in-farm Co-60 and Eu-154 signatures around this depth. The dry well 60-10-07 continues to display an elevated Cs-137 signature to a depth approximately 55.8 ft (17 m) bgs (620.1 ft [189 m] amsl). Although not directly comparable to the resistivity data, the gamma information can provide an indication of past releases. The remaining dry wells within U Tank Farm showed very low gamma activity.

In addition, a large low resistivity region is seen encompassing the area below the northernmost nine tanks (U-101 through U-109), between approximately 82 and 137.8 ft (25 and 42 m) bgs (between 593.8 and 538.1 ft [181 and 164 m] amsl). This target could result from an increase in soil moisture at depth, although the low resistivity values, between 1 and 3 ohm-m, would tend to indicate a high percentage of ionic constituents present. There is little corroborating information in the gamma logging to support a release at these depths, although it is possible that the more mobile ionic constituents could potentially have migrated deeper than the radioactive isotopes.

The second modeling effort used wells as long electrodes in a WTW inversion, and included approximately 2,800 voltage measurements. The results of the modeling for the FY2013 survey

displayed low resistivity targets between storage tanks U-102 and U-103, in between storage tanks U-104, U-105, U-107, and U-108, and between storage tanks U-110 and U-111. The footprints of the latter two low resistivity targets coincided with expectations based on knowledge of past releases in the tank farm and gamma logging results in the dry wells. These results correspond well to similar target locations observed in the FY2006 WTW survey; the difference in intensity and size of the targets is most likely an effect of the different remote locations used during data acquisition for each survey.

In summary, the different inverse modeling efforts conducted for the U Tank Farm displayed corresponding low resistivity targets in the vicinity of storage tanks U-103, U-104, U-107, and U-108 (in-between the four tanks) and storage tanks U-110 and U-111 (in-between and to the south of the two tanks). These targets are shallow, extending a minimal distance below the bottom of the storage tanks, and appear to agree with what is known about past releases in the tank farm. Overall, the shallow nature of these resistivity targets would likely support the value of an interim barrier should the targets prove to be waste related.

The success of this first whole tank farm SGE survey was realized through the deployment of the Geotecton-180 Resistivity Monitoring System. The 180 channel system allowed all measurement combinations of the 554 electrodes (surface, depth, and long (dry well) electrodes) to be collected 10 to 15 times more rapidly than previous SGE surveys using the eight-channel SuperSting R8 system.

6.0 REFERENCES

- CEES-0360, 2007, *Surface Geophysical Exploration System Design Description*, Rev. 0, Columbia Energy & Environmental Services, Inc., Richland, Washington.
- DOE/RL-2013-22, 2013, *Hanford Site Groundwater Monitoring Report for 2012*, Rev. 0, U.S. Department of Energy, Richland Operations Office, Richland, Washington.
- DOE/RL-88-30, 2013, *Hanford Site Waste Management Units Report*, Rev. 22, U.S. Department of Energy, Richland Operations Office, Richland, Washington.
- GJO-97-1-TARA, *Hanford Tank Farms Vadose Zone: Addendum to the U Tank Farm Report*, GJO-HAN-8, U.S. Department of Energy, Grand Junction Office, Grand Junction, Colorado.
- HNF-EP-0182, 2013, *Waste Tank Summary Report for Month Ending July 31, 2013*, Rev. 304, Washington River Protection Solutions, LLC, Richland, Washington.
- PNNL-17163, 2007, *Characterization of Direct Push Vadose Zone Sediments from the 241-U Single-Shell Tank Farm*. Pacific Northwest National Laboratory, Richland, Washington.
- RPP-7580, 2001, *Historical Vadose Zone Contamination from U Farm Operations*, Rev. 0, CH2M HILL Hanford Group, Inc., Richland, Washington.
- RPP-15808, 2003, *Subsurface Conditions Description of the U Waste Management Area*, Rev. 0, CH2M HILL Hanford Group, Inc., Richland, Washington.
- RPP-23405, 2008, *Tank Farm Vadose Zone Contamination Volume Estimates*, Rev. 3, CH2M HILL Hanford Group, Inc., Richland, Washington.
- RPP-23748, 2006, *Geology, Hydrogeology, Geochemistry, and Mineralogy Data Package for the Single-Shell Tank Waste Management Areas at the Hanford Site*, Rev. 0, CH2M HILL Hanford Group, Inc., Richland, Washington.
- RPP-26744, 2005, *Hanford Soil Inventory Model*, Rev. 1, Rev. 0, CH2M HILL Hanford Group, Inc., Richland, Washington.
- RPP-34690, *Surface Geophysical Exploration of the B, BX, and BY Tank Farms at the Hanford Site*
- RPP-35485, 2007, *Field Investigation Report for Waste Management Area U*, CH2M HILL Hanford Group, Richland, Washington.
- RPP-35968, 2007, *Completion Report for U Tank Farm Hydraulic Rotary Hammer Direct Push Drilling, Probe Installation and Sampling*, Rev. 0, CH2M HILL Hanford Group, Inc., Richland, Washington.
- RPP-PLAN-53808, 2012, *200 West Area Tank Farms Interim Measures Investigation Work Plan*, Rev 0., CH2M HILL Hanford Group, Inc., Richland, Washington.
- RPP-PLAN-54501, *Work Plan for 3D Electrical Resistivity Survey at the 241-U Tank Farm*. Rev. 0, Washington River Protection Solutions, LLC, Richland, Washington.

RPP-RPT-31557, 2006, *Surface Geophysical Exploration of U Farm at the Hanford Site*, Rev. 0, CH2M HILL Hanford Group, Inc., Richland, Washington.

RPP-RPT-50097, *Hanford 241-U Farm Leak Inventory Assessment Report*, Rev. 0, Washington River Protection Solutions, LLC, Richland, Washington.

RPP-RPT-54500, 2013, *241-U Farm: Two-Dimensional Electrical Resistivity Reanalysis*, Rev. 0, Washington River Protection Solutions, LLC, Richland, Washington

RPT-2013-004, 2013, *Summary of U-farm Site Clearance Survey*, Rev. 0, hydroGeophysics, Inc., Tucson, Arizona.

APPENDIX A

QUALITY ASSURANCE

A1.0 QUALITY ASSURANCE

Collection and analysis of surface geophysical exploration (SGE) data are performed under a project-specific quality assurance plan using a graded approach that conforms to applicable requirements from Columbia Energy quality assurance procedures (CEES-0333, *Quality Assurance Plan for Surface Geophysical Exploration Projects*). These procedures implement the requirements of ASME NQA-1, *Quality Assurance Requirements for Nuclear Facility Applications* and DOE O 414.1C, *Quality Assurance*. Work not covered in the quality assurance plan will conform to accepted industry standards for SGE and sound engineering principles.

This quality assurance plan implements the criteria of DOE O 414.1C and the following requirements from ASME NQA-1:

- Requirement 1 Organization
- Requirement 2 Quality Assurance Program
- Requirement 5 Instructions, Procedures, and Drawings
- Requirement 6 Document Control
- Requirement 16 Corrective Action
- Requirement 17 Quality Assurance Records.

Columbia Energy and Environmental Services, Inc. (Columbia Energy) and hydroGEOPHYSICS, Inc. (HGI) collect data using designed systems or off-the-shelf commercially available hardware. Designed systems conform to applicable requirements in approved procedures that address design, design analysis, design verification, and engineering drawing.

A project specific software management plan, CEES-0338, *Software Management Plan for Surface Geophysical Exploration Projects*, was prepared to implement a graded approach to software management in accordance with the following requirements documents:

- ASME NQA-1, Subpart 2.7, "Quality Assurance Requirements for Computer Software for Nuclear Facility Applications"
- CEES-0333
- Software Engineering (CE-ES-3.5)
- Contract 28090, *High Resolution Resistivity Characterization of Single Shell Tank Farm Waste Management Areas*
- DOE O 414.1C.

A1.1 CALIBRATION AND MAINTENANCE OF EQUIPMENT AND INSTRUMENTS

Calibration and maintenance of equipment used for data collection is addressed in CEES-0360, *Surface Geophysical Exploration System Design Description*. Where periodic calibration and/or maintenance of instruments used to collect quality affecting data is recommended those instruments were current on calibration at the time the instrument was used for data collection and the calibration certificate is maintained in the project files.

Field notes are used to document the specific instruments used. Electronic logs are utilized to provide traceable documentation for each data set collected. Information recorded in the

electronic field log includes date, instrument identification, operator, and applicable settings for each data set collected. All instruments have current calibration certificates and documentation is maintained in the project files. Instrument calibration frequency and calibration tests performed in the field are documented in the system design description (CEES-0360).

A1.2 DATA COLLECTION

The setup, operation, and maintenance of the SGE equipment used in collecting and analyzing resistivity data is described in CEES-0360. This document identifies the requirements for the hardware/software used for data collection and analysis and provides a rationale for the hardware/software selected for use.

Data accuracy will be evaluated by performing reciprocal data collection. Reciprocal collection is used as a tool to assure the data collected is accurate and repeatable. The transfer, storage, and management of data collected in the field are described in the system design description (CEES-0360).

A1.2.1 Selection of Resistivity Data Acquisition Equipment

In response to Washington River Protection Solutions, LLC (WRPS) desire for rapid data acquisition to reduce tank farm work restriction times, the Geotecton™ -180 Resistivity Monitoring System, designed and fabricated by HGI, is to be used. Similar equipment is currently in use at the C Tank Farm as part of the leak detection and monitoring program. HGI will deploy a larger and easily portable version of this system for this project, which is typically used for commercial applications. This new system has several capabilities that make it ideal for this application:

- **Improved Speed:** The system has 180 channels in comparison to the 8 channels available on the SuperSting R8® system previously used. This equates to a data collection rate that is 15 to 20 times faster.
- **Improved Data Quality:** Side by side comparison testing performed as part of acceptance testing for the leak detection and monitoring project showed the Geotecton™ system is more sensitive, more accurate, has a larger dynamic range, and is better equipped to deal with electrical interference.
- **Better Depth Electrode Sampling:** Geotecton has a greater number of channels, which in turn decreases the number of times the depth electrodes are transmitted on by a factor of 20. On previous surveys it was possible to overuse the depth electrodes through continuous current transmission, which reduced the available moisture. In addition, the improved dynamic range allows us to reduce the output electrical power while still producing a usable signal; improving the lifespan of the, historically fragile, depth electrodes.
- **Improved Safety:** Geotecton is UL-compliant, whereas the previously used equipment was not UL listed which required additional inspection for approved use. In addition, Geotecton automatically detects breaks in cables and will suspend current transmission to any conductors that are broken.

® SuperSting R8 is a registered trademark of Advanced Geosciences, Inc.

™ Geotecton is a trademark of hydroGEOPHYSICS, Inc.

- Improved Lock Out/Tag Out: Lock Out/Tag Out procedures are already in place within the Hanford complex as part of use on the leak detection and monitoring program.

A specific listing of the functional requirements and how the selected instruments meet those requirements is contained in Tables A-1, A-2, and A-3.

Table A-1. Physical Characteristics of the Geotection™-180 Resistivity Data Acquisition System.


| Physical Characteristics | Requirement | Selected Resistivity Data Acquisition Instrument |
|--------------------------|--|--|
| Portability | Must be field portable such that the components can be easily operated within the cab of a vehicle or field trailer. |  <p>Geotection™-180 system is mounted in a mobile, trailer based enclosure that can be temporarily or permanently deployed at a project site using mains or generator power.</p> |
| Temperature Range | 32° Fahrenheit to 105° Fahrenheit (0° Celsius to 40° Celsius). | Trailer based enclosure is fully climate controlled. |
| Power | Input power should be minimum of 12V dc. | 220 Volt AC, Single Phase, 3 pole, 50 A. (requires neutral) |
| Water Protection | Must be able to operate in rainy conditions. | Trailer based enclosure can operate in any weather conditions. |

Table A-2. Performance Characteristics of the Geotection™-180 Resistivity Data Acquisition System.

| Performance Characteristic | Requirement | Selected Resistivity Data Acquisition Instrument |
|----------------------------|---|---|
| Availability | Commercially available hardware with support for part repair/replacement. | Geotection™-180 Resistivity Monitoring System manufactured by hydroGEOPHYSICS, Inc, Tucson Arizona. Website: http://www.hgiworld.com/equipment/geotection/ |
| Use | Acquire Earth resistivity data using the pole-pole electrode array. | Resistivity imaging surveys using the pole-pole electrode array. |
| Operating Modes | Must be capable of automated multi-channel (minimum of six channels) data acquisition using a user defined set of electrode measurement instructions. | Automated data acquisition for up to 180-channels using a command file that is created manually by an operator. |
| Measurement Modes | Apparent resistivity and resistance. | Apparent resistivity, resistance, self-potential, contact resistance, transmitter current and voltage, receiver voltage, weather (in/out temp, rain, wind, humidity). |
| Number of Electrodes | Must be able to integrate with a minimum of 200 electrodes. | System can support a maximum of 66,000 electrode channels. |
| Measurement range | ±5 V dc. | ±10 V dc. |
| Measurement Resolution | Not defined. | 16-bit (15 µV per ±10 V range) |
| Output Current | Minimum of 1 A. | 1 mA - 8 A. |
| Output Power | Minimum of 100W. | 200W. |
| Input Impedance | >10 MOhms. | >10 MOhms. |
| Data Storage | Greater than 56,280 data points in resistivity mode. | Redundant enterprise grade laptop hard drives, SQL database storage, ASCII CSV summary files, binary full waveform files. |
| Depth of Investigation | Up to 82 feet (25 meters) to image target body. | Dependent on electrode spacing, total number of electrodes, array type, power output and signal-to-noise ratio. Under optimal conditions, a depth greater than 82 feet (25 meters) can be achieved with 262 feet (80 meters) x 216 feet (60 meters) survey grid. |
| Calibration | System must provide a manual/external calibration protocol, instrument must contain internal calibration function, or manufacturer must specify that no calibration is required for the intended purpose. | Externally calibrated using NIST traceable calibration box or upgradeable to internal calibration modules. |

ASCII = American Standard Code for Information Interchange.
 CSV = comma separated values.
 SQL = structured query language.

Table A-3. Interface Requirements of the Geotection™ -180 Resistivity Data Acquisition System.

| Interface Requirements | Requirement | Selected Resistivity Data Acquisition Instrument |
|------------------------|---|--|
| Data Storage Channels | Data output file must include: record, data, time, V/I, I, V, Error. | Geotection™ -180 data stored in SQL database and contain the following information: Decimal Time, Sequence Filename, Hardware Ver, Software Ver, Operator, Current Sense Scale (V/A), Site, Tx Frequency, Tx Duty Cycle (%), Tx Num Cycles, Tx Max Voltage (V), Tx Max Current (mA), Rx Sampling Rate, Data Window Min (%), Data Window Max (%), Error Cutoff (%), Trigger Multiplier, Trigger Duration Pts, Contact Resistance Test Current (mA), Contact Resistance Test Voltage (V), Max Contact Resistance (Ohms), Tx Voltage Divider, Overvoltage Protection (V), Error Type, Num Step Retries, GPIB Delay Compensation (msecs), Pwr Relay Delay Compensation (msecs), Auto Gain, Auto Gain Num Cycles, Auto Gain Scaling Factor, Low-Pass Filter, Site Notes, Record, Date, Time, Dec Time, Tx Chn, Rx Chn, File Name, Step Skipped, Reason Skipped, Contact Resistance (Ohms), Tx Voltage (V), Tx Voltage Saturated, Tx Voltage Gain, Tx Current (mA), Tx Current Saturated, Tx Current Gain, Rx Voltage (V), Resistance (Ohms), Pulse Error (%), Point Error (%), SP (V), Gain, Data Status |
| Output Channels | Must have a serial or universal serial bus channel to download data to a personal computer using Microsoft Windows XP®. | Data is written direct to desktop hard drive in trailer. |

* Microsoft Windows XP® is a registered trademark of the Microsoft Corporation.

| | | | | | |
|------|---|--------------------------------|-----|---|----------------------------|
| GPIB | = | General Purpose Interface Bus. | SP | = | Self Potential. |
| Max | = | Maximum. | SQL | = | Structured Query Language. |
| Min | = | Minimum. | Ver | = | Version. |

A1.3 ELECTRICAL INTERFERENCE MONITORING

Electrical interference can affect resistivity measurements in two ways:

1. Grounded conductive infrastructure (pipes, tanks, fences) may provide a preferential current pathway that distorts predictable current flow paths within the earth.
2. Electrical noise (voltage/current) sources from electrical systems (cathodic protection, pumps, motors, earth grounding arrays, etc.) may inject a competing signal.

Electrical noise interference can be minimized by identifying noise sources and then turning off electrical sources where possible for the duration of the resistivity surveying.

A passive monitoring system will be used to detect and map possible electrical noise interference prior to the start of resistivity measurements. For previous surveys, the process consisted of temporarily wiring several electrodes or steel-cased monitoring wells, distributed over a tank farm (inside and outside of the farm fence), to a distribution panel. A digital recording

oscilloscope was connected the electrode measuring points (two at a time) and the background electrical field was digitally recorded via a laptop computer. The oscilloscope operates via the universal serial bus port on the laptop computer and does not transmit signal into the ground. The data would be assessed at an offsite location and recommendations to minimize electrical interference will be made.

However, the new Geotecton™-180 System has a built in passive monitoring system that is capable of detecting electrical noise from any grounded electrical system. For this survey, the Geotecton-180 System will be used to identify the magnitude, frequency, and cycle time of possible interference. Noise will be monitored on all sensor types (well, surface electrode, and depth electrode) to generate a representative snapshot of electrical noise conditions. The primary focus will be to validate the suspension of cathodic protection systems.

A1.4 EQUIPMENT TESTING

A1.4.1 Geotecton™-180

Daily inspection of the entire system calibration is performed onsite using the manufacturer-supplied calibration resistor test box. The supplied test box is connected to the Geotecton™-180 before commencing the daily survey. A specific calibration test sequence file is used to test all possible measurement combinations. The resulting data file is copied into a controlled spreadsheet that contains the known National Institute of Standards and Technology (NIST) resistance values. The sheet identifies if any of the channels fail, a recalibration or repair is required.

A1.4.2 Passive Resistivity Cables

The passive resistivity cables shall be tested for continuity and current leakage in accordance with test procedure CEES-0399, *Test Procedure for SGE Passive Cables Using Porta Scan*. The cable sections shall be tested prior to initiating the survey, opportunistically during the survey, and at the completion of the survey. The test instrument is designed to provide a screening level field test to verify cable integrity and functionality. Test records shall be maintained in the project files.

A1.4.3 SuperSting

Daily inspection of the receiver calibration is performed onsite using the manufacturer-supplied calibration resistor test box. The supplied test box is connected to the SuperSting R8 before commencing the daily survey. A specific calibration test firmware is provided within the SuperSting® and provides the operator with a pass/fail indication for each of the eight receiver channels. If any of the channels fail, a recalibration or repair is required.

A1.4.1 SwitchBoxes

The operator connects a switchbox or switchboxes to the SuperSting R8 and performs the relay test that is incorporated into the SuperSting R8 firmware. This test sends a signal to each switchbox electrode to assess the functionality of the relays on each switchbox electrode channel. The SuperSting reports the success or failure of each relay (switchbox electrode channel) as a pass or fail. The relay test only inspects the operability of each relay.

As part of field equipment testing on all resistivity surface exploration geophysics deployments at the Hanford site, it is necessary to provide equipment evaluation specifically with regard to the functionality of the Advanced Geosciences Inc. Super Sting R8 Resistivity meter ("Sting") electrode multiplexors (switchboxes). The switchboxes come in three standard capacities, all in increments of 28 switches, e.g., 28, 56, and 84 switches. Any combination of these switchboxes may be used on a Hanford Site deployment of SGE.

A Switchbox test was performed on all switchboxes used on a weekly, and as needed basis. For the Switchbox test, the operator connects a switchbox to the SuperSting R8 and to a switchbox diagnostic tester (SBDT) (HGI). The SBDT simulates an actual resistivity survey using a network of resistors of known resistance. The measured data is compared to the known resistances for the SBDT and success or failure is reported for each switchbox electrode channel as a pass or fail. The switchbox test evaluates the operability of each relay and in addition evaluates any possible shorting, lack of isolation or failures of internal electronics that control the relays. If a relay fails in the opened or closed state during typical testing, relatively high measurement errors, sometimes exceeding 100 percent relative to the standard baseline results recorded for the SBDT by the High Resolution Resistivity® Leak Detection and Monitoring® Data Acquisition System (DAS), can be expected.

The selection of an appropriate error threshold for passing or failing needs to be consistent with the type of survey being performed and environmental conditions that could be encountered during testing. A 5 percent error threshold is typical for industry use in bench-scale testing of equipment and this level could be very appropriate for some applications. Under a bench testing setting, where environmental conditions are generally controlled, our own experience shows that recorded Sting measurements for operational relays within a switchbox can be much less than 5 percent of standard baseline values for the SBDT. The 5 percent level is also supported by the manufacturer, Advanced Geosciences, Inc. in bench-scale evaluation of switchbox relays in their facilities.

However, under field conditions, where changes in ambient temperature, wind conditions, and electrical interference can potentially affect measurement error during data acquisition, it is possible that this 5 percent pass/fail threshold may not be adequate and could potentially result in apparent relay failures in a fully operational switchbox. Geophysical resistivity data taken in less than ideal environment conditions can often exceed a 5 percent error in repeatability, but can still be used to produce usable results. Therefore, to account the additional effects of field conditions, our professional judgment is that a 10 percent threshold would be a more appropriate level to use and this level was initially used in switchbox testing for this project. As we gain additional experience with SBDT field testing, we will reevaluate this value as an effective pass/fail threshold.

A1.5 DATA PROCESSING

The process used to filter the raw data is described in the system design description (CEES-0360). Data are downloaded from the resistivity instrument and parsed into a usable format. Data filtering techniques are then used to remove data spikes or anomalous data caused by data acquisition card instabilities, or extraneous current sources.

® High Resolution Resistivity (HRR) is a registered trademark of hydroGEOPHYSICS, Inc.

® Leak Detection and Monitoring (LDM) is a registered trademark of hydroGEOPHYSICS, Inc.

Data filtering is performed by copying the parsed raw data into an Excel data filtering template that contains a series of graphs that show the various data parameters. The process of filtering eliminates data points, but no data modification (rounding, averaging, smoothing, or splining) is permitted. The rationale is to seek out and remove spurious points that do not conform to the data population or points that violate potential theory.

The final step is to inverse model the measured data to obtain the spatio-temporal distribution of electrical resistivity. Inverse modeling is accomplished using either EarthImager3DCL (EI3DCL) or RES3DINVx64 (RES3D). Verification and testing of the inversion software was performed and documented in RPP-34974, *Verification and Testing of the EarthImager Series of Electrical Resistivity Inversion Codes – A Benchmark Comparison*. Verification and testing was performed on the existing two-dimensional (2D) and three-dimensional (3D) versions of the software as well as the upgraded 64-bit, multi-threaded versions developed for tank farm projects.

The objective of the verification and testing study was to demonstrate that the resistivity inversion codes were comparable to known conditions from a pilot-scale field resistivity experiment. The pilot-scale field experiment was used to test the WTW inversion methodology by establishing a known conductive target in the subsurface and making measurements with a set of 27 simulated wells. To date, there is no industry standard for the WTW resistivity imaging technique, which necessitated the field experiment. The field experiment was designed to test the inversion code's ability to replicate a target of known geometry. The subsurface geophysical target was an amended, electrically conductive soil, buried approximately 1.6 feet (0.5 meters) below ground surface. The 27 wells were distributed around the target in a pattern similar to tank B-105 in the B Tank Farm.

From the above descriptions, it is obvious that data processing is performed using a number of software packages. The requirements and responsibilities for the identification, evaluation, development, testing, and maintenance of quality-affecting software acquired, developed, or modified in support of the SGE efforts are defined in CEES-0338.

A2.0 REFERENCES

- ASME NQA-1, 2004, *Quality Assurance Requirements for Nuclear Facility Applications*, American Society of Mechanical Engineers, New York, New York.
- CEES-0333, 2006, *Quality Assurance Plan for Surface Geophysical Exploration Projects*, as revised, Columbia Energy and Environmental Services Inc., Richland, Washington.
- CEES-0338, 2006, *Software Management Plan for Surface Geophysical Exploration Projects*, Rev. 0, Columbia Energy and Environmental Services Inc., Richland, Washington.
- CEES-0360, *Surface Geophysical Exploration System Design Description*, Columbia Energy and Environmental Services Inc., Richland, Washington.
- Contract 28090, Requisition 123974, *High Resolution Resistivity Characterization of Single Shell Tank Farm Waste Management Areas*, Revision 3, CH2M HILL Hanford Group, Inc.
- DOE O 414.1C, *Quality Assurance*, U.S. Department of Energy, Washington, D.C.

RPP-34974, *Verification and Testing of the EarthImager Series of Electrical Resistivity Inversion Codes – A Benchmark Comparison*, Rev. 0, CH2M HILL Hanford Group, Inc., Richland, Washington.